ISSN: 1945-3078 (Print), 1945-3086 (Online) Volume 1, Number 1, April 2009

Wireless Sensor Network

Chief Editor : Kosai Raoof

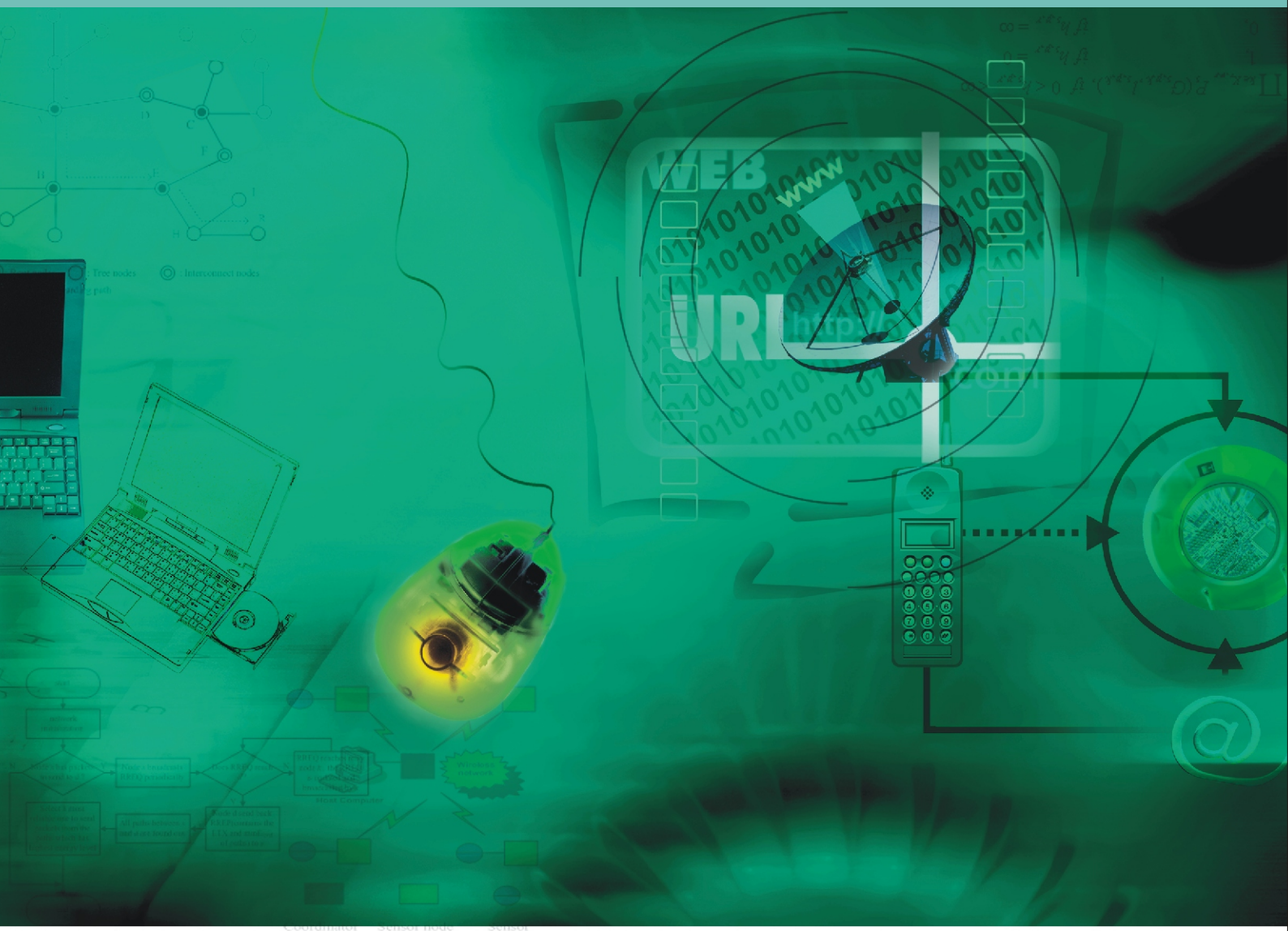

www.scirp.org/journal/wsn/

Scientific Research Publishing

Journal Editorial Board

ISSN 1945-3078 (Print) ISSN 1945-3086 (Online)

http://www.scirp.org/journal/wsn/

Wireless Sensor Network, 2009, 1, 1-60
Published Online April 2009 in SciRes (http://www.SciRP.org/journal/wsn/).

TABLE OF CONTENTS

Volume 1 Number 1 **April 2009**

Bandwidth Efficient Three-User Cooperative Diversity Scheme Based on Relaying Superposition Symbols

M. W. CAO, G. G. BI, X. F. JIN……..…….….. 1

The Influence of LOS Components on the Statistical Properties of the Capacity of Amplify-and-Forward Channels

G. RAFIQ, M. PÄTZOLD……...……...…….. 7

Parameter Optimization for Amplify-and-Forward Relaying Systems with Pilot Symbol Assisted Modulation Scheme

Y. WU, M. PÄTZOLD……...……..….. 15

An Energy Balanced Reliable Routing Metric in WSNs

J. ZHU, H. ZHAO, J. Q. XU…….……..……... 22

Extending the Network Lifetime Using Optimized Energy Efficient Cross Layer Module (OEEXLM) in Wireless Sensor Networks

T. V. PADMAVATHY……...……...…….. 27

Subarea Tree Routing (STR) in Multi-Hop Wireless Ad hoc Networks

G. K. LIU, C. L. SHAN, G. WEI, H. J. WANG.……..……... 36

Research on ZigBee Wireless Sensors Network Based on ModBus Protocol

C. B. YU, Y. F. LIU, C. WANG……...…..……..…. 43

Policy Based Self-Adaptive Scheme in Pervasive Computing

J. Q. OUYANG, D. X. SHI, B. DING, J. FENG, H. M. WANG……..……..……..….. 48

The Analysis of the Structure and Security of Home Control Subnet

C. Y. WANG, Y. ZHANG……..……..….. 56

Wireless Sensor Network (WSN)

Journal Information

SUBSCRIPTIONS

The *Wireless Sensor Network* (Online at Scientific Research Publishing, www.SciRP.org) is published quarterly by Scientific Research Publishing, Inc. 5005 Paseo Segovia, Irvine, CA 92603-3334, USA.

E-mail: wsn@scirp.org

Subscription rates: Volume 1 2009

Print: $50 per copy.

Electronic: free, available on www.SciRP.org.

To subscribe, please contact Journals Subscriptions Department, E-mail: wsn@scirp.org

Sample copies: If you are interested in subscribing, you may obtain a free sample copy by contacting Scientific Research Publishing, Inc at the above address.

SERVICES

Advertisements

Advertisement Sales Department, E-mail: wsn@scirp.org

Reprints (minimum quantity 100 copies)

Reprints Co-ordinator, Scientific Research Publishing, Inc. 5005 Paseo Segovia, Irvine, CA 92603-3334, USA.
E-mail: wsn@scirp.org

COPYRIGHT

PRODUCTION INFORMATION

For manuscripts that have been accepted for publication, please contact:
E-mail: wsn@scirp.org

Wireless Sensor Network, 2009, 1, 1-60
Published Online April 2009 in SciRes (http://www.SciRP.org/journal/wsn/).

Bandwidth Efficient Three-User Cooperative Diversity Scheme Based on Relaying Superposition Symbols

Mingwei CAO, Guangguo BI, Xiufeng JIN
National Mobile Communications Research Laboratory, Southeast University, Nanjing, China
E-mail: mwcao@163.com, {bigg, xiufeng.jin}@seu.edu.cn
Received February 3, 2009; *revised February* 17, 2009; *accepted February* 19, 2009

Abstract

Recently, Cooperative diversity in wireless communication systems has gained much attention. A simple two-user cooperative diversity scheme called decode-and-forward cooperation scheme has been presented by Laneman (2004). Each user has one partner to decode its information and retransmit it by employing repetition coding. This scheme can offer diversity order of two. But the bandwidth efficiency is low. In this paper, we propose a bandwidth efficient three-user cooperative diversity scheme based on relaying superposition symbols. Each user has two partners and each partner relays superposition symbols of the other two users instead of repetition. Thus, the bandwidth efficiency is improved compared to the baseline decode-and-forward cooperative diversity scheme presented by Laneman. Moreover, the proposed scheme can also offer diversity order of two. Then, in order to improve the system performance, a new constellation labeling for the superposition 8PSK modulation is designed. It is a simple way to exploit the symbol mapping diversity and a gain of about 2 dB can be obtained. Furthermore, the performance improvement comes at no additional power or bandwidth expense.

Keywords: Cooperative Diversity, Bandwidth Efficiency, Superposition Symbols, Symbol Mapping Diversity

1. Introduction

Multiple-antenna technique has been studied extensively, and it is an efficient technique to exploit spatial diversity and offer capacity gain compared to single-antenna systems [1,2]. Transmit diversity [3] has been proposed to improve the performance for systems with multiple transmit antennas.

However, in wireless communication systems, users may not be able to support multiple antennas because of the limitation of the size or cost. In this scenario, cooperative diversity, which has been proposed to achieve the transmit diversity, has gained much attention when each user only has a single antenna [4,5]. In cooperative communication systems [6,7], each user transmits its information to a destination and receives its partners' information and then serves as a relay for its partners. Hence, the destination can receive each user's information from several independent paths to efficiently resist the slowly fading effect. In baseline decode-and-forward cooperation scheme [7], two users transmit their information on orthogonal channels. Each user has one partner and decodes the partner's information and re-encodes and retransmits it through its own channel, thus, the diversity order is two. However, the bandwidth efficiency is decreased by 1/2 compared to a non-cooperative diversity scheme. In order to reduce the bandwidth loss, some cooperation schemes are proposed in [8−12]. In [8], distributed space-time codes are used for cooperating transmission. Multi-source cooperation coding approach is introduced in [9−12]. In those cooperation schemes, data of multiple users are jointly encoded by relays. The bandwidth efficiency of these schemes presented in [8−12] is improved greatly, but the decoding complexity is too high.

In this paper, we propose a cooperative diversity scheme based on superposition modulation, which offers the same diversity order as the baseline decode-and-forward cooperation scheme does. The bandwidth efficiency of the proposed scheme is only decreased by 1/3 compared to a non-cooperative diversity scheme and the decoding complexity is much lower than that of these schemes presented in [8−12]. Moreover, a new constellation labeling for the superposition modulation is designed to improve the bit error rate (BER) performance when the system employs 8PSK modulation. Using the

new constellation labeling, the system performance can be improved without any additional power or bandwidth expense.

Also, a cooperation scheme of two-node system based on superposition BPSK modulation is proposed in [13]. In this system, each node transmits a superposition of its own data with the data received from its partner in the previous slot. The performance of this scheme presented in [13] is further analyzed in [14,15]. In [16], the generalization of the scheme proposed in [13] to a multiple-user scenario is considered. In [17], a novel cooperation scheme based on the algebraic superposition of channel codes over a finite field is proposed. In [18], user and relay use the in-phase and the quadrature components of a QPSK signal, respectively for cooperating transmission. These schemes proposed in [13−18] are different from our scheme in which each partner retransmits the superposition symbols received from different users and each user's own symbols are not superposed with its partners' symbols.

The rest of this paper is organized as follows. In Section 2, system model is introduced, and a bandwidth efficient cooperative diversity scheme is proposed. The diversity order is discussed in Section 3 and a new symbol mapping is designed in Section 4. The simulation results are described in Section 5. Finally, conclusions are summarized in Section 6.

2. System Model

In this scheme, three users (A, B, and C) transmit their information to a destination (D). Assume that all channels between users and the destination (uplink channels) are Rayleigh flat slowly fading channels, which remain constant over at least six slots. We consider multiple access channels as time-division multiple access (TD MA). Thus, these users transmit in their own slots, respectively. If symbols a_i, b_i and c_i, which take values from an M-ary alphabet $\{s_0, s_1, \ldots, s_{M-1}\}$, are transmitted from these users through three orthogonal channels, respectively, then the received baseband signals r_{1i}, r_{2i} and r_{3i} in the destination can be written as

$$r_{1i} = h_{AD} a_i + n_1 \quad \textbf{(1)}$$

$$r_{2i} = h_{BD} b_i + n_2 \quad \textbf{(2)}$$

$$r_{3i} = h_{CD} c_i + n_3. \quad \textbf{(3)}$$

where h_{AD}, h_{BD}, and h_{CD} are channel fading coefficients between users A, B, C, and the destination D, respectively, and n_1, n_2, and n_3 are additive noises. They are all modeled as independent complex zero-mean Gaussian random variables, and

$$\varepsilon\left\{|h_{AD}|^2\right\} = \varepsilon\left\{|h_{BD}|^2\right\} = \varepsilon\left\{|h_{CD}|^2\right\} = 1. \quad \textbf{(4)}$$

and

$$\varepsilon\left\{|n_1|^2\right\} = \varepsilon\left\{|n_2|^2\right\} = \varepsilon\left\{|n_3|^2\right\} = N_0 \quad \textbf{(5)}$$

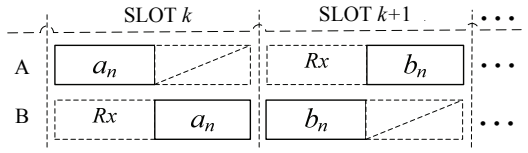

(a) System model of the baseline two-user cooperation scheme.

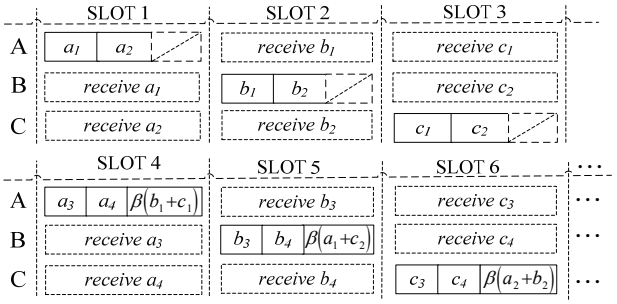

(b) System model of the proposed cooperation scheme.

Figure 1. System models of the baseline and the proposed cooperation schemes.

Note that ε denotes the expectation operator.

Simultaneously, each user receives the other users' information through the channels between users (inter-user channels) and relays its partners' information only if it decodes correctly, which can be determined by the cyclic redundancy check (CRC). The destination is assumed to be informed of whether relays decode correctly or not. Generally speaking, the user is close to its partners and they may have line-of-sight connections. Thus, the quality of inter-user channels is better than that of uplink channels. In this paper, we take inter-user channels to be additive white Gaussian noise (AWGN) when line-of-sight connections exist.

2.1. Baseline Scheme

The decode-and-forward cooperation scheme presented in [7] is regarded as a baseline scheme. The system model of two-user cooperation scheme is shown in Figure 1 (a). Each slot is divided into two segments with the same length of time. Each user transmits its own symbols in the first segment and remains inactive in the second segment. The partner receives these symbols in the first segment, and then retransmits these symbols by employing repetition coding in the second segment if it decodes correctly, otherwise, it remains inactive.

2.2. Proposed Scheme

The system model of the proposed cooperation scheme is shown in Figure 1(b). Each slot is divided into three segments with the same length of time. In the first slot, user A transmits its own symbols a_1 and a_2 in the first two segments, respectively, and remains inactive in the third segment. User B only detects a_1 in the first segment and user C only detects a_2 in the second segment. Coopera-

tion processes are similar in the second and third slots (see Figure 1(b)).

In the fourth slot, user A transmits its own symbols a_3 and a_4 in the first two segments, respectively, and the superposition symbol $\beta(b_1 + c_1)$ in the third segment if both of b_1 and c_1 are decoded correctly, where β is a power-normalizing scalar. In this paper, we set $\beta = \sqrt{2}/2$ to satisfy the transmit-power constraint. If user A can only decode the symbol of user B (or user C) correctly, then user A only retransmits b_1 (or c_1) instead of $\beta(b_1 + c_1)$ in the third segment. If neither of the symbols of user B and user C can be decoded correctly, then user A remains inactive in the third segment. User B detects a_3 in the first segment and user C detects a_4 in the second segment. Also, cooperation processes are similar in the fifth and sixth slots (see Figure 1(b)).

In the following slots, similar cooperation processes to those executed in the fourth to sixth slots are executed. In the last three slots, each user remains inactive in the first two segments and only retransmits the superposition symbol in the third segment.

Each user transmits its own symbols in two segments and serves as a relay for other users in only one segment. We assume that the total number of slots is large so that the loss of overhead in the first three slots can be neglected. Therefore, the bandwidth efficiency is only decreased by 1/3 compared to a non-cooperative diversity scheme.

In this scheme, symbols received from two different partners are superposed, and then the superposition symbols are retransmitted from the user. This can provide diversity order of two. However, if symbols received from each partner are superposed, respectively, and then retransmitted from the user, the diversity order of two will not be achieved.

3. Diversity Order

Assume that perfect channel state information is available in the receiver and ideal cooperation is considered, which means each user can always decode other users' information correctly. The maximum-likelihood (ML) decoder in the destination works with pairs of transmitted symbols instead of single symbols. Thus, the decoding complexity is higher, but it is still much lower than that of the schemes presented in [8−12].

Assume that M-PSK ($M \geq 4$) modulation is employed and Gray code is used to map bits to symbols. Without loss of generality, we consider the pair of symbols a_i and b_i, where $a_i, b_i \in \{s_0, s_1, \ldots, s_{M-1}\}$. Assume that a_i, b_i and $\frac{\sqrt{2}}{2}(a_i + b_i)$ are transmitted from user A, B and C, respectively, the corresponding received baseband signals are r_{1i}, r_{2i} and r_{3i}. The receiver computes the decision metric

$$\left|r_{1i} - h_{AD}a_i\right|^2 + \left|r_{2i} - h_{BD}b_i\right|^2 + \left|r_{3i} - \frac{\sqrt{2}h_{CD}(a_i + b_i)}{2}\right|^2 \quad \textbf{(6)}$$

over all possible pairs of symbols $\{a_i, b_i\}$, and a decision is made in favor of the pair of symbols that minimizes the metric.

There will be three cases for each decision.

case 0: The decision is correct.

case 1: The decision results in one symbol error.

case 2: The decision results in two symbol errors.

The probability of *case* 1 for each decision is

$$\begin{aligned}&\Pr(case\,1)\\ &= \Pr(a_i \text{ is decoded correctly}, b_i \text{ is decoded incorrectly})\\ &\quad + \Pr(a_i \text{ is decoded incorrectly}, b_i \text{ is decoded correctly})\end{aligned} \quad \textbf{(7)}$$

Equation (7) can be approximated as

$$\begin{aligned}\Pr(case\,1) \approx 2\varepsilon\Bigg\{&Q\left(\sqrt{\frac{\left(|h_{AD}|^2 + |h_{CD}|^2/2\right)d_{\min}^2}{2N_0}}\right)\\ &+ Q\left(\sqrt{\frac{\left(|h_{BD}|^2 + |h_{CD}|^2/2\right)d_{\min}^2}{2N_0}}\right)\Bigg\}\end{aligned} \quad \textbf{(8)}$$

where $Q(\cdot)$ is the Gaussian Q-function and d_{min} is the minimum Euclidean distance between pairs of signal points in the constellation. Let

$$\gamma = d_{\min}^2/(8N_0). \quad \textbf{(9)}$$

then (8) can be simplified as [19]

$$\Pr(case\,1) \approx 2 + 2\sqrt{\frac{\gamma}{1+\gamma}} - 4\sqrt{\frac{2\gamma}{1+2\gamma}}. \quad \textbf{(10)}$$

when $\gamma >> 1$, the probability is

$$\Pr(case\,1) \approx \frac{3}{8}\gamma^{-2} \quad \textbf{(11)}$$

If the receiver decides erroneously in favor of symbols a_i' ($a_i \neq a_i'$) and b_i' ($b_i \neq b_i'$), the value $a_i' + b_i'$ may be probably equal to the value $a_i + b_i$. Thus, the probability of *case* 2 for each decision can be upper-bounded as

$$\begin{aligned}\Pr(case\,2) &< 2\varepsilon\left\{Q\left(\sqrt{\frac{\left(|h_{AD}|^2 + |h_{BD}|^2\right)d_{\min}^2}{2N_0}}\right)\right\}\\ &= \frac{1}{2}\left(2 + \sqrt{\frac{2\gamma}{1+2\gamma}}\right)\left(1 - \sqrt{\frac{2\gamma}{1+2\gamma}}\right)^2\end{aligned} \quad \textbf{(12)}$$

when $\gamma >> 1/2$, we obtain

$$\Pr(case\ 2) < \frac{3}{32}\gamma^{-2} \tag{13}$$

From (11) and (13), we can conclude that each erroneous decision most results in one symbol error and the average BER for each user is approximated as

$$\begin{aligned} p_b &\approx \frac{1}{\log_2 M} \times \frac{1}{2} \Pr(case\ 1) \\ &\approx \frac{1}{\log_2 M} \times \frac{3}{16}\gamma^{-2} \end{aligned} \tag{14}$$

which shows that the diversity order of two is achieved.

In baseline decode-and-forward cooperation scheme, the average BER for each user is approximated as

$$p_b' \approx \frac{1}{\log_2 M} \times \frac{3}{32}\gamma^{-2}. \tag{15}$$

4. Design of Symbol Mapping

We observed from (14) and (15) that there is signal-to-noise ratio (SNR) loss for the proposed scheme compared to the baseline scheme. That is mainly because the power of the superposition symbol is equal to that of a single symbol transmitted in the first two segments in the proposed scheme. The total average energy for each symbol in the proposed scheme is 3/4 times as large as that in the baseline scheme. However, we can mitigate the SNR loss by exploiting symbol mapping diversity.

In most communication systems, multi-level modulation techniques such as *M*-PAM, *M*-PSK and *M*-QAM are employed to improve the bandwidth efficiency and the bit-to-symbol mapping for those modulation constellations is Gray code bit mapping. However, some enhanced Automatic Repeater request (ARQ) schemes [20−23] to extract additional diversity called symbol mapping diversity between retransmissions have been proposed. In those schemes, for exploiting the symbol mapping diversity, the bit-to-symbol mapping for the second transmission (first retransmission) is not Gray code bit mapping. For example, in the scheme proposed in [21], Gray code bit mapping is employed in the first transmission and another different symbol mapping is employed for maximizing the minimum combined squared Euclidean distance (CESD) [21] in the second transmission. The method proposed in [21] is further discussed in [22] and a symbol mapping diversity scheme in Multiple-Input Multiple-Output (MIMO) systems is presented in [23]. The symbol mapping diversity can provide great BER gains in AWGN and Rayleigh flat fading channels. In this paper, we design a new symbol mapping for superposition 8PSK modulation.

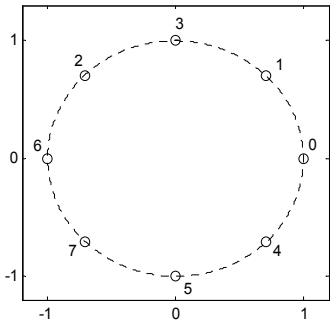

Figure 2. Signal constellation of 8PSK modulation.

The superposition symbols lead to a superposition modulation and we use Gray code bit mapping for 8PSK modulation and another symbol mapping for superposition modulation. The constellation of 8PSK modulation is showed in Figure 2. Each point represents an 8PSK symbol, which is labeled by 3 bits represented as an octal number. Since each erroneous decision most results in one symbol error and erroneous selection of an adjacent symbol, these distances between pairs of signal points, such as

$$\begin{Bmatrix} \{(s_i s_j \leftrightarrow s_i s_k)\} \\ \{(s_j s_i \leftrightarrow s_k s_i)\} \end{Bmatrix}, 0 \le i, j, k \le 7 \ and \ j \ne k. \tag{16}$$

which differ in only a symbol and two different symbols s_j and s_k are adjacent in 8PSK constellation, should be increased as large as possible in the superposition constellation. Based on this principle, the constellation of the superposition 8PSK modulation is designed and shown in Figure 3. Each point represents the superposition of two 8PSK symbols, which is labeled by 6 bits represented as two octal numbers.

5. Simulation Results

In the simulation, we assume that uplink channels are Rayleigh flat slowly fading channels. When we suppose that there exist line-of-sight connections, inter-user channels are assumed to be AWGN channels. Otherwise, inter-user channels are assumed to be Rayleigh flat slowly fading channels. In baseline decode-and-forward cooperation scheme, each user employs repetition coding to relay its partner's information. Set the symbol energy as *Es* and assume that all inter-user channels have equal average SNR and so do all uplink channels.

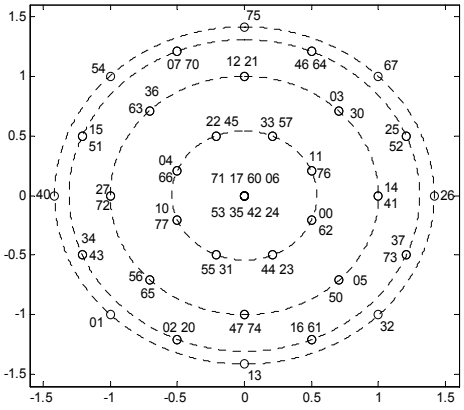

Figure 3. Signal constellation of superposition 8PSK modulation.

Figure 4 shows the simulation results of the BER performance versus the uplink SNR per symbol (Es/N_0) for ideal cooperation and real cooperation (all inter-user channels are assumed to be AWGN and they have equal average SNR=15 dB). All cooperative diversity schemes employ QPSK modulation with Gray code bit mapping and the non-cooperative diversity scheme employs BPSK modulation. Hence, the transmission rate is 4/3 bit /s/Hz for the proposed cooperation scheme and 1 bit/s/Hz for baseline cooperation scheme and the non-cooperative diversity scheme. The analysis result of the proposed scheme is also given and it matches the simulation result very well when Es/N_0 is large and they all indicate that the diversity order of two is achieved. It is shown that the performance of real cooperation is almost the same as that of ideal cooperation when inter-user channel SNR= 15 dB.

When line-of-sight connections do not exist, we take inter-user channels as Rayleigh flat slowly fading channels and set that inter-user channel SNR is always 10dB higher than uplink channel SNR. The similar simulation is performed, and the results of the BER performance are shown in Figure 5. It is observed that the results are similar to those in Figure 4.

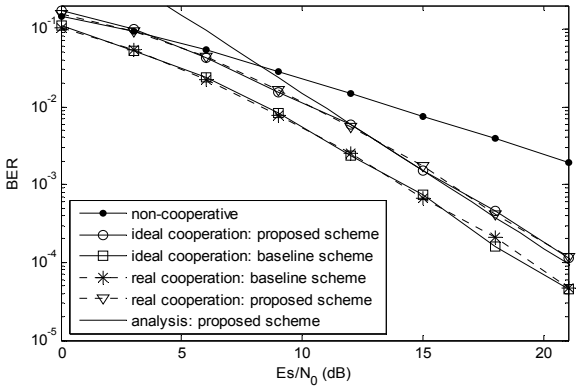

Figure 4. BER performance of ideal cooperation and real cooperation.

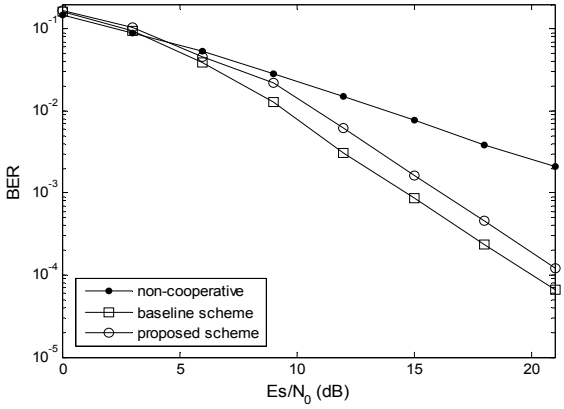

Figure 5. BER performance of cooperation schemes employing QPSK modulation and non-cooperative scheme employing BPSK modulation when inter-user channels are Rayleigh flat slowly fading channels.

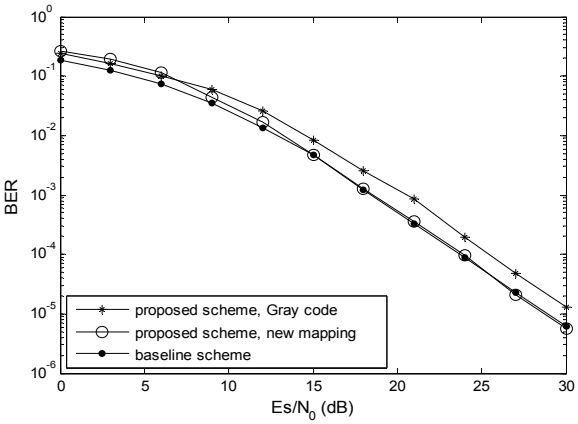

Figure 6. BER performance of cooperation schemes employing 8PSK modulation when inter-user channels are AWGN channels.

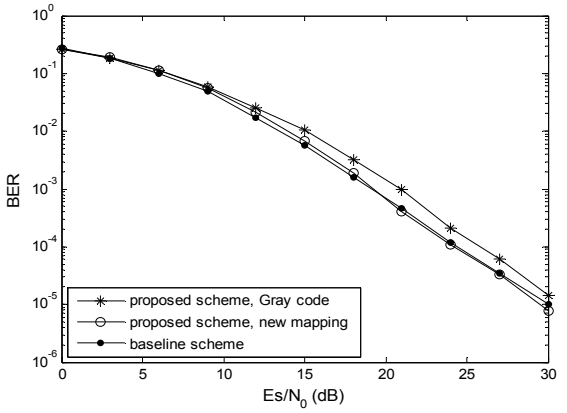

Figure 7. BER performance of cooperation schemes employing 8PSK modulation when inter-user channels are Rayleigh flat slowly fading channels.

Figure 6 shows the simulation results of the BER performance versus Es/N_0 for real cooperation (all inter-user channels are assumed to be AWGN and they have equal average SNR=20 dB). All schemes employ 8PSK modulation. It is shown that there is about 2 dB SNR loss for the proposed scheme employing Gray code bit mapping compared to the baseline scheme. However, using the new symbol mapping, a gain of about 2 dB can be obtained and the performance of the proposed scheme is similar to that of the baseline scheme when Es/N_0 is large.

When inter-user channels are Rayleigh flat slowly fading channels, the simulation is also performed and the results are shown in Figure 7. Also, the inter-user channel SNR is always 10dB higher than uplink channel SNR. The proposed scheme with proposed symbol mapping has similar performance with the baseline scheme, and they both outperform the proposed scheme without symbol mapping diversity.

6. Conclusions

A cooperative diversity scheme using superposition modulation is proposed and a new symbol mapping is

designed. The bandwidth efficiency of the proposed scheme is more efficient than that of the baseline decode-and-forward cooperation scheme because of superposition modulation. Moreover, it is demonstrated that the BER performance of the proposed scheme with the proposed symbol mapping is almost the same as that of the baseline cooperation scheme employing 8PSK modulation and the decoding complexity is moderate.

7. Acknowledgement

This work was supported by the Research Fund of National Mobile Communications Research Laboratory, Southeast University under Grant No. 2008A05, by the National Basic Research Program of China under Grant 2007CB310603, by China 863 Project under Grant No. 2007AA01Z2B1, and by NSFC Project under Grant No. 60802005.

9. References

[1] G. J. Foschini and M. J. Gans, "On limits of wireless communications in a fading environment when using multiple antennas," Wireless Personal Communications, Vol. 6, No. 3, pp. 311−335, 1998.

[2] E. Telatar, "Capacity of multi-antenna Gaussian channels," European Transactions on Telecommuni- cations, Vol. 10, No. 6, pp. 585−596, 1999.

[3] S. M. Alamouti, "A simple transmit diversity technique for wireless communications," IEEE Journal on Selected Areas in Communications, Vol. 16, No. 8, pp. 1451−1458, 1998.

[4] A. Sendonaris, E. Erkip, and B. Aazhang, "User cooperation diversity Part I: System description," IEEE Transactions on Communications, Vol. 51, No. 11, pp. 1927−1938, November 2003.

[5] A. Sendonaris, E. Erkip, and B. Aazhang, "User cooperation diversity Part II: Implementation aspects and performance analysis," IEEE Transactions on Communications, Vol. 51, No. 11, pp. 1939−1948, November 2003.

[6] A. Nosratinia, T. E. Hunter, and A. Hedayat, "Cooperative communication in wireless networks," IEEE Communications Magazine, Vol. 42, No. 10, pp. 74−80, October 2004.

[7] J. N. Laneman, D. N. C. Tse, and G. W. Wornell, "Cooperative diversity in wireless networks: Efficient protocols and outage behavior," IEEE Transactions on Information Theory, Vol. 50, No. 12, pp. 3062−3080, December 2004.

[8] J. N. Laneman and G. W. Wornell, "Distributed space-time-coded protocols for exploiting cooperative diversity in wireless networks," IEEE Transactions on Information Theory, Vol. 49, No. 10, pp. 2415−2425, October 2003.

[9] O. Shalvi, "Multiple source cooperation diversity," IEEE Communications Letters, Vol. 8, No. 12, pp. 712−714, December 2004.

[10] R. Q. Wang, W. L. Zhao, and G. B. Giannakis, "Multi-source cooperative networks with distributed convolutional coding," 2005 Conference Record of the Thirty-Ninth Asilomar Conference on Signals, Systems and Computers, pp. 1056−1060, 2005.

[11] R. Q. Wang, W. L. Zhao, and G. B. Giannakis, "Distributed trellis coded modulation for multi-source cooperative networks," Radio and Wireless Symposium, 2006 IEEE, San Diego, CA, pp. 271−274, January 2006.

[12] R. Q. Wang and G. B. Giannakis, "Complex field coding in multi-source cooperative networks for full diversity," 2006 IEEE International Conference on Communications, Vol. 10, pp. 4485−4488, June 2006.

[13] E. G. Larsson and B. R. Vojcic, "Cooperative transmit diversity based on superposition modulation," IEEE Communications Letters, Vol. 9, No. 9, pp. 778−780, September 2005.

[14] Z. G. Ding, T. Ratnarajah, and C. Cowan, "On the performance of superposition cooperative diversity in wireless networks," 2006 IEEE International Symposium on Information Theory, pp. 2714−2718, July 2006.

[15] K. Ishii, "Cooperative transmit diversity utilizing superposition modulation," Radio and Wireless Symposium, 2007 IEEE, pp. 337−340, January 2007.

[16] Z. G. Ding, T. Ratnarajah, and C. C. F. Cowan, "On the divesity-multiplexing tradeoff for wireless cooperative multiple access systems," IEEE Transactions on Signal Processing, Vol. 55, No. 9, pp. 4627−4638, September 2007.

[17] L. Xiao, T. E. Fuja, J. Kliewer, and D. J. Costello, "Cooperative diversity based on code superposition," 2006 IEEE International Symposium on Information Theory, pp. 2456−2460, July 2006.

[18] V. Mahinthan, J. W. Mark, and X. M. Shen, "A cooperative diversity scheme based on quadrature signaling," IEEE Transaction on Wireless Communications, Vol. 6, No. 1, pp. 41−45, January 2007.

[19] M. K. Simon and M. Alouini, "A unified approach to the performance analysis of digital communication over generalized fading channels," Proceedings of IEEE, Vol. 86, No. 9. pp. 1860−1877, September 1998.

[20] C. Wengerter, A. G. Edler von Elbwart, E. Seidel, G. Velev, and M. P. Schmitt, "Advanced hybrid ARQ technique empolying a signal constellation rearrangement," in Proceedings of IEEE VTC 2002 Fall, Vol. 4, pp. 2002−2006, September 2002.

[21] H. Samra, Z. Ding, and P. M. Hahn, "Symbol mapping diversity design for multiple packet transmissions," IEEE Transactions on Communications, Vol. 53, No. 5, May 2005.

[22] M. Gidlund, "Performance of hybrid ARQ scheme based on bit-to-symbol mapping," 2008 IET International Conference on Wireless, Mobile and Multimedia Networks, pp. 303−306, January 2008.

[23] S. H. Moon, H. H. Park, A. Goldsmith, and M. S. Oh, "Bit rearrangement for MIMO retransmissions," Global Telecommunications Conference, 2007, GLOBECOM '07 IEEE, pp. 3509–3513, November 2007.

Wireless Sensor Network, 2009, 1, 1-60
Published Online April 2009 in SciRes (http://www.SciRP.org/journal/wsn/).

The Influence of LOS Components on the Statistical Properties of the Capacity of Amplify-and-Forward Channels

Gulzaib RAFIQ, Matthias PÄTZOLD
Faculty of Engineering and Science, University of Agder, Grimstad, Norway
E-mail: {gulzaib.rafiq, matthias.paetzold}@uia.no
Received February 26, 2009; *revised March* 5, 2009; *accepted March* 7, 2009

Abstract

Amplify-and-forward channels in cooperative networks provide a promising improvement in the network coverage and system throughput. Under line-of-sight (LOS) propagation conditions in such cooperative networks, the overall fading channel can be modeled by a double Rice process. In this article, we have studied the statistical properties of the capacity of double Rice fading channels. We have derived the analytical expressions for the probability density function (PDF), cumulative distribution function (CDF), level-crossing rate (LCR), and average duration of fades (ADF) of the channel capacity. The obtained results are studied for different values of the amplitudes of the LOS components in the two links of double Rice fading channels. It has been observed that the statistics of the capacity of double Rice fading channels are quite different from those of double Rayleigh and classical Rice fading channels. Moreover, the presence of an LOS component in any of the two links increases the mean channel capacity and the LCR of the channel capacity. The validity of the theoretical results is confirmed by simulations. The results presented in this article can be very useful for communication system designers to optimize the performance of cooperative networks in wireless communication systems.

Keywords: Amplify-and-Forward Channels, Channel Capacity, Cooperative Networks, Line-of-Sight Component, Double Rice Process, Double Rayleigh Process, Level-Crossing Rate, Average Duration of Fades

1. Introduction

Increased network coverage, improved link quality, and provision of new applications with increased mobility support are the basic demands imposed on future wireless communication systems. One promising solution to fullfil these requirements is the use of cooperative diversity techniques [1−3]. Single-antenna mobile stations in cooperative networks assist each other to relay the transmitted signal from the source mobile station (SMS) to the destination mobile station (DMS). The cooperation of single-antenna mobile stations in such networks to share their antennas for transmission of the signal makes it possible to form the so-called virtual multiple-input multiple-output (MIMO) system [4], thus, achieving the diversity gain. Moreover, such cooperation between mobile stations results in increased network coverage with enhanced mobility support.

For the development and analysis of wireless communication systems that exploit cooperative diversity, a solid knowledge of the multipath fading channel characteristics is required. Recent studies illustrate that mobile-to-mobile (M2M) fading channels associated with relay-based cooperative networks under non-line-of-sight (NLOS) propagation conditions in different propagation scenarios can be modeled either as a double Rayleigh process [5−8] or an NLOS second-order scattering (NLSS) process [9]. On the other hand, different scenarios under LOS propagation conditions lead to modeling the overall M2M fading channel either by a double Rice process [10], a single-LOS double-scattering (SLDS) process [11], a single-LOS second-order scattering (SLSS) process [9], or a multiple-LOS second-order scattering (MLSS) process [12,13]. These studies provide results for the statistical characterization of M2M fading channels in cooperative networks under different propagation conditions. The impact of double Rayleigh fading on the performance of a communication system is investigated in [14]. Even with all this research going on,

February 26, 2009. The material in this paper is based on "On the Statistical Properties of the Capacity of Amplify-and-Forward Channels Under LOS Conditions", by Gulzaib Rafiq and Matthias Pätzold which appeared in the proceedings of 11th IEEE International Conference on Communications Systems, ICCS 2008, Guangzhou, China, November 2008.

the important question regarding the maximum possible information transfer rate in such fading channels is still unanswered. Thus, the purpose of this paper is to fill in this gap in information regarding the capacity of amplify-and -forward channels in cooperative networks.

Studies pertaining to the analysis of the outage capacity of double Rayleigh channels can be found in [15,16]. However, to the best of the authors' knowledge, the statistical properties of the capacity of double Rice channels have never been investigated. The analysis of the statistical properties of the channel capacity can be very helpful to study the dynamic behavior of the channel capacity. Here, the statistical properties of interest include the PDF, CDF, LCR, and ADF of the channel capacity. The PDF and CDF of the channel capacity provide the information regarding mean value and variance of the channel capacity. The LCR and ADF of the channel capacity, on the other hand, give a deep insight into the temporal variations of the channel capacity [17]. The LCR of the channel capacity is a measure of the rate at which the channel capacity crosses a certain threshold level from up to down or vice versa. However, the ADF of the channel capacity is defined as the average duration of time over which the channel capacity is below a certain threshold level [18,19].

In this paper, we have investigated the statistical properties of the capacity of amplify-and-forward channels in cooperative networks. The transmitted signal from the SMS is received at the DMS via a mobile relay (MR). The MR amplifies the received signal and forwards it to the DMS. We have assumed that there is no direct transmission link between the SMS and the DMS. Moreover, it is also assumed that the LOS components exist in both of the transmission links, i.e., the SMS-MR and MR-DMS links. Hence, the overall fading channel is modeled by a double Rice process [10]. We have derived exact analytical expressions for the PDF, CDF, LCR, and ADF of the channel capacity of double Rice channels. The results are studied for different values of the amplitudes of the LOS components in the two transmission links of double Rice channels. It has been observed that the statistics of the capacity of double Rice channels are quite different from those of double Rayleigh and classical Rice/Rayleigh channels. Specifically, for medium and high signal levels, the presence of LOS components in the two cascaded transmission links increases the mean channel capacity and the LCR of the channel capacity. However, it results in a decrease in the ADF of the channel capacity.

The rest of the paper is organized as follows. In Section 2, we describe briefly the double Rice channel model and some of its statistical properties. The statistical properties of the capacity of double Rice channels are studied in Section 3. Section 4 presents the statistical properties of the capacity of double Rayleigh channels. Numerical results are discussed in Section 5. Finally, the concluding remarks are given in Section 6.

2. The Double Rice Channel Model

In cooperative networks employing amplify-and-forward relay, the channel between the SMS and the DMS via a MR can be represented as a concatenation of the SMS-MR and MR-DMS channels [8,10]. Figure 1 depicts an example of the transmission link from the SMS to the DMS via the MR in such amplify-and-forward relay-based networks. For the case when an LOS component is present in both of the transmission links, i.e., the SMS-MR link and the MR-DMS link, the overall fading channel can be modeled as a product of two non-zero- mean complex Gaussian processes given by [10].

$$\chi(t) = A_{\mathrm{MR}}\,\mu_{\rho}^{(2)}(t)\mu_{\rho}^{(1)}(t) \tag{1}$$

where A_{MR} is a real positive constant representing the relay gain and $\mu_{\rho}^{(i)}(t) = \mu^{(i)}(t) + m^{(i)}(t) \quad (i = 1,2)$ models the fading in the ith link. Here, $\mu^{(i)}(t)$ denotes the scattered component and $m^{(i)}(t)$ is the LOS component. The scattered component $\mu^{(i)}(t)$ can be modeled in the complex baseband as a complex Gaussian process with zero mean and variance $2\sigma_i^2$, i.e., $\mu^{(i)}(t) = \mu_1^{(i)}(t) + j\mu_2^{(i)}(t)$ where, $\mu_1^{(i)}(t)$ and $\mu_2^{(i)}(t)$ are the underlying zero-mean real-valued Gaussian processes. The LOS component $m^{(i)}(t)$ having amplitude ρ_i, Doppler frequency f_{ρ_i}, and phase θ_{ρ_i} i can be expressed as $m^{(i)}(t) = \rho_i e^{j(2\pi f_{\rho i}t + \theta_{\rho i})}$. Let $f_{\rho_{\mathrm{SMS}}}$, $f_{\rho_{\mathrm{MR}}}$, and $f_{\rho_{\mathrm{DMS}}}$ represent the respective Doppler frequencies of the SMS, MR, and DMS, then it can be easily observed from Figure 1 that $f_{\rho_1} = f_{\rho_{\mathrm{SMS}}} + f_{\rho_{\mathrm{MR}}}$ and $f_{\rho_2} = f_{\rho_{\mathrm{MR}}} + f_{\rho_{\mathrm{DMS}}}$. The envelope of the process $\chi(t)$ in (1) results in a double Rice process given by [10]

$$\begin{aligned}\Xi(t) &= |\,\chi(t)\,| = |\,A_{\mathrm{MR}}\mu_{\rho}^{(1)}(t)\mu_{\rho}^{(2)}(t)\,| \\ &= A_{\mathrm{MR}}\,\xi_1(t)\,\xi_2(t)\end{aligned} \tag{2}$$

where $\xi_i(t) \quad (i = 1,2)$ represents the classical Rice process.

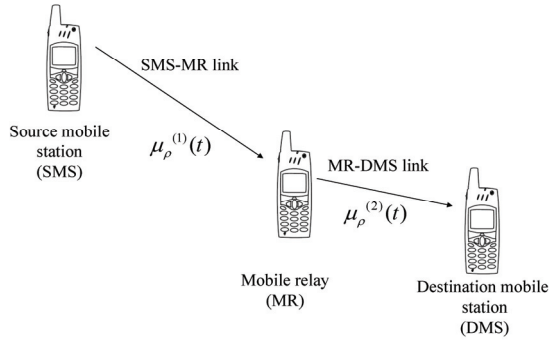

Figure 1. The propagation scenario describing double Rice fading channels.

The PDF of double Rice processes $\Xi(t)$ is given by [10]

$$p_{\Xi}(z)=\frac{z}{\sigma_1^2\sigma_{\mathrm{MR}}^2}\int_0^{\infty}\frac{1}{y}e^{-\frac{(z/y)^2+\rho_1^2}{2\sigma_1^2}}e^{-\frac{y^2+\rho_{\mathrm{MR}}^2}{2\sigma_{\mathrm{MR}}^2}} I_0\left(\frac{z\rho_1}{y\sigma_1^2}\right)I_0\left(\frac{y\rho_{\mathrm{MR}}}{\sigma_{\mathrm{MR}}^2}\right)dy,\quad z\ge 0 \tag{3}$$

where $I_0(\cdot)$ is the modified Bessel function of the first kind of order zero [20], $\sigma_{\mathrm{MR}}^2=(A_{\mathrm{MR}}\sigma_2)^2$, and $\rho_{\mathrm{MR}}=A_{\mathrm{MR}}\rho_2$.

In order to derive the expressions for the statistical properties of the capacity of double Rice channels, we need the PDF $p_{\Xi^2}(z)$ of the squared process $\Xi^2(t)$ as well as the joint PDF $p_{\Xi^2\dot{\Xi}^2}(z,\dot{z})$ of $\Xi^2(t)$ and its time derivative $\dot{\Xi}^2(t)$[1]. The joint $p_{\Xi^2\dot{\Xi}^2}(z,\dot{z})$ can be found using the joint PDF $p_{\Xi\dot{\Xi}}(z,\dot{z})$ [10] and by using the concept of transformation of random variables [21] as

$$\begin{aligned}p_{\Xi^2\dot{\Xi}^2}(z,\dot{z})&=\frac{1}{4z}p_{\Xi\dot{\Xi}}\left(\sqrt{z},\frac{\dot{z}}{2\sqrt{z}}\right)\\&=\frac{1}{\sqrt{2\pi z}(4\pi\sigma_1\sigma_{\mathrm{MR}})^2}\int_0^{\infty}\frac{1}{\sqrt{\beta_1y^4+\beta_2z}}e^{-\frac{z/y^2+\rho_1^2}{2\sigma_1^2}}e^{-\frac{y^2+\rho_{\mathrm{MR}}^2}{2\sigma_{\mathrm{MR}}^2}}\int_{-\pi}^{\pi}e^{-\frac{y\rho_{\mathrm{MR}}\cos\theta_2}{\sigma_{\mathrm{MR}}^2}}\int_{-\pi}^{\pi}e^{-\frac{1}{2}K^2(\sqrt{z},y,\theta_1,\theta_2)}\\&\quad\times e^{-\frac{(\sqrt{z}/y)\rho_1\cos\theta_1}{\sigma_1^2}}e^{-\frac{(y\dot{z})^2}{8z(\beta_1y^4+\beta_2z)}-\frac{y\dot{z}}{2\sqrt{\beta_1zy^4+\beta_2z^2}}K(\sqrt{Z},Y,\theta_1,\theta_2)}d\theta_1d\theta_2dy,\quad z\ge 0,|\dot{z}|<\infty\end{aligned} \tag{4}$$

where

$$\beta_1=2(\pi\sigma_1)^2(f_{\max_1}^2+f_{\max_2}^2) \tag{5}$$

$$\beta_2=2(\pi\sigma_{\mathrm{MR}})^2(f_{\max_2}^2+f_{\max_3}^2) \tag{6}$$

and

$$K(z,y,\theta_1,\theta_2)=\frac{2\pi\rho_1f_{\rho_1}y^2\sin\theta_1+2\pi\rho_{\mathrm{MR}}f_{\rho_2}z\sin\theta_2}{\sqrt{\beta_1zy^4+\beta_2z^2}}. \tag{7}$$

Here $f_{\max_1}$, $f_{\max_2}$, and $f_{\max_3}$ denote the maximum Doppler frequencies of the SMS, MR and DMS, respectively. The expression for the PDF $p_{\Xi^2}(z)$ can be obtained by integrating the joint PDF $p_{\Xi^2\dot{\Xi}^2}(z,\dot{z})$ over $\dot{z}$. Alternatively, in our case the PDF $p_{\Xi^2}(z)$ can also be found from the PDF $p_{\Xi}(z)$ in (3) using the concept of transformation of random variables [21] as

$$\begin{aligned}p_{\Xi^2}(z)&=\frac{1}{2\sqrt{z}}p_{\Xi}(\sqrt{z})\\&=\frac{1}{2\sigma_1^2\sigma_{\mathrm{MR}}^2}\int_0^{\infty}\frac{1}{y}e^{-\frac{z/y^2+\rho_1^2}{2\sigma_1^2}}e^{-\frac{y^2+\rho_{\mathrm{MR}}^2}{2\sigma_{\mathrm{MR}}^2}} I_0\left(\frac{\sqrt{z}\rho_1}{y\sigma_1^2}\right)I_0\left(\frac{y\rho_{\mathrm{MR}}}{\sigma_{\mathrm{MR}}^2}\right)dy,\quad z\ge 0.\end{aligned} \tag{8}$$

In the next section, we will derive the statistical properties of the capacity of double Rice channels using the results found in this section.

[1]Throughout this paper, we will represent the time derivative of a process by an overdot.

3. Statistical Properties of the Capacity of Double Rice Channels

The instantaneous capacity $C(t)$ of double Rice channels can be expressed using a similar formula found in [22] as

$$\begin{aligned}C(t)&=\log_2\left(1+\gamma_s|\Xi(t)|^2\right)\\&=\log_2\left(1+\gamma_s\Xi^2(t)\right)\ (\text{bits/s/Hz})\end{aligned} \tag{9}$$

where γ_s denotes the average received signal-to-noise ratio (SNR) at the DMS. Equation (9) can be considered as a mapping of a random process $\Xi(t)$ to another random process $C(t)$. Hence, the expressions for the statistical properties of the channel capacity $C(t)$ can be derived by using the results for the statistical properties of the process $\Xi(t)$ obtained in the previous section. The PDF $p_C(r)$ of the channel capacity $C(t)$ can be found using (8), (9), and by applying the concept of transformation of random variables as

$$\begin{aligned}p_C(r)&=\frac{2^r\ln(2)}{\gamma_s}p_{\Xi^2}\left(\frac{2^r-1}{\gamma_s}\right)\\&=\frac{2^r\ln(2)}{2\gamma_s\sigma_1^2\sigma_{\mathrm{MR}}^2}\int_0^{\infty}\frac{1}{y}e^{-\frac{2^r-1/\gamma_s,y^2+\rho_1^2}{2\sigma_1^2}}e^{-\frac{y^2+\rho_{\mathrm{MR}}^2}{2\sigma_{\mathrm{MR}}^2}} I_0\left(\frac{\sqrt{2^r-1}\rho_1}{y\sqrt{\gamma_s}\sigma_1^2}\right)I_0\left(\frac{y\rho_{\mathrm{MR}}}{\sigma_{\mathrm{MR}}^2}\right)dy,\ r\ge 0.\end{aligned} \tag{10}$$

The CDF $F_C(r)$ of the channel capacity $C(t)$ can now be obtained by solving the integral given by

$$F_C(r) = \int_0^r p_C(z)dz. \tag{11}$$

By substituting (10) in (11) and doing some mathematical manipulations, the CDF of the channel capacity can be expressed as follows

$$F_C(r) = 1 - \frac{1}{\sigma_{\mathrm{MR}}^2}\int_0^\infty y e^{-\frac{y^2+\rho_{\mathrm{MR}}^2}{2\sigma_{\mathrm{MR}}^2}} I_0\left(\frac{y\rho_{\mathrm{MR}}}{\sigma_{\mathrm{MR}}^2}\right) Q_1\left(\frac{\rho_1}{\sigma_1}, \frac{\sqrt{2^r-1}}{y\sqrt{\gamma_s}\sigma_1}\right) dy, \quad r \geq 0 \tag{12}$$

where $Q_1(\cdot,\cdot)$ is the generalized Marcum Q-function [20]. The LCR $N_C(r)$ of the channel capacity $C(t)$ is defined as [19]

$$N_C(r) = \int_0^\infty \dot{z}\, p_{C\dot{C}}(r,\dot{z})\, d\dot{z}, \quad r \geq 0 \tag{13}$$

where $p_{C\dot{C}}(z,\dot{z})$ represents the joint PDF of $C(t)$ and its time derivative $\dot{C}(t)$. The joint PDF $p_{C\dot{C}}(z,\dot{z})$ can be obtained from the joint PDF $p_{\Xi^2\dot{\Xi}^2}(z,\dot{z})$ by applying again the concept of transformation of random variables as

$$\begin{aligned} p_{C\dot{C}}(z,\dot{z}) &= \left(\frac{2^z \ln(2)}{\gamma_s}\right)^2 p_{\Xi^2\dot{\Xi}^2}\left(\frac{2^z-1}{\gamma_s}, \frac{2^z \dot{z}\ln(2)}{\gamma_s}\right) \\ &= \frac{\left(2^z\ln(2)\right)^2\left(2^z-1\right)^{-1/2}}{(4\pi)^2\sqrt{2\pi}\gamma_s^{3/2}\sigma_1^2\sigma_{\mathrm{MR}}^2}\int_0^\infty \frac{e^{-\frac{2^z-1/\gamma_s y^2+\rho_1^2}{2\sigma_1^2}}}{\sqrt{\beta_1 y^4+\beta_2\left(2^z-1/\gamma_s\right)}} e^{-\frac{y^2+\rho_{\mathrm{MR}}^2}{2\sigma_{\mathrm{MR}}^2}} \int_{-\pi}^{\pi} e^{-\frac{y\rho_{\mathrm{MR}}\cos\theta_2}{\sigma_{\mathrm{MR}}^2}} \int_{-\pi}^{\pi} e^{-\frac{\sqrt{2^z-1/\gamma_s y^2}\rho_1\cos\theta_1}{\sigma_1^2}} \\ &\quad \times e^{-\frac{\left(y\dot{z}\ln(2)2^z\right)^2\left(2^z-1\right)^{-1}}{8\left(\gamma_s\beta_1 y^4+\beta_2\left(2^z-1\right)\right)}} e^{-\frac{y\dot{z}\ln(2)2^z\left(2^z-1\right)^{-1/2}}{2\sqrt{\gamma_s\beta_1 y^4+\beta_2\left(2^z-1\right)}}K\left(\sqrt{\frac{2^z-1}{\gamma_s}},y,\theta_1,\theta_2\right)} e^{-\frac{1}{2}K^2\left(\sqrt{\left(2^z-1/\gamma_s\right)},y,\theta_1,\theta_2\right)} d\theta_1\, d\theta_2 dy \end{aligned} \tag{14}$$

for $z \geq 0$, $|\dot{z}| < \infty$, where $K(\cdot,\cdot,\cdot,\cdot)$ is defined in (7). After substituting (14) in (13) and carrying out some algebraic calculations, we obtain

$$\begin{aligned} N_C(r) &= \frac{\sqrt{2^r-1}}{(2\pi)^{5/2}\sqrt{\gamma_s}\sigma_1^2\sigma_{\mathrm{MR}}^2}\int_0^\infty \sqrt{\beta_1+\beta_2\left(\frac{2^r-1}{y^4\gamma_s}\right)} e^{-\frac{2^r-1/\gamma_s y^2+\rho_1^2}{2\sigma_1^2}} e^{-\frac{y\rho_{\mathrm{MR}}\cos\theta_2}{\sigma_{\mathrm{MR}}^2}} \int_{-\pi}^{\pi} e^{-\frac{\sqrt{2^r-1/\gamma_s y^2}\rho_1\cos\theta_1}{\sigma_1^2}} \\ &\quad \times \int_{-\pi}^{\pi}\left[1+\sqrt{\frac{\pi}{2}}\; e^{\frac{1}{2}K^2\left(\sqrt{\left(2^r-1/\gamma_s\right)},y,\theta_1,\theta_2\right)}\; K\left(\sqrt{\frac{2^r-1}{\gamma_s}},y,\theta_1,\theta_2\right)\left\{1+\Phi\left(\frac{K\left(\sqrt{\frac{2^r-1}{\gamma_s}},y,\theta_1,\theta_2\right)}{\sqrt{2}}\right)\right\}\right] \\ &\quad \times e^{-\frac{y^2+\rho_{\mathrm{MR}}^2}{2\sigma_{\mathrm{MR}}^2}} e^{-\frac{1}{2}K^2\left(\sqrt{\left(2^r-1/\gamma_s\right)},y,\theta_1,\theta_2\right)} d\theta_1 d\theta_2 dy,\; r \geq 0 \end{aligned} \tag{15}$$

where $\Phi(\cdot)$ denotes the error function [20]. Finally, from (15) and (12), the ADF $T_C(r)$ of the channel capacity $C(t)$ can be obtained using [19]

$$T_C(r) = \frac{F_C(r)}{N_C(r)}. \tag{16}$$

The results found in this section will be used in the following section to derive the statistical properties of the capacity of double Rayleigh channels.

4. Statistical Properties of the Capacity of Double Rayleigh Channels

The double Rayleigh channel follows as a special case of

the double Rice channel when $\rho_i \to 0$ $(i=1,2)$. Hence, by letting $\rho_i \to 0$ $(i=1,2)$ in (10), (12), and (15), the PDF, CDF, and LCR of the channel capacity of double Rayleigh channel can be expressed as

$$p_C(r)\Big|_{\rho_i\to 0} = \frac{2^r \ln(2)}{2\gamma_s \sigma_1^2 \sigma_{\mathrm{MR}}^2} \int_0^\infty \frac{1}{y} e^{-\frac{2^r-1}{2\sigma_1^2\gamma_s y^2}} e^{-\frac{y^2}{2\sigma_{\mathrm{MR}}^2}} dy,\ r \geq 0 \tag{17}$$

$$F_C(r)\Big|_{\rho_i\to 0} = 1 - \frac{1}{\sigma_{\mathrm{MR}}^2} \int_0^\infty y e^{-\frac{y^2}{2\sigma_{\mathrm{MR}}^2}} e^{-\frac{2^r-1}{2\sigma_1^2\gamma_s y^2}} dy,\ r \geq 0 \tag{18}$$

and

$$N_C(r)\Big|_{\rho_i\to 0} = \frac{\sqrt{2^r-1}}{\sqrt{2\pi\gamma_s}\sigma_1^2\sigma_{\mathrm{MR}}^2} \int_0^\infty \sqrt{\beta_1 + \beta_2\left(\frac{2^r-1}{y^4\gamma_s}\right)} e^{-\frac{2^r-1}{2\sigma_1^2\gamma_s y^2}} e^{-\frac{y^2}{2\sigma_{\mathrm{MR}}^2}} dy,\ r \geq 0 \tag{19}$$

respectively. The ADF of the channel capacity $C(t)$ of double Rayleigh channel can be found using (16), (18), and (19).

5. Statistical Properties of the Capacity of Rayleigh and Rice Channels

In this section, we will present the PDF, CDF, and LCR of the capacity of Rayleigh and Rice channels. We will study these results along with the statistical properties of the capacity of double Rice channels in the next section for comparison purposes. The PDF $p_C(r)$ of the capacity $C(t)$ of Rice channels can be found using the PDF $p_{\xi^2}(r)$ of the squared Rice process $\xi^2(t)$ and by employing the expression presented in (9) corresponding to Rice processes $\xi(t)$ as

$$p_C(r) = \frac{2^r \ln(2)}{\gamma_s} p_{\xi^2}\left(\frac{2^r-1}{\gamma_s}\right) = \frac{2^r \ln(2)}{2\gamma_s\sigma_0^2} e^{-\frac{2^r-1+\gamma_s\rho^2}{2\sigma_0^2\gamma_s}} I_0\left(\sqrt{\frac{\left(2^r-1\right)\rho^2}{\sigma_0^4\gamma_s}}\right),\quad r \geq 0 \tag{20}$$

where ρ represent the amplitude of the LOS component and σ_0^2 denotes the variance of the underlying Gaussian processes. By substituting (20) in $F_C(r) = \int_0^r p_C(x)dx$, the CDF $F_C(r)$ of the capacity of $C(t)$ of Rice channels can be written as

$$F_C(r) = 1 - Q_1\left(\frac{\rho}{\sigma_0}, \sqrt{\frac{\left(2^r-1\right)}{\sigma_0^2\gamma_s}}\right),\quad r \geq 0 \tag{21}$$

By solving $N_C(r) = \int_0^\infty p_{C\dot{C}}(r,\dot{z})d\dot{z}$, the LCR $N_C(r)$ of the capacity of $C(t)$ of Rice channels can be represented by

$$N_C(r) = \sqrt{\frac{\left(2^r-1\right)\beta}{\pi 2\sigma_0^4\gamma_s}} e^{-\frac{2^r-1+\gamma_s\rho^2}{2\sigma_0^2\gamma_s}} I_0\left(\sqrt{\frac{\left(2^r-1\right)}{\sigma_0^4\gamma_s/\rho^2}}\right),\quad r \geq 0 \tag{22}$$

where β under isotropic scattering conditions is given by $\beta = 2\left(\pi f_{\max}\sigma_0\right)^2$. Here, $p_{C\dot{C}}(z,\dot{z})$ represents the joint PDF of the capacity $C(t)$ and its time derivative $\dot{C}(t)$ and $f_{\max}$ denotes the maximum Doppler frequency.

The results for the PDF, CDF, and LCR of the capacity $C(t)$ of Rayleigh channels can be obtained from (20)−(22), respectively, by letting $\rho \to 0$ as follows:

$$p_C(r)\Big|_{\rho\to 0} = \frac{2^r \ln(2)}{2\gamma_s\sigma_0^2} e^{-\left(\frac{2^r-1}{2\gamma_s\sigma_0^2}\right)},\ r \geq 0 \tag{23}$$

$$F_C(r)\Big|_{\rho\to 0} = 1 - e^{-\left(\frac{2^r-1}{2\gamma_s\sigma_0^2}\right)},\ r \geq 0 \tag{24}$$

$$N_C(r)\Big|_{\rho\to 0} = \frac{1}{\sigma_0^2}\sqrt{\frac{\beta\left(2^r-1\right)}{2\pi\gamma_s}} e^{-\left(\frac{2^r-1}{2\gamma_s\sigma_0^2}\right)},\ r \geq 0. \tag{25}$$

The expressions (23)−(25) have already been presented in [23, Equations (23−25)]. However, we have presented these equations here for the sake of completeness.

6. Numerical Results

This section aims at the validation and analysis of the analytical results presented in the previous section, using simulations. We have also included the results for double Rayleigh, classical Rayleigh [19], and classical Rice channels in our study for comparison purposes. For the case of classical Rice channels, we denote the amplitude of the LOS component as ρ. The Rice processes $\mu_\rho^{(i)}(t) = \mu^{(i)}(t) + m^{(i)}(t)$ $(i=1,2)$ were simulated using the sum-of-sinusoids model [24]. The model parameters were computed using the generalized method of exact Doppler spread (GMEDS$_1$) [25]. The number of sinusoids ($N_1^{(i)}$ and $N_2^{(i)}$) for the resulting deterministic processes $\tilde{\mu}_1^{(i)}(t)$ and $\tilde{\mu}_2^{(i)}(t)$ in GMEDS$_1$ were chosen to be $N_1^{(i)} = N_2^{(i)} = 20$ for $i=1,2$, respectively. The maximum Doppler frequencies $f_{\max_2}$ and $f_{\max_3}$ were taken to be 91 and 125 Hz, respectively. We have assumed that the Doppler frequency $f_{\rho_{\mathrm{SMS}}}$ equals 0. Unless stated otherwise, the values of the Doppler fre-

quencies $f_{\rho_{\mathrm{MR}}}$ and $f_{\rho_{\mathrm{DMS}}}$ were set to be equal to $f_{\max_2}$ and $f_{\max_3}$, respectively. The SNR γ_s was set to 20 dB. The parameters A_{MR} and σ_i $(i=1,2)$ were chosen to be unity. Finally, using (2) and (9) the simulation results for the statistical properties of the channel capacity were found.

The PDF $p_{\Xi}(z)$ of double Rice processes $\Xi(t)$ are shown in Figure 2 for different values of the amplitudes of the LOS components ρ_i $(i=1,2)$. In Figure 2, the PDF of the double Rayleigh process is also shown, which represents a special case of the double Rice process when $\rho_1=\rho_2=0$. It is observed that the presence of the LOS components has a dominant effect on the mean value and spread of the PDF of double Rice processes. It can also be seen that the PDF of double Rice processes is identical for the cases $\rho_2=0$; $\rho_1=2$ and $\rho_2=2$; $\rho_1=0$.

Figures 3 and 4 present the PDF and CDF of the capacity of double Rice channels, respectively. It is observed that the amplitude of the LOS component has a significant influence on the PDF and CDF of the channel capacity. Specifically, the presence of an LOS component in one or both of the links (i.e., the SMS-MR and MR-DMS links) increases the mean channel capacity. Hence, double Rayleigh channels have a lower mean channel capacity compared to double Rice channels, (e.g., when $\rho_2=\rho_1=2$). It is also observed that the capacity of classical Rice channels has a lower mean value compared to that of double Rice channels. These facts are specifically studied in Figure 5, where the mean channel capacity of classical Rice as well as double Rice channels is studied for different values of the amplitudes of the LOS component. Figure 6 shows the influence of the amplitude of LOS component on the variance of the classical Rice and double Rice channels. It is observed that increasing the value of ρ decreases the spread of the channel capacity for medium and large values of ρ, say $\rho\geq 1$. Moreover, the variance of the capacity of double Rice channels is much higher as compared to that of classical Rice channels.

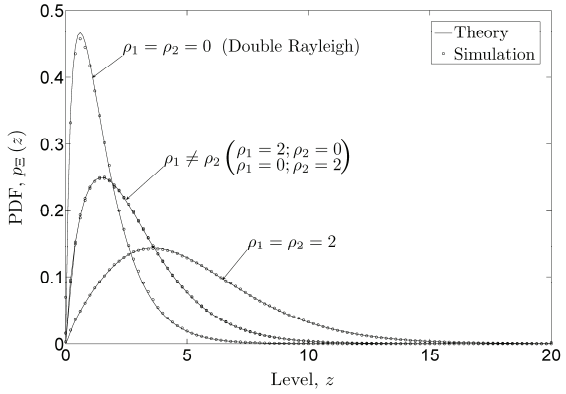

Figure 2. The PDF $p_{\Xi}(z)$ of double Rice processes $\Xi(t)$.

The LCR and ADF of the channel capacity of double Rice channels are presented in Figures 7 and 8, respectively. It is evident from Figure 7 that the maximum value of the LCR of the channel capacity increases with an increase in the value of the amplitude of the LOS component ρ_i $(i=1,2)$. It is also observed that the LCR of the capacity of classical Rice channels is much lower compared to that of double Rice channels. The converse statements with respect to the LCR of the channel capacity are true for the ADF, as can be seen in Figure 8.

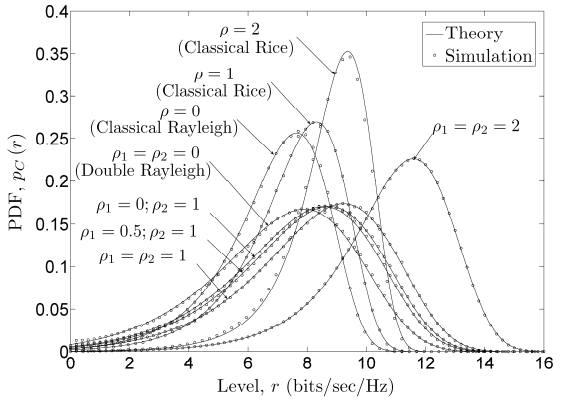

Figure 3. The PDF $p_C(r)$ of the capacity of double Rice channels.

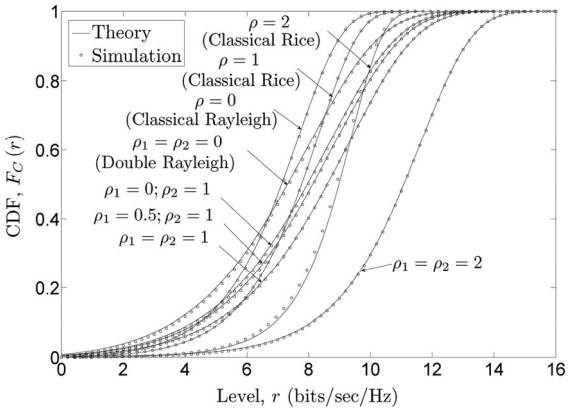

Figure 4. The CDF $F_C(r)$ of the capacity of double Rice channels.

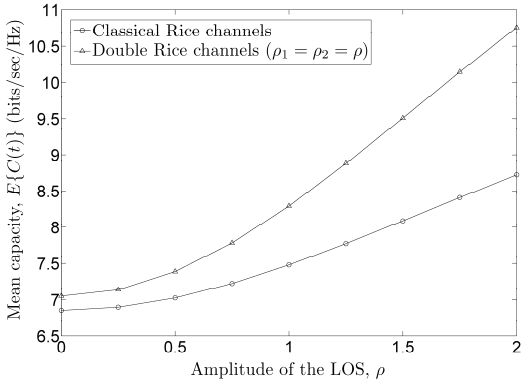

Figure 5. The mean capacity E{C(t)} of classical Rice and double Rice channels.

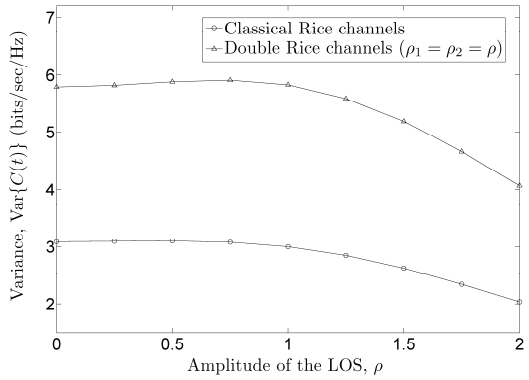

Figure 6. The variance Var{C(t)} of the capacity of classical Rice and double Rice channels.

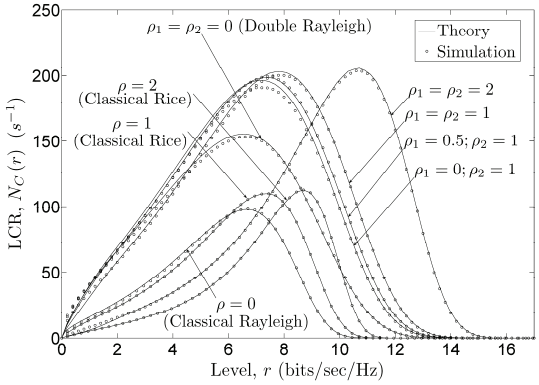

Figure 7. The LCR $N_C(r)$ of the capacity of double Rice channels.

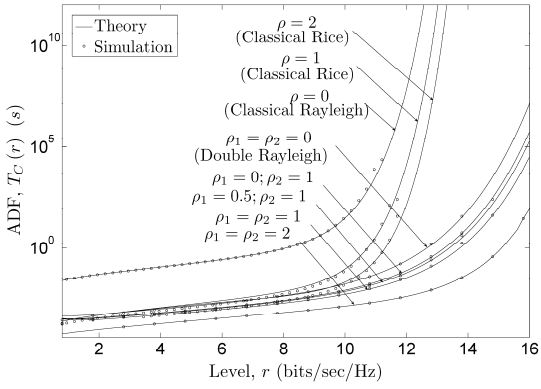

Figure 8. The ADF $T_C(r)$ of the capacity of double Rice channels.

Figures 9 and 10 illustrate the effect of the Doppler frequency on the LCR and ADF of the channel capacity. From Figures 9 and 10, it can clearly be seen that the LCR and ADF are strongly dependent on the Doppler frequencies of the MR and the DMS. It is observed that increasing the Doppler frequencies $f_{\rho_{\mathrm{MR}}}$ and $f_{\rho_{\mathrm{DMS}}}$ from 0 to $f_{\max_2}$ and $f_{\max_3}$, respectively, results in a significant increase in the LCR. However, the ADF decreases by increasing the Doppler frequencies of the MR and the DMS.

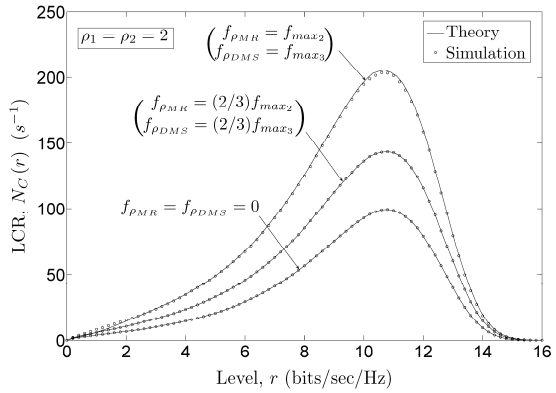

Figure 9. The LCR $N_C(r)$ of the capacity of double Rice channels.

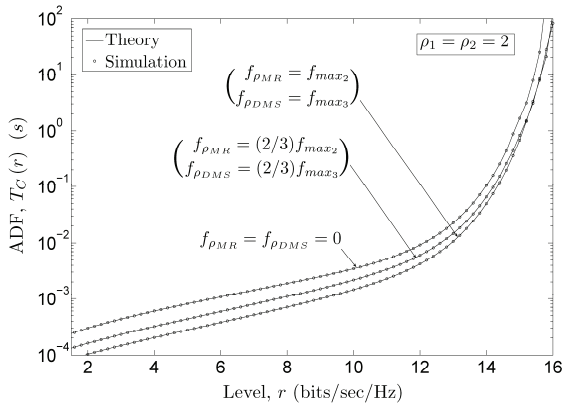

Figure 10. The ACF $T_C(r)$ of the capacity of double Rice channels.

7. Conclusions

In this paper, we have studied the statistical properties of the channel capacity of the double Rice channels. We have derived analytical expressions for the PDF, CDF, LCR, and ADF of the channel capacity. The findings of this paper give a deep insight into the influence of the LOS components, corresponding to the two links of amplify-and-forward channels, on the statistical properties of the channel capacity. It has been observed that for medium and high signal levels, the presence of the LOS components in one or both of the links of the double Rice channel model increases the mean channel capacity and the LCR of the channel capacity. However, it decreases the ADF of the channel capacity. Moreover, the Doppler frequencies of the MR and the DMS have a significant impact on the LCR and ADF of the channel capacity. The validity of all the presented analytical results is confirmed by simulations, whereby a very good fitting between the analytical and simulation results is found.

8. References

[1] A. Sendonaris, E. Erkip, and B. Aazhang, "User coopera-

tion diversity—Part I: System description," IEEE Transactions on Communications, Vol. 51, No. 11, pp. 1927−1938, November 2003.

[2] A. Sendonaris, E. Erkip, and B. Aazhang, "User cooperation diversity—Part II: Implementation aspects and performance analysis," IEEE Transactions on Communications, Vol. 51, No. 11, pp. 1939−1948, November 2003.

[3] J. N. Laneman, D. N. C. Tse, and G. W. Wornell, "Cooperative diversity in wireless networks: Efficient protocols and outage behavior," IEEE Transactions on Information Theory, Vol. 50, No. 12, pp. 3062−3080, December 2004.

[4] M. Dohler, "Virtual antenna arrays," Ph. D. dissertation, King's College, London, United Kingdom, 2003.

[5] J. B. Andersen, "Statistical distributions in mobile communications using multiple scattering," in Proceedings of 27th URSI General Assembly, Maastricht, Netherlands, August 2002.

[6] I. Z. Kovacs, P. C. F. Eggers, K. Olesen, and L. G. Petersen, "Investigations of outdoor-to-indoor mobile-to-mobile radio communication channels," in Proceedings of IEEE 56th Vehicular Technology Conference, VTC'02 Fall, Vancouver BC, Canada, pp. 430−434, September 2002.

[7] V. Ercerg, S. J. Fortune, J. Ling, A. J. Rustako Jr., and R. A. Valenzuela, "Comparison of a computer based propagation prediction tool with experimental data collected in urban microcellular environment," IEEE Journal on Selected Areas in Communications, Vol. 15, No. 4, pp. 677−684, May 1997.

[8] C. S. Patel, G. L. Stüber, and T. G. Pratt, "Statistical properties of amplify and forward relay fading channels," IEEE Transactions on Vehicular Technology, Vol. 55, No. 1, pp. 1−9, January 2006.

[9] J. Salo, H. M. El Sallabi, and P. Vainikainen, "Statistical analysis of the multiple scattering radio channel," IEEE Transactions on Antennas Propagation, Vol. 54, No. 11, pp. 3114−3124, November 2006.

[10] B. Talha and M. Pätzold, "On the statistical properties of double Rice channels," in Proceedings of 10th International Symposium on Wireless Personal Multimedia Communications, WPMC 2007, Jaipur, India, pp. 517−522, December 2007.

[11] B. Talha and M. Pätzold, "On the statistical properties of mobile to mobile fading channels in cooperative networks under line of sight conditions," in Proceedings of 10th International Symposium on Wireless Personal Multimedia Communications, WPMC 2007. Jaipur, India, pp. 388−393, December 2007.

[12] B. Talha and M. Pätzold, "A novel amplify-and-forward relay channel model for mobile-to-mobile fading channels under line-of-sight conditions," in Proceedings of 19th IEEE International Symposium on Personal, Indoor and Mobile Radio Communications, PIMRC 2008, Cannes, France, September 2008.

[13] B. Talha and M. Pätzold, "Level-crossing rate and average duration of fades of the envelope of mobile-to-mobile fading channels in cooperative networks under line-of-sight conditions," in IEEE Conference Proceedings Globecom'08, New Orleans, LA, USA, November /December 2008.

[14] J. Salo, H. M. El-Sallabi, and P. Vainikainen, "Impact of double-Rayleigh fading on system performance," in Proceedings of 1st IEEE International Symposium on Wireless Pervasive Computing, ISWPC 2006. Phuket, Thailand, January 2006.

[15] P. Almers, F. Tufvesson, and A. F. Molisch, "Keyhole effect in MIMO wireless channels: Measurements and theory," IEEE Transactions on Wireless Communications, Vol. 5, No. 12, pp. 3596−3604, 2006.

[16] D. Gesbert, H. Bölcskei, D. A. Gore, and A. J. Paulraj, "Outdoor MIMO wireless channels: Models and performance prediction," IEEE Transactions on Wireless Communications, Vol. 50, No. 12, pp. 1926−1934, December 2002.

[17] A. Giorgetti, P. J. Smith, M. Shafi, and M. Chiani, "MIMO capacity, level crossing rates and fades: The impact of spatial/temporal channel correlation," Journal of Communications and Networks, Vol. 5, No. 2, pp. 104−115, June 2003.

[18] B. O. Hogstad and M. Pätzold, "Capacity studies of MIMO models based on the geometrical one-ring scattering model," in Proceedings of 15th IEEE International Symposium on Personal, Indoor and Mobile Radio Communications, PIMRC 2004, Vol. 3. Barcelona, Spain, pp. 1613−1617, September 2004.

[19] B. O. Hogstad and M. Pätzold, "Exact closed-form expressions for the distribution, level- crossing rate, and average duration of fades of the capacity of MIMO channels," in Proceedings of 65th Semiannual Vehicular Technology Conference, IEEE VTC 2007-Spring, Dublin, Ireland, pp. 455−460, April 2007.

[20] I. S. Gradshteyn and I. M. Ryzhik, "Table of Integrals, Series, and Products," 6th edition, Academic Press, 2000.

[21] A. Papoulis and S. U. Pillai, Probability, "Random variables and stochastic processes," 4th edition, New York: McGraw-Hill, 2002.

[22] G. J. Foschini and M. J. Gans, "On limits of wireless communications in a fading environment when using multiple antennas," Wireless Personal Communications, Vol. 6, pp. 311−335, March 1998.

[23] G. Rafiq and M. Pätzold, "A study of the influence of shadowing on the statistical properties of the capacity of mobile radio channels," Wireless Personal Communications, DOI 10.1007/s11277-008-9545-7, June 2008.

[24] M. Pätzold, "Mobile fading channels," Chichester: John Wiley & Sons, 2002.

[25] M. Pätzold and B. O. Hogstad, "Two new methods for the generation of multiple uncorrelated Rayleigh fading waveforms," in Proceedings of 63rd IEEE Semiannual Vehicular Technology Conference, IEEE VTC 2006-Spring, Vol. 6, Melbourne, Australia, pp. 2782−2786, May 2006.

Wireless Sensor Network, **2009, 1, 1-60**
Published Online April 2009 in SciRes (http://www.SciRP.org/journal/wsn/).

Parameter Optimization for Amplify-and-Forward Relaying Systems with Pilot Symbol Assisted Modulation Scheme

Yi WU, Matthias PÄTZOLD
Faculty of Engineering and Science, University of Agder, Grimstad, Norway
E-mail: {yi.wu, matthias.paetzold}@uia.no
Received March 7, 2009; *revised March* 16, 2009; *accepted March* 18, 2009

Abstract

Cooperative diversity is a promising technology for future wireless networks. In this paper, we consider a cooperative communication system operating in an amplify-and-forward (AF) mode with a pilot symbol assisted modulation (PSAM) scheme. It is assumed that a linear minimum mean square estimator (LMMSE) is used for the channel estimation at the receiver. A simple and easy-to-evaluate asymptotical upper bound (AUB) of the symbol-error-rate (SER) is derived for uncoded AF cooperative communication systems with quadrature amplitude modulation (QAM) constellations. Based on the AUB, we propose a criterion for the parameter optimization in the PSAM scheme. We discuss how the pilot spacing and the length of the Wiener filter should be chosen under the constraint of a tradeoff between pilot overhead, estimation accuracy, and receiver complexity. We also formulate an power allocation problem for the considered system. It is shown that the power allocation problem can optimally be solved by means of a gradient search method. Numerical simulations are presented to verify the correctness of the theoretical results and to demonstrate the benefits of the parameter optimization.

Keywords: Amplify-and-Forward, Cooperative Communication System, Imperfect Channel Estimations, Parameter Optimization

1. Introduction

Recently, a new form of spatial diversity called "cooperative diversity" has attracted much research interest because it provides effective diversity benefits for those devices that cannot be equipped with multiple antennas due to their size, complexity, and cost. The main idea behind cooperative diversity is that the mobile users in the neighborhood share the use of their antennas to assist each other with data transmission. Cooperative diversity is realized by collaboration among the users. If the channel fading from a user to the destination terminal is severe, then the information might be successfully transmitted through the cooperative users. Different cooperative protocols have been proposed to exploit the diversity that cooperative systems offer (see, e.g., [1-4] and the references therein). One commonly used protocol is the amplify-and-forward (AF) protocol, in which the relay terminal simply re-transmits a scaled version of the received signal to the destination terminal. Depending on the scaling factor, the AF relaying scheme can be further divided into two types which are called fixed gain AF systems and variable gain AF systems [5].

The performance of AF cooperative systems has been studied in the past from different perspectives. For example, [4,6,7] analyzed the performance of AF systems in terms of the outage probability and diversity gain under different assumptions for the amplifier gain. On the other hand, the authors of [8−12] derived exact expressions for the symbol-error-rate (SER) and presented various SER bounds for AF cooperative communication systems. However, all these papers have assumed that the perfect channel state information (CSI) is available at both the relay and destination terminal. More recently, [5] and [13] have studied the performance of AF cooperative communication systems with channel estimation errors by means of Monte Carlo simulations. The accurate SER expression for cooperative communication systems with a pilot symbol assisted modulation (PSAM) scheme employing a linear minimum mean square estimator (LMMSE) is derived in [14]. To the authors' best knowledge, no research has been conducted to solve the

This paper will be presented in part at the 69th IEEE Semiannual Vehicular Technology Conference, VTC2009-Spring, Barcelona, Spain, April 2009.

problem of parameter optimization and optimum power allocation for variable gain AF cooperative communication systems with a PSAM scheme.

The difficulty in optimizing the system design lies in the fact that the accurate SER expression is given in form of a double integral [14]. This prevents us from minimizing the SER directly. In this paper, we propose to use the asymptotic upper bound (AUB) of the SER to overcome these difficulties. In particular, we derive a tight expression for the AUB of the SER for the AF cooperative communication system with a PSAM scheme. The derived AUB has a simple form and no integrating operation is involved. Using the AUB of the SER, we present the criterion for the parameter choice in the PSAM scheme and show that two parameters used in this scheme, i.e., pilot spacing and Wiener filter length, can be chosen in a tradeoff between system performance, pilot overhead, and receiver complexity. With the derived tight AUB, an optimum power allocation problem is also formulated for the AF cooperative communication system. Since the optimization of the power allocation is very complicated, as it is related to many terms, and obtaining an analytical solution is unlikely, we propose to find the optimum power allocation by means of a gradient search over a continuous range.

The rest of the paper is organized as follows. In Section 2, we describe the system model and some preliminaries of the AF cooperative system with a PSAM scheme. In Section 3, we derive an AUB of the SER for an AF cooperative communication system with LMMSE. In Section 4, we first deal with the parameter optimization for the PSAM scheme. Then, an optimum power allocation problem is formulated. A gradient search algorithm is also proposed to find the solution of the optimization problem. Various simulation results and their discussions are presented in Section 5. Finally, Section 6 contains the conclusions.

The following notation is used throughout the paper: $(\cdot)^*$, $(\cdot)^T$, $(\cdot)^H$, and $(\cdot)^{-1}$ denote the complex conjugate, vector (or matrix) transpose, conjugate transpose, and matrix inverse, respectively. The symbol $E[\cdot]$ denotes the expectation operator, $|z|$ represents the absolute value of a complex number z, and the complex Gaussian distribution with mean m and covariance P is denoted by $\mathcal{CN}(m,P)$.

2. System Model

We consider an AF cooperative communication system which consists of a source, relay, and destination terminal. The block diagram of the system is shown in Figure 1. We assume that each terminal is equipped with a single transmit and receive antenna and operates in a half-duplex mode, i.e., it cannot transmit and receive simultaneously. We adopt the so-called Protocol II proposed by Nabar *et al*. [6] as the user cooperative protocol. This means that two time slots are used to transmit one data symbol. The source terminal communicates with the relay and destination terminal during the first time slot. In the second time slot, only the relay terminal communicates with the destination terminal. This protocol realizes a maximum degree of broadcasting and exhibits no receive collisions [6]. To simplify the following analysis, we consider a symbol-by-symbol transmission, so that the time slot index 1 and 2 can be dropped. Throughout this paper, we assume that the system operates in a Rayleigh flat fading environment with perfect synchronization, and imperfect channel estimation is assumed at the receiver. As in [5], we use a PSAM scheme for the channel estimation. Pilot symbols are periodically inserted in data symbols with an insertion period of L symbols. Since the design of an optimal channel estimator is very complex, we resort to a suboptimal LMMSE. We further assume that the data information symbols are equally probable over a constellation set composed of quadrature amplitude modulation (QAM) symbols of size M, and the pilot symbols are selected from a binary phase-shift keying (BPSK) constellation.

With these assumptions, let us look at the received signals corresponding to the k th transmitted symbol. The received signals in the first time slot at the destination terminal and the relay terminal are given by

$$r_{SD}(k) = \sqrt{P_S}\,h_{SD}(k)x(k) + n_{SD}(k) \quad \textbf{(1)}$$

$$r_{SR}(k) = \sqrt{P_S}\,h_{SR}(k)x(k) + n_{SR}(k) \quad \textbf{(2)}$$

respectively, where P_S is the average power of the transmitted signal at the source terminal, $h_{SD}(k)$ and $h_{SR}(k)$ are the channel coefficients from the source terminal to the destination terminal with distribution $\mathcal{CN}(0,\sigma_{SD}^2)$ and from the source terminal to the relay terminal with distribution $\mathcal{CN}(0,\sigma_{SR}^2)$, respectively. The symbol $x(k)$ is the k th transmitted symbol from the source terminal, and $n_{SD}(k)$ and $n_{SR}(k)$ are the additive receiver noises at the destination terminal and the relay terminal, respectively, with the same distribution $\mathcal{CN}(0,N_0)$. Throughout this paper, we assume

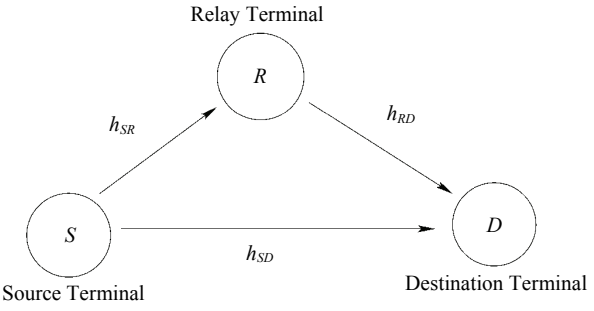

Figure 1. Block diagram of the AF cooperative communication system.

that $E[|x(k)|^2]=1$, i.e., the transmitted symbols have an average energy of 1. According to the Protocol II, the relay terminal will first normalize the received signal by a factor of $\sqrt{E(|r_{SR}(k)|^2)}$ (to ensure the unity of average energy). Then, the normalized signal will be amplified and forwarded to the destination terminal during the second time slot. Therefore, the received signal at the destination terminal within the second time slot is given by

$$r_{RD}(k)=\frac{\sqrt{P_R}}{\sqrt{P_S\,|h_{SR}(k)|^2+N_0}}h_{RD}(k)\,r_{SR}(k)+n_{RD}(k) \quad \textbf{(3)}$$

where P_R is the average power of the transmitted signal at the relay terminal, $h_{RD}(k)$ is the channel coefficient from the relay terminal to the destination terminal with distribution $\mathcal{CN}(0,\sigma_{RD}^2)$, and $n_{RD}(k)$ is the additive receiver noise at the destination terminal with distribution $\mathcal{CN}(0,N_0)$. Using (2), we can rewrite (3) as

$$r_{RD}(k)=\frac{\sqrt{P_S P_R}}{\sqrt{P_S\,|h_{SR}(k)|^2+N_0}}h_{SR}(k)\,h_{RD}(k)\,x(k)+n'_{RD}(k) \quad \textbf{(4)}$$

where

$$n'_{RD}(k)=\frac{\sqrt{P_R}}{\sqrt{P_S\,|h_{SR}(k)|^2+N_0}}h_{RD}(k)\,n_{SR}(k)+n_{RD}(k) \quad \textbf{(5)}$$

Assuming that $n_{SR}(k)$ and $n_{RD}(k)$ are independent, it can be shown that the noise term $n'_{RD}(k)$ is a complex Gaussian random variable with distribution $\mathcal{CN}(0,(\sqrt{P_R}/\sqrt{P_S\,|h_{SR}(k)|^2+N_0}+1)N_0)$. Since the PSAM scheme is used for the channel estimation, the packed transmission can be divided into blocks by pilot symbols. In each block, there are L symbols in which the first time slot is assigned to a pilot symbol and the remaining $L-1$ symbols are assigned to data symbols. The channel estimation at each symbol position in a block is obtained using N_1 pilot symbols on the left-hand side of the symbol position and N_2 pilot symbols on the right-hand side of the symbol position. Therefore, $N=N_1+N_2$ pilot symbols are used to estimate the channel coefficient of the desired symbol position.

Let us denote the pilot symbols employed to estimate the channel gain $h_{SD}(k)$ of the desired data symbol $x(k)$ as an $N\times 1$ vector $\mathbf{p}_{SD}=[x(k-L(N_1-1)-l),...,x(k-l),x(k+L-l),...,x(k+LN_2-l)]^T$, where $l=1,2,...,L-1$ is the offset of the desired data symbol $x(k)$ to the closest pilot symbol on its left side. Using (1), we obtain the received signal vector $\mathbf{r}_{SD}$, corresponding to the transmitted pilot vector $\mathbf{p}_{SD}$, at the destination terminal as

$$\mathbf{r}_{SD}=\sqrt{P_S}\;diag(\mathbf{p}_{SD})\mathbf{h}_{SD}+\mathbf{n}_{SD} \quad \textbf{(6)}$$

where $\mathbf{h}_{SD}=[h_{SD}(k-L(N_1-1)-l),...,h_{SD}(k-l),h_{SD}(k+L-l),...,h_{SD}(k+LN_2-l)]^T$ and $\mathbf{n}_{SD}=[n_{SD}(k-L(N_1-1)-l),...,n_{SD}(k-l),n_{SD}(k+L-l),...,n_{SD}(k+LN_2-l)]^T$ are the channel coefficient and noise component at the pilot symbols' position for estimating $h_{SD}(k)$, respectively.

Without loss of generality, we assume that positive unit energy symbols are transmitted as pilot symbols, i.e., $\mathbf{p}_{SD}$ is an all-one vector. Then, (6) simplifies to

$$\mathbf{r}_{SD}=\sqrt{P_S}\mathbf{h}_{SD}+\mathbf{n}_{SD} \quad \textbf{(7)}$$

With these observations, the channel estimate for $h_{SD}(k)$ can be obtained by the LMMSE as [15]

$$\hat{h}_{SD}(k)=\mathbf{w}_{SD}\,\mathbf{r}_{SD} \quad \textbf{(8)}$$

where $\mathbf{w}_{SD}=\mathbf{c}_{h_{SD},\mathbf{r}_{SD}}(l)\mathbf{C}_{\mathbf{r}_{SD}}^{-1}$ is an $1\times N$ LMMSE filter vector, $\mathbf{C}_{\mathbf{r}_{SD}}=E[\mathbf{r}_{SD}\mathbf{r}_{SD}^H]$ and $\mathbf{c}_{h_{SD},\mathbf{r}_{SD}}(l)=E[h_{SD}^*(k)\mathbf{r}_{SD}]$ are the autocorrelation matrix of $\mathbf{r}_{SD}$ and cross-correlation vector $h_{SD}(k)$ and $\mathbf{r}_{SD}$, respectively. From the LMMSE theory [15], we know that $\hat{h}_{SD}(k)$ is distributed as $\mathcal{CN}(0,\mathbf{c}_{h_{SD},\mathbf{r}_{SD}}(l)\;(\mathbf{C}_{\mathbf{r}_{SD}}^{-1})^H\;\mathbf{c}_{h_{SD},\mathbf{r}_{SD}}^H(l))$. Let us define the discrete autocorrelation function of $h_{SD}(k)$ as $R_{SD}(\kappa)=E[h_{SD}(k)\;\;h_{SD}(k+\kappa)^*]$. Then, using the system model under consideration of the channel properties described above, we can finally express $\mathbf{C}_{\mathbf{r}_{SD}}$ and $\mathbf{c}_{h_{SD},\mathbf{r}_{SD}}(l)$ as

$$\mathbf{C}_{\mathbf{r}_{SD}}=\begin{bmatrix} P_S R_{SD}(0)+N_0 & P_S R_{SD}(L) & \cdots & P_S R_{SD}((N-1)L) \\ P_S R_{SD}(L) & P_S R_{SD}(0)+N_0 & \cdots & P_S R_{SD}((N-2)L) \\ \vdots & \vdots & \ddots & \vdots \\ P_S R_{SD}((N-1)L) & P_S R_{SD}((N-2)L) & \cdots & P_S R_{SD}(0)+N_0 \end{bmatrix} \quad \textbf{(9)}$$

$$\mathbf{c}_{h_{SD},\mathbf{r}_{SD}}(l)=[\sqrt{P_S}R_{SD}(-L(N_1-1)-l),\cdots,\sqrt{P_S}R_{SD}(L-l),\cdots\sqrt{P_S}R_{SD}(L(N_2-1)-l)] \quad \textbf{(10)}$$

From the LMMSE filter vector $\mathbf{w}_{SD}$, we can see that each data symbol position in a block requires a different estimator. However, due to the periodic pilot insertion, an identical estimator will be adopted at the same data symbol positions across all blocks in a packet. Therefore, without loss of generality, we will only consider $L-1$

different estimators for the data symbol positions in one particular block in the following analysis and employ the index l instead of k to distinguish them. With this in mind, we can express the estimation error of the lth estimator as

$$e_{SD}(l) = h_{SD}(l) - \hat{h}_{SD}(l) \quad \textbf{(11)}$$

Furthermore, the estimation error $e_{SD}(l)$ is distributed as $\mathcal{CN}(0, \sigma^2_{e,SD}(l))$, where $\sigma^2_{e,SD}(l)) = \sigma^2_{SD} - \mathbf{c}_{h_{SD},\mathbf{r}_{SD}}(l)$ $(\mathbf{C}^{-1}_{\mathbf{r}_{SD}})^H \mathbf{c}^H_{h_{SD},\mathbf{r}_{SD}}(l)$. From (11) it follows that we can model the channel gain $h_{SD}(l)$ as the sum of the channel estimate $\hat{h}_{SD}(l)$ and the estimation error $e_{SD}(l)$, i.e.,

$$h_{SD}(l) = \hat{h}_{SD}(l) + e_{SD}(l) \quad \textbf{(12)}$$

Similarly, we can model the channel gain from the source terminal to the relay terminal $h_{SR}(l)$ and the channel gain from the relay terminal to the source terminal $h_{RD}(l)$ as

$$h_{SR}(l) = \hat{h}_{SR}(l) + e_{SR}(l) \quad \textbf{(13)}$$

$$h_{RD}(l) = \hat{h}_{RD}(l) + e_{RD}(l) \quad \textbf{(14)}$$

where $\hat{h}_{SR}(l)$, $e_{SR}(l)$, $\hat{h}_{RD}(l)$, and $e_{RD}(l)$ can be attained using the same procedure as above.

3. AUB Analysis for AF Cooperative Systems

With the above assumption and the estimated channel gains, maximum ratio combining (MRC) [16] can be applied at the destination terminal to minimize the SER of the system. Define $B = 1 - 1/\sqrt{M}$ and $K_Q = 3/(M-1)$. The accurate SER expression for the considered system with M-QAM is [14]

$$\overline{P} = \frac{1}{L-1}\sum_{l=1}^{L-1} P(l) \quad \textbf{(15)}$$

where

$$P(l) = \frac{1}{\pi}\int_0^{\pi/2}\int_0^1 \frac{4B\eta(l)}{\alpha_1(l) + \dfrac{K_Q}{2\sin^2\theta}} f(l,x,\frac{K_Q}{2\sin^2\theta})\ dxd\theta$$

$$-\frac{1}{\pi}\int_0^{\pi/4}\int_0^1 \frac{4B^2\eta(l)}{\alpha_1(l) + \dfrac{K_Q}{2\sin^2\theta}} f(l,x,\frac{K_Q}{2\sin^2\theta})\ dxd\theta$$

$$f(l,x,s) = exp\left(-\frac{\alpha_3(l)\beta(l)x}{1-x}\right)\left[a(l,x,s) + b(l,x,s)\right]$$

$$a(l,x,s) = \frac{\beta(l)}{\alpha_2(l) + (s - 2\alpha_2(l) + \alpha_3(l))x + \upsilon(l,x,s)}$$

$$\upsilon(l,x,s) = (-2s + \alpha_2(l) - \alpha_3(l))x^2 + sx^3$$

$$b(l,x,s) = \frac{1}{\left(\alpha_2(l) + [s - \alpha_2(l) + \alpha_3(l)]x - sx^2\right)^2}$$

$$\eta(l) = \alpha_1(l)\alpha_2(l)\alpha_3(l)\, exp[\alpha_3(l)\beta(l)]$$

$$\alpha_1(l) = \frac{[P_S\sigma^2_{e,SD}(l) + N_0]}{[P_S\sigma^2_{\hat{h},SD}(l)]}$$

$$\alpha_2(l) = \frac{(P_R + N_0)\sigma^2_{e,RD}(l) + N_0}{P_R\sigma^2_{\hat{h},RD}(l)}$$

$$\alpha_3(l) = \frac{P_S\sigma^2_{e,SR}(l) + N_0}{P_S\sigma^2_{\hat{h},SR}(l)}$$

$$\beta(l) = \frac{P_SP_R\sigma^2_{e,SR}(l)\sigma^2_{e,RD}(l) + (1 + \sigma^2_{e,RD}(l))N_0^2}{(P_S\sigma^2_{e,SR}(l) + N_0)[(P_R + N_0)\sigma^2_{e,RD}(l) + N_0]}$$

Note that although the numerical evaluation of the above expression of the SER is straightforward, it is not insightful in terms of its dependence on the system parameters like the pilot spacing or power allocation between the source terminal and relay terminal. To optimize the system parameters using (15) seems to be intractable. Therefore, a simple and insightful AUB of the SER is of special interest.

As derived in [14], we know that the instantaneous SNR of the output signal from the MRC detector is the sum of two terms: the first term is determined by the direct signal from the source terminal and the second term is determined by the relay signal from the relay terminal. Using the result in [14], the instantaneous SNR determined by the relay signal can be rewritten as

$$\gamma_2(l) = \frac{x_1(l)x_2(l)}{x_1(l) + x_2(l) + \beta(l)} \quad \textbf{(16)}$$

where

$$x_1(l) = \frac{|\hat{h}_{RD}(l)|^2}{\alpha_2(l)\sigma^2_{\hat{h},RD}(l)}$$

$$x_2(l) = \frac{|\hat{h}_{SR}(l)|^2}{\alpha_3(l)\sigma^2_{\hat{h},SR}(l)}$$

From the definition of $\beta(l)$ in (15), it can be found that $\beta(l) > 0$. Therefore, if we set $\beta(l) = 0$ in (16), we get an upper bound of the $\gamma_2(l)$. With this observation, we obtain an upper bound of the SER by simply setting $\beta(l) = 0$ in (15). After some manipulations, we obtain the AUB of the SER

$$\overline{P}_{UB} = \frac{1}{L-1}\sum_{l=1}^{L-1}\frac{4B}{K_Q}\alpha_1(l)\left[\alpha_2(l) + \alpha_3(l)\right] \quad \textbf{(17)}$$

Note that N_0 / P_R tends to zero in high SNR regions.

Therefore, the AUB of the SER can be further simplified as

$$\overline{P}_{UB} = \frac{1}{L-1}\sum_{l=1}^{L-1}\frac{4B}{K_Q}\alpha_1(l)\left[\alpha_2'(l)+\alpha_3(l)\right] \quad \textbf{(18)}$$

where

$$\alpha_2'(l) = \frac{P_R\sigma_{e,RD}^2(l)+N_0}{P_R\sigma_{\hat{h},RD}^2(l)} \approx \alpha_2(l)$$

As shown in Section 5, the AUB of the SER in (18) is very close to the exact SER, especially in high SNR regions.

4. Parameter Optimization

As can be seen from (18), the AUB of the SER is determined by the function

$$M(L,N,P_S,P_R) = \sum_{l=1}^{L-1}\alpha_1(l)\left[\alpha_2'(l)+\alpha_3(l)\right] \quad \textbf{(19)}$$

It should be pointed out that $\alpha_1(l),\alpha_2'(l),\alpha_3(l)$, for $l=1,2,\cdots,L-1$ are related to the parameters L,N,P_S, and P_R. This can be deduced from their definition in (15). As a result, we establish the relation between the AUB of the SER and the parameters which need to be optimized. Using the above metric as an optimality criterion, we can now study the parameter optimization problem of the considered system. In principle, we should optimize the four parameters L,N,P_S, and P_R jointly to get the optimum system performance. However, the joint optimization problem is difficult to solve due to the form of the metric in (19). Therefore, we propose to optimize the parameters of the PSAM and the power allocation separately as shown below. Although this method is suboptimal, our simulation results show that this method provides a satisfactory performance.

4.1. PSAM Parameter Optimization

For the PSAM scheme, there exists a tradeoff between the system performance, pilot overhead, and receiver complexity. While a smaller pilot spacing L leads to a better channel estimation, the overhead imposed by the pilot symbols reduces the effective SNR and transmission efficiency. A similar conflict also exists for the choice of the Wiener filter length N. A larger value of N is required to improve the channel estimation, but this will increase the receiver complexity. Therefore, the parameters L and N should be accordingly chosen by taking all these factors into account. We will use the metric in (19) as the optimality criterion for determining appropriate values of L and N. In particular, we will set $P_S = P_R = P/2$, where P is the total transmitted power, and try to minimize the metric $M(L,N,P_S,P_R)$ which characterizes (asymptotically) the performance of the considered system. Since there is no closed-form solution to this minimization problem, the suitable values of L and N can only be obtained by examining the metric $M(L,N,P_S,P_R)$, which is presented in the next section.

4.2. Power Allocation Optimization

Now, we will study the power allocation problem for the considered system. We assume that the parameters L, N are fixed and the total transmitted power is $P = P_S + P_R$. Under these constraints, we are going to optimize P_S and P_R so that the SER performance of the system is minimized. Since the metric $M(L,N,P_S,P_R)$ characterizes (asymptotically) the SER performance of the considered system, we can state the power allocation problem as follows.

Problem Statement: Given positive integers L, N, find a pair of real numbers P_S and P_R such that the metric function $M(L,N,P_S,P_R)$ is minimized under the power constraint of the transmitted power which is fixed to P, i.e.,

$$\{P_S,P_R\} = arg \min_{\substack{P_S,P_R \\ P_S+P_R=P}} M(L,N,P_S,P_R) \quad \textbf{(20)}$$

Note that the derivatives of the metric $M(L,N,P_S,P_R)$ with respect to P_S and P_R will be expressed as the sum of several high-order polynomials. This prevents us from finding a closed-form solution for P_S and P_R. Therefore, we propose to find the optimum power allocation by means of a gradient search over a continuous range.

5. Numerical Results

In this section, we will first verify by simulations the correctness of the derived expression found for the AUB of the SER. We will then present some examples illustrating the parameter optimization procedure. We consider an AF cooperative communication system with 4-QAM modulation formats using the PSAM scheme for the channel estimation. Unless stated otherwise, the following parameters are used in the numerical work. We set $P_S = P_R$ and assume that the variance of the noise was chosen to be $N_0 = 1$. We also assume that the complex channel gains are described by the autocorrelation functions $R_{SD}(\kappa) = R_{SR}(\kappa) = R_{RD}(\kappa) = J_0(2\pi f_{\max}\kappa T_s)$, where $J_0(x)$ is the zeroth order Bessel function of the first kind, $f_{\max}$ is the maximum Doppler frequency, and T_s is the symbol duration. Note that the variances of the complex channel gains are normalized to unity. We further assume that a pilot spacing of $L = 6$ is used

in the PSAM scheme and the LMMSE with $N = 6$ is used for the channel estimation. Note that the power loss resulting from the pilots is accounted for all curves.

Figure 2 shows the theoretical AUB and the Monte Carlo simulation results of the SER for the AF cooperative communication system with 4-QAM. The results are presented for two different levels of the normalized maximum Doppler frequency, i.e $f_{\max}T_s = 0.01$ and $f_{\max}T_s = 0.05$. From Figure 2, we observe that the AUB fits very well with the simulated SER for both cases in high SNR regions.

Assuming $P_S = P_R$, Figure 3 plots the metric $M(L,N,P_S,P_R)$ as a function of the pilot spacing L and the Wiener filter length N at SNR=20 dB with a normalized maximum Doppler frequency of $f_{\max}T_s = 0.05$. We observe that for a given N, the metric $M(L,N,P_S,P_R)$ decreases rapidly with L for $L \le 4$. This is because the energy spent by pilot symbols decreases rapidly with L for $L \le 4$. As a result, the energy assigned to each data symbol increases, and this leads to a fast decrease in the SER. On the other hand, we also find that the metric $M(L,N,P_S,P_R)$ increases with L for $L > 7$. This is easy to understand since large L will increase the channel estimation error, and thus increase the SER. By taking all these factors into account, we suggest to choose $L = 6$. Now let us consider the choice of N. From Figure 3, we observe that for a given L, the metric $M(L,N,P_S,P_R)$ decreases rapidly with N for $N \le 6$. However, the decrease in $M(L,N,P_S,P_R)$ obtained by increasing N beyond 6 is minor. Since large N leads to a high receiver complexity, we suggest to choose $N = 6$ for this particular case.

Now, we turn our attention to the power allocation strategies. As discussed earlier, we use a constrained gradient-search algorithm to find the power tradeoff between the source terminal and the relay terminal. For example, in case of $\sigma_{SD}^2 = \sigma_{SR}^2 = \sigma_{RD}^2 = 1$, and $f_{\max}T_s = 0.01$ we find the optimum power allocation is $P_S / P = 0.66$, and $P_R/P = 0.34$. The performance comparison of the equal power scheme and the optimum power allocation scheme is presented in Figure 4. This figure illustrates that the performance of the system with optimum power allocation is better than that of the system with equal power allocation. We can see that a greater performance improvement can be achieved from

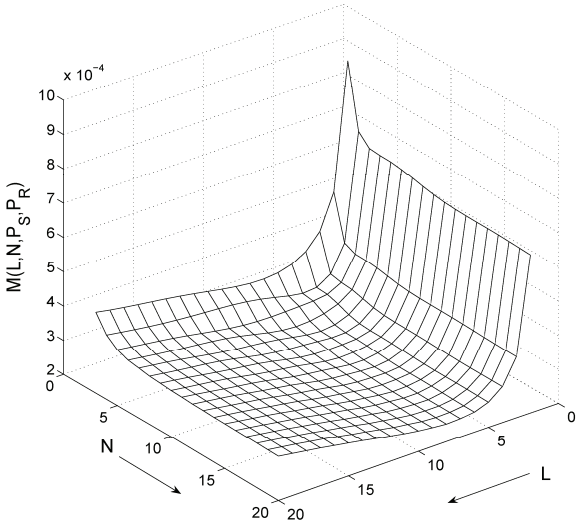

Figure 3. The metric $M(L,N,P_S,P_R)$ at SNR=20 dB with a normalized maximum Doppler frequency of $f_{\max}T_s = 0.05$.

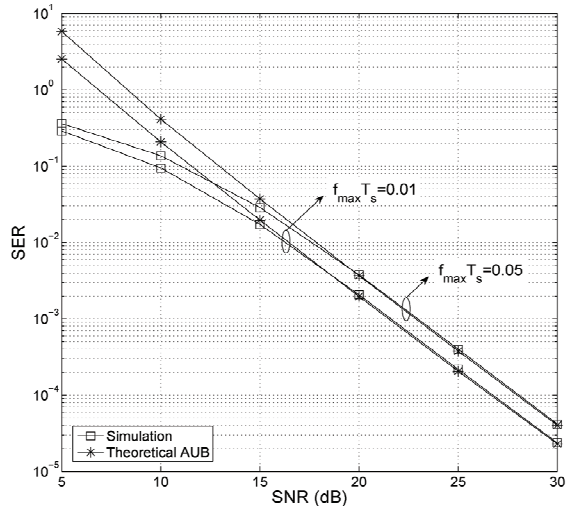

Figure 2. Comparison of the theoretical AUB and simulation results of the SER for the AF cooperative communication systems with various values of the normalized maximum Doppler frequency $f_{\max}T_s$.

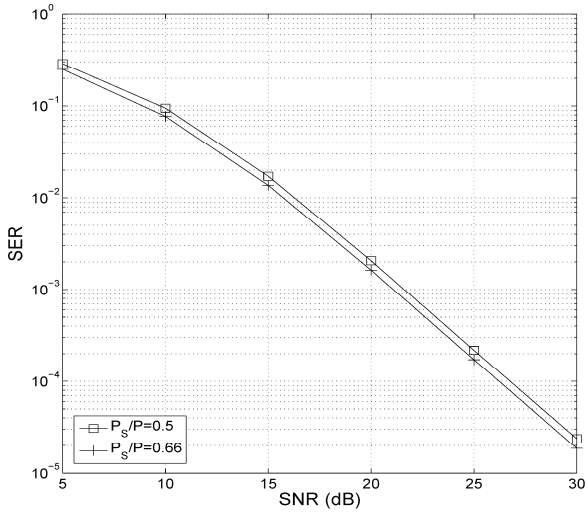

Figure 4. SER performance of the AF cooperative communication systems assuming equal power allocation and optimum power allocation.

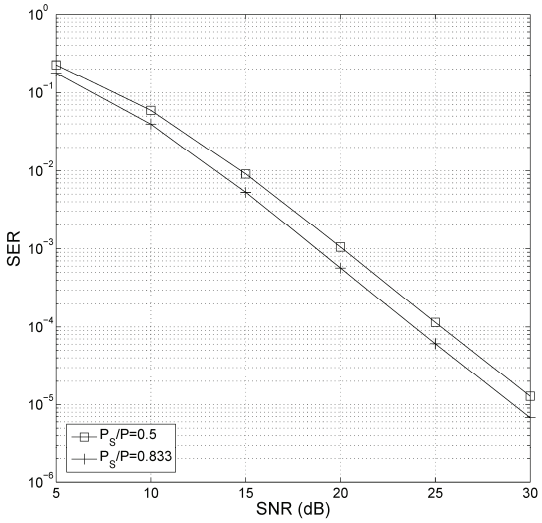

Figure 5. SER performance of the AF cooperative communication systems assuming equal power allocation and optimum power allocation.

the optimum power allocation scheme if the ratio $\sigma_{SR}^2 / \sigma_{RD}^2$ decreases. For example, in case of $\sigma_{SD}^2 = \sigma_{SR}^2 = 1$, $\sigma_{RD}^2 = 10$ and $f_{max}T_s = 0.01$, we find the optimum power allocation is $P_S/P = 0.83$, and $P_R/P = 0.17$. The corresponding performance comparison is plotted in Figure 5. As can be seen from this figure, the optimum power allocation scheme leads to an improvement of 1.5 dB over the equal power scheme. This further demonstrates the effectiveness of the power allocation optimization.

6. Conclusions

We dealt with the problem of parameter optimization of AF cooperative communication systems with a PSAM-based LMMSE scheme used for the channel estimation. A tight and easy to-evaluate AUB of the SER was derived for the considered system with QAM constellations. Using the derived AUB, we proposed a criterion for the choice of parameters in the PSAM scheme, i.e., pilot spacing and Wiener filter length. We also formulated an optimum power allocation problem for the considered system. The optimum power allocation was found by means of a gradient search over a continuous range. Some illustrative examples for the parameter optimization were presented. The benefits of parameter optimization were demonstrated by the numerical results.

7. References

[1] G. Kramer, M. Gastpar, and P. Gupta, "Cooperative strategies and capacity theorems for relay networks," IEEE Transactions on Information Theory, Vol. 51, No. 9, pp. 3037−3063, September 2005.

[2] A. Reznik, M. R. Kulkarni, and S. Verdu, "Degraded Gaussian multirelay channel: Capacity and optimal power allocation," IEEE Transactions on Information Theory, Vol. 50, No. 12, pp. 3037−3046, December 2004.

[3] A. Host-Madsen and J. Zhang, "Capacity bounds and power allocation for wireless relay channels," IEEE Transactions on Information Theory, Vol. 51, No. 6, pp. 2020−2040, June 2005.

[4] J. N. Laneman, D. N. C. Tse, and G. W. Wornell, "Cooperative diversity in wireless networks: Efficient protocols and outage behavior," IEEE Transactions on Information Theory, Vol. 50, No. 12, pp. 3062−3080, December 2004.

[5] C. S. Patel and G. L. Stüber, "Channel estimation for amplify and forward relay based cooperation diversity systems," IEEE Transactions on Wireless Communications, Vol. 6, No. 6, pp. 2348–2356, June 2007.

[6] R. U. Nabar, H. Bölcskei, and F. W. Kneubühler, "Fading relay channels: Performance limits and space-time signal design," IEEE Journal on Selected Areas in Communications, Vol. 22, No. 6, pp. 1099−1109, August 2004.

[7] M. O. Hasna and M.-S. Alouini, "Harmonic mean and end-to-end performance of transmission systems with relays," IEEE Transactions on Communications, Vol. 52, No. 1, pp. 130−135, January 2004.

[8] M. O. Hasna and M.-S. Alouini, "A performance study of dual-hop transmissions with fixed gain relays," IEEE Transactions on Wireless Communications, Vol. 3, No. 6, pp. 1963−1968, November 2004.

[9] P. A. Anghel and M. Kaveh, "Exact symbol error probability of a cooperative network in a Rayleigh-fading environment," IEEE Transactions on Wireless Communications, Vol. 3, No. 5, pp. 1416−1421, September 2004.

[10] A. Ribeiro, X. Cai, and G. B. Giannakis, "Symbol error probabilities for general cooperative links," IEEE Transactions on Wireless Communications, Vol. 4, No. 3, pp. 1264−1273, March 2005.

[11] Y. Li and S. Kishore, "Asymptotic analysis of amplify-and-forward relaying in Nakagami-fading environments," IEEE Transactions on Wireless Communications, Vol. 6, No. 12, pp. 4256−4262, December 2007.

[12] W. Su, A. K. Sadek, and K. J. R. Liu, "Cooperative communication protocols in wireless networks: Performance analysis and optimum power allocation," Wireless Personal Communications (Springer), Vol. 44, No. 2, pp. 181−217, January 2008.

[13] B. Gedik and M. Uysal, "Two channel estimation methods for amplify-and-forward relay networks," in Proceedings of Canadian Conference on Electrical and Computer Engineering , pp. 615−618, May 2008.

[14] Y. Wu and M. Pätzold, "Performance analysis of cooperative communication systems with imperfect channel estimation," IEEE International Conference on Communications, IEEE ICC 2009, accepted for publication, June 2009.

[15] L. L. Scharf, "Statistical signal processing: Detection, estimation, and time-series analysis," Reading, MA: Addison-Wesley, 1990.

[16] D. G. Brennan, "Linear diversity combining techniques," Proceedings of the IEEE, Vol. 91, No. 2, pp. 331−356, February 2003.

Wireless Sensor Network, 2009, 1, 1-60
Published Online April 2009 in SciRes (http://www.SciRP.org/journal/wsn/).

An Energy Balanced Reliable Routing Metric in WSNs

Jian ZHU, Hai ZHAO, Jiuqiang XU
The Northeastern University, ShenYang, China
*E-mail: zhujian*1981710@163.*com*
Received November 13, 2008; *revised February* 16, 2009; *accepted February* 18, 2009

Abstract

In WSNs' applications, not only the reliable end-to-end communications are must be ensured, but also the reduction of energy consumption and the entire network's lifetim e should be optimized. All of the above have become to be an important way to evaluate the performance of routing protocols. In this paper, an optimization model for WSNs' lifetime is firstly advanced. Secondly, the shortage of ETX based routing metric is solved with the help of the optimization model. Thirdly, an energy balanced routing metric is advanced which is called EBRM in this paper. The result of simulation in NS-2 shows that, the EBRM metric can not only prolong the network's lifetime, but also can ensure the reliable end-to-end communication.

Keywords: WSN, Routing Metric, Reliable Communication, Lifetime, Energy Balance

1. Introduction

The WSNs (Wireless Sensor Networks) is a kind of self-organized network which mainly aims at applications. The wireless links are not stable, and the loss of packets happens frequently in communications [1,2]. To solve this problem, some routing metrics are adopted in routing protocol, for example, the ETX (expected transmission) metric can make a most reliable link to be used. But, the WSNs is mainly battery-powered, the energy is restricted, whether the sensor or monitor applications often need a network with more than one year lifetime. If we only consider the reliability of communication, some of the WSNs nodes will be exhausted rapidly. Unfortunately, the few exhausted nodes are always very important to the entire network, if they can't work, the network's performance will be pulled down and the entire network's lifetime will be reduced. So, how to balance the load on the base of reliable communication become to be a key problem in WSNs [3,4].

Aiming at the problems above, an energy balanced reliable routing metric is advanced-EBRM (Energy Balanced Reliable Metric). This metric can not only ensure the reliable communication, but also balance the network's load, and prolong the networks' lifetime.

2. Mode of Lifetime's Optimization

Before optimizing the lifetime of network, we must know that, how to measure the lifetime. In different applications, the common ways are as follow: the ratio of remained active nodes in network [5], packets reception ratio [6] and the time of first blind covering's appearance [7]. The mutual character of above ways is that, while the index of network reaches a set value, the network's lifetime is considered to be over. But, in different applications, it is very difficult to make out a universal index value to judge the network's life.

So, in this paper, we use the time of the network node's first death as the measurement of network's lifetime [8]. This metric's usage range is wider, and it is used more early, it supposes that, all the nodes place the same part in the network. Its excellence is that, it reflects the hypostasis of the lifetime maximization problem, and this hypostasis is network's load balance.

Thus, we can set up the model of network's lifetime. It is supposed that, there are S sensor nodes in a network, every node sends a packet an second, and every node s has D_s paths to destination node r. Make $h_{s,p,r}$ as the hops between node s and node r in path p, if node r doesn't belong to path p, the $h_{s,p,r}$ is set to be $+\infty$. So, the probability of relaying the packet which comes from node s is $s^{tx}_{s,p,r}$, its expression is as follow:

$$\begin{cases} \prod_{k\in K_{s,p,r}} P_s(G_{s,p,k}, l_{s,p,k}), & if\ \ 0 < h_{s,p,r} < \infty \\ 1, & if\ h_{s,p,r} = 0 \\ 0, & if\ h_{s,p,r} = \infty \end{cases} \quad (1)$$

In the above expression:
$K_{s,p,r} \equiv \{k \mid 0 \le h_{s,p,k} < h_{s,p,r}\}$, $G_{s,p,k}$ is the channel gain of correspond links, $l_{s,p,k}$ is the sending power level of

node *k*. The probability of the packets which come from node s received by node *r* is $s^{rx}_{s,p,r}$, and it equals to the probability of the packets sent by node *r*'s upstream node, it is node k and $h_{s,p,k}=h_{s,p,r-1}$. So,

$$s^{rx}_{s,p,r} = s^{tx}_{s,p,k} \quad (2)$$

Therefore, if sensor node *i* want to send some packets, the energy's decrease speed of node *i* is V_E:

$$\sum_{s=1}^{S}\sum_{p=1}^{Ds} A(s^{tx}_{s,p,i}E^{tx}_{s,p,i} + s^{rx}_{s,p,i}E^{rx}_{s,p,i})u_{s,p} \quad (3)$$

And

$$E^{tx}_{s,p,i} = E^{tx}(P_{l_{s,p,i}}) + E^{ack-rx} \quad (4)$$

$$E^{rx}_{s,p,i} = E^{rx} + E^{ack-tx} \quad (5)$$

The $u_{s,p}$ is ratio of path *p*'s holding time which is used by node *s*. So, node *i*'s lifetime can be expressed by: $T_i = \frac{E_i}{V_E}$, E_i is the initialization energy of node *i*.

$$V_E = \sum_{s=1}^{S}\sum_{p=1}^{Ds} A(E^{tx}_{s,p,i}N^{tx}_{s,p,i} + E^{rx}_{s,p,i}N^{rx}_{s,p,i} + E^{ack-tx}_{s,p,i}N^{ack-tx}_{s,p,i} + E^{ack-rx}_{s,p,i}N^{ack-rx}_{s,p,i})u_{s,p} \quad (6)$$

According to the above metric, the WSNs' lifetime can be defined as $T = \min_i T_i$.

So, the problem of WSNs' lifetime can be transformed to be a linear programming problem: Minimizing $1/T$.

$$\frac{1}{T} = \frac{A}{E_i}\sum_{s=1}^{S}\sum_{p=1}^{Ds}(s^{tx}_{s,p,i}E^{tx}_{s,p,i} + s^{rx}_{s,p,i}E^{rx}_{s,p,i})u_{s,p} \quad (7)$$

$$\sum_{p=1}^{Ds} u_{s,p} = 1, \text{ for all s} \quad (8)$$

$$u_{s,p} \geq 0, \text{ for all s, p} \quad (9)$$

The expression (7) indicates the speed of node's energy consumption, it is easy to find that, if we decrease the power consumption in network's communication, the longer lifetime of network can be got, the correlation researches mostly focus on physical layer and link layer. From the expression (8), we can got that, the node *i* is used in D_s paths and following a specifically time ratio $u_{s,p}$, for example, if the ratio $u_{s,q}$ equals to zero, it is said that, the node *i* will not be used in path *q*. So, we can adjust the value of $u_{s,p}$ to solve the above linear programming problem. In this paper, we increase the network's lifetime mainly by balancing the network's load.

3. Energy Balanced Reliable Routing Metric

Because of the complexity and un-reliability in wireless communications, there are many differences between wired network and wireless network, so, their routing protocols are also different. The routing metrics place a more and more important part in routing protocols' design and performance; every routing metric indicates the cost of path selection and routing capability.

While in routing finding or routing table's maintenance, the value of routing metric should firstly be got from routing table, and then decide the next hop according to the metric values. ETX is a metric which aims at high reliable communication [9], and the value equals to the final logic transmission times while one packet wants to be successfully transmitted, it includes retransmissions, the value ETX=1/*pq* (*p* is the forward packet reception ratio, *q* is the reverse packet reception ratio). The ETX value of a path equals to the summation of every hop's ETX in the path.

The ETX mainly aims at reliable communication, however, if only the ETX is used in WSNs, it maybe cause a too many hops path, and the high quality paths are frequently used. So the lifetime of the high quality paths will be decreased, thereby, the entire network's lifetime and quality will be decreased. On the basis of ETX, a reliable and network load balanced routing metric—EBRM is advanced.

The main idea of EBRM is that, the time ratio of a node is according to the node's remainder energy, for example, the initialization energy is set to be E, and the energy has N levels, in several reachable paths, the M paths with the highest energy level are firstly selected, and secondly, the most reliable path in the selected M path is finally selected. The routing method can not only ensure the end-to-end reliability, but also can decrease the load of the nodes whose energy is in lowest level. So the load of network is optimized, and the lifetime of the network can be prolonged.

The EBRM is not a routing protocol, it is a metric, so, it can only be used in a routing protocol, it is said that, the existed protocol's metric will be changed by EBRM. The AODV [10] is a very classical protocol; it is very suitable for WSNs' applications. The most important is that, the AODV uses hello packets to maintenance the routing table, the hello packets are useful for EBRM. The metric of AODV is Hops; it selects the path which has the least Hops. Because of the character of wireless channel, the Hops-AODV can't be used in WSNs. So the AODV is improved in this paper, it is called EBRM-AODV; the main processes are as follow:

1) In the network initialization, every nodes send fifty packets to each other, and compute the forward and reverse packet reception ratio *p* and *q*, so, the ETX between two neighbor nodes can be got; In this paper, the remainder energy of a node is defined to be four level {Elevel | Elevel=1,2,3,4}, actually the number of energy level can equal to be any natural numbers according to the requirements of user. A small number of energy levels will cause a low performance in energy balance, but a high performance in reliable communication, for example, if the number of energy level is set to be one, it means that, all the paths will always have the same energy level, and the most reliable path will be in used until

it is dead; Accordingly, a big number of energy level will cause a high performance in energy balance, but a low performance in reliable communication. In our experiment, we define the energy to be four levels subjectively.

2) The source node *s* broadcasts a routing request packet (RREQ). The RREQ of AODV is advanced as Figure 1, the original metric-Hops is replaced by ETX and minElevel, the value of ETX in Figure 1 is ETX of a path, it is an accumulative total, for example, if there are three hops between two nodes, every hop has a ETX, and the path's ETX equals to the summation of the three hop ETXs; The value of minElevel is the lowest energy level of all the nodes in a candidate path.

3) The relay node M_i which receives the RREQ adds the $ETX_{i,i-1}$ (the ETX between node M_i and node M_{i-1}) and the current ETX value in Figure 1. So, while the RREQ reaches to a destination node, the ETX in Figure 1 equal the path's ETX.

4) At the time of sending packets, source node *s* will firstly broadcast RREQ to find out the reachable paths P_i to destination node *d*, after the RREQ reaches in *d*, a packet called RREP will be send back to *s* in paths P_i. In the broadcasting, every relay node which receives the RREQ will count its energy level, if it is less than the minElevel which is recorded in received RREQ, the value of minElevel in RREQ packet will be updated to be the node's lower energy level.

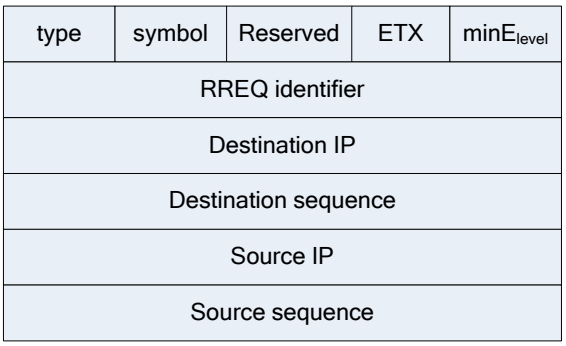

Figure 1. The advanced format of RREQ.

5) After receiving the RREQ, the destination node will firstly select several paths with highest energy level. In these paths, the most reliable path can be got by the use of ETX.

6) The RREQ is sent periodically by source node to update the routing table, and check the power levels' change of the nodes. Along with the usage of nodes, if a currently used path's minElevel is lower than a candidate path's, then, the candidate path will be used. By this, the network's load can be balanced, and the energy cost is also balanced.

The flow figure of EBRM-AODV is as follow:

So, while the EBRM is used in a network, the recorded information will be updated frequently, the path which has a bigger minElevel will be selected. This means that, if a path's energy is decreased, the EBRM will select another path which has more energy. So, every path's lifetime is prolonged, and the quality of the network is advanced.

4. Simulation of EBRM Metric

The EBRM's capability is analyzed by the result of simulation in NS-2. The scene is as follow: there are eighty nodes in a 100m×100m square area, the detailed parameters of nodes are as Table 1:

The routing protocol is AODV whose routing metric is Hops, ETX or EBRM; the three metrics' capability will be compared. In the simulations, the Energy Model is used, and the parameters of a node are set to be as follow: the initial energy equals to 1, and every packet's sending costs 0.002, every hello packet's cost 0.001 and every packet's receiving costs 0.0005.

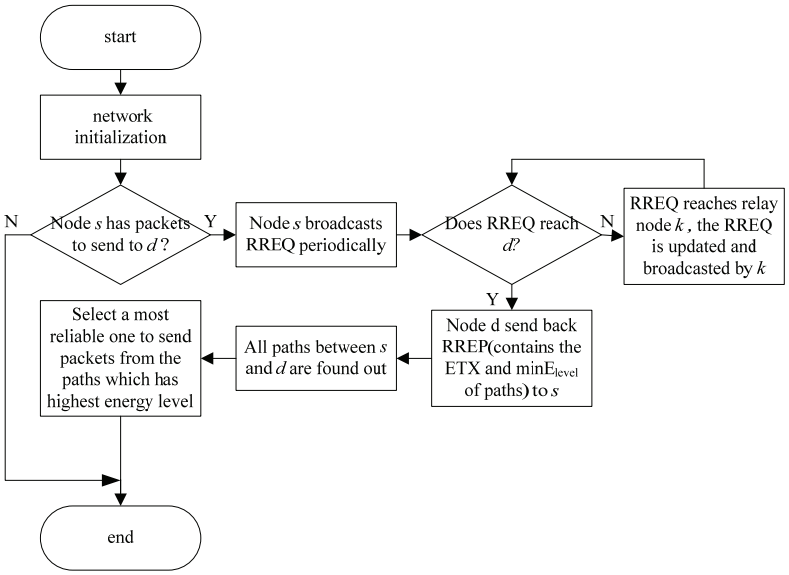

Figure 2. The flow figure of EBRM-AODV.

Table 1. The detailed parameters of nodes in NS-2.

Parameter	Value
Nodes distribution	Random
Channel bandwidth	250kbps
Frequency	2.4GHz
Wireless model	Shadowing
MAC protocol	IEEE 802.15.4
Power for transmission (mWatt)	2.0
Power for idle (mwatt)	1.0
Power for reception(mwatt)	1.0
Power for sleep (mwatt)	0.001
Power for sleep/idle transition (mWatt)	0.2
Time for sleep/idle transition (s)	0.005

Aiming at the three metrics' capabilities, two experimentations are designed. The first experiment is that, the *plr* (packet lost ratio) and the remainder energy are tested without packet retransmissions; the second experiment is that, the network's lifetime with different reliability requirements is tested with packet retransmissions.

In the first experiment, the *plr*'s calculation is

$$P_{\text{lost}} = \frac{N_{source} - \text{N}_{\text{destination}}}{N_{source}} \quad \textbf{(10)}$$

The N_{source} is a number of the packets which are sent by source node, $\text{N}_{\text{destination}}$ is a number of the packets which are received by destination node, and the result is as Figure 3.

It shows that, the routing's set up is almost finished after thirty seconds, the *plr* of ETX-AODV is lowest, this is because that, the ETX metric mainly aims at reliable communications, however, the Hops metric aims at shortest path, it doesn't consider the reliability, so, Hops-AODV causes a highest *plr*. The EBRM metric gives attention to energy balance, so, its reliability is a little bigger than Hops' and smaller than ETX's.

In the same setting, the relationship between the average remainder energy of all nodes in entire network and time is shown in Figure 4.

Figure 4 shows that, the EBRM metric can cause lower energy consumption than ETX metric, and cause higher energy consumption than Hops metric. This is because that, Hops-AODV aims at shortest path, and shortest path can decrease the number of working nodes, so the shorter path will cause lower energy consumption.

The ETX metric will not select the shortest path to transmit packets. For a low *plr*, it only selects the path with highest reliability, so it causes lower average remainder energy than EBRM.

In the second experiment, a retransmission mechanism is added into IEEE802.15.4 to ensure the reliability communication. With the increase of reliability, the three metrics based on network's lifetime are shown in Figure 5.

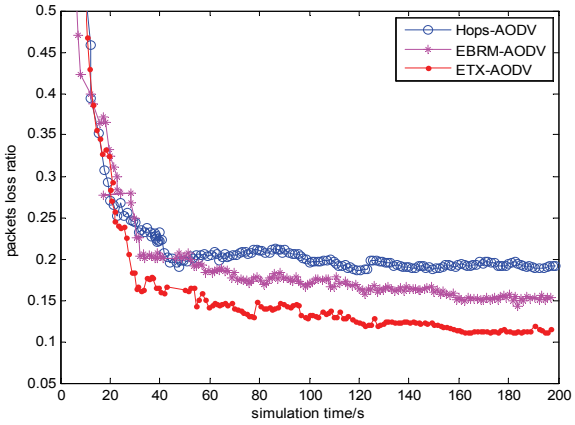

Figure 3. The relationship between *plr* and time.

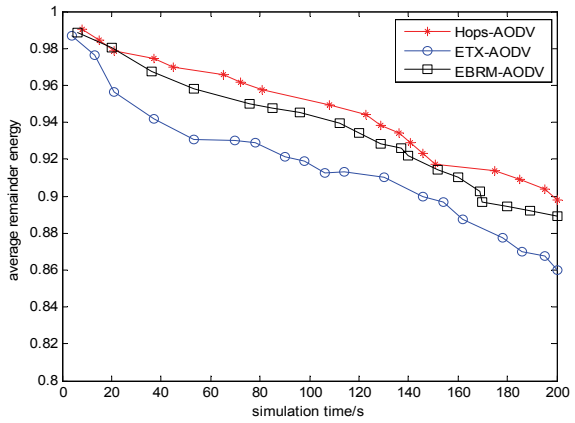

Figure 4. The relationship between remainder energy and time.

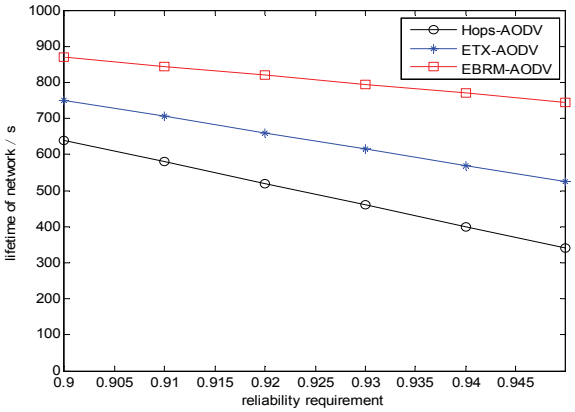

Figure 5. Lifetime with different reliability requirements.

From Figure 5, the EBRM metric can cause a longest lifetime, and with the reliability's increase, the three lifetimes are all decreased. The lifetime with Hops metric drops fastest, it is because that, Hops based protocol will cause a large number of retransmission packets, it will not only consume a mass of energy, but also can make some important nodes dead quickly. The ETX metric considers the reliability, and the number of retransmission packets is decreased, so it will decrease the energy

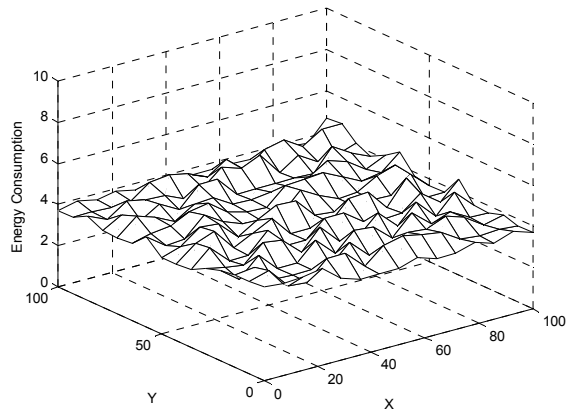

Figure 6. Energy consumption in energy balanced network.

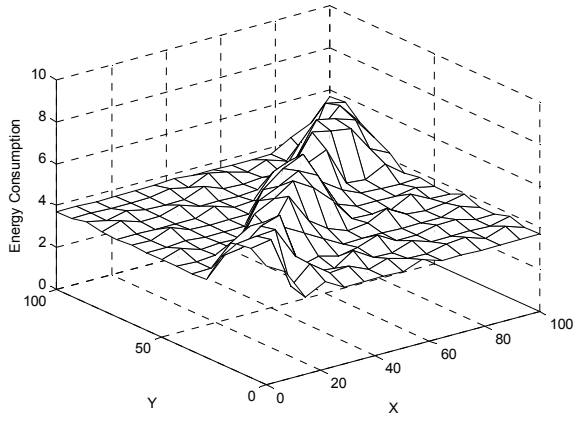

Figure 7. Energy consumption in no energy balance network.

consumption. But, ETX doesn't consider the entire network's energy balance; some important nodes will die quickly as the Hops metric.

To describe the energy balance lively, the result of energy balanced network and no energy balance network in a same setting are shown in Figure 6 and Figure 7.

In Figure 6 and Figure 7, axis X and axis Y construct a square area where the nodes are distributed. The two figures show that, the energy consumption in Figure 7 is very unbalanced, some nodes are consumed heavily, but, the other nodes are consumed lightly. While the heavily consumed nodes dead, the entire network is almost dead, so, the lifetime of the network is decreased heavily. In Figure 6, the problem of energy balance is solved, the network's load is balanced in the all nodes, every node's energy is almost exhausted, this can prolong the network's lifetime as long as possible. So the EBRM metric is advanced, it can balance the energy consumption and ensure the reliability, the entire network's lifetime is prolonged.

5. Conclusions

This paper optimizes the WSNs' reliability and lifetime, and advances a routing metric called EBRM. From the result of simulation, the metric can balance the entire network's lifetime by balancing the energy consumption on the base of reliable communication, this metric is more suitable for low reliability and energy restricted WSNs' applications.

6. References

[1] I. F. Akyildiz, W. Su, Y. Sankarasubramaniam, *et al*., "A survey on sensor networks," [J]. IEEE Communications Magazine, 40(8), pp. 102−105, 2002.

[2] C. Suh, Y. B. Ko, D. M. Son, *et al*., "Energy efficient cross-layer MAC protocol for wireless sensor networks," [A]. Proceedings of the APWeb 2006 International Workshops: XRA, IWSN, MEGA, and ICSE[C]., Harbin, Springer Verlag, pp. 410−419, 2006.

[3] H. L. Van, T. Nieberg, J. Wu, *et al*., "Prolonging the lifetime of wireless sensor networks by cross-layer interaction," [J]. IEEE Wireless Communications, 11(6), pp. 78−86, 2004.

[4] I. Y. Kong and W. J. Hwang, "Lifetime maximization by cross-layer interaction in wireless sensor networks," [A]. Proceedings of the 8th International Conference Advanced Communication Technology (ICACT 2006) [C]. Phoenix Park: Institute of Electrical and Electronics Engineers Computer Society, pp. 2055−2060, 2006.

[5] P. J. Wan, G. Calinescu, and X. Li, "Minimum-energy broadcast routing in static ad-hoc wireless networks," [C]. Proceedings of INFOCOM'01, Anchorage, AK, pp. 1162−1171, 2001.

[6] C. K. Toh, "Maximum battery life routing to support ubiquitous mobile computing in wireless ad hoc networks," [J]. IEEE Communications Magazine, pp. 138−147, 2001.

[7] M. Bhardwaj, T. Garnett, A. P. Chandrakasan, "Upper bounds on the lifetime of sensor networks," [C]. Proceedings of ICC, Helsinki, Finland, pp. 785−790, 2001.

[8] S. Singh, M. Woo, and C. S. Raghavendra, "Power-aware routing in mobile ad hoc networks," [C]. Proceedings of the 4th Annual ACM/IEEE International Conference on Mobile Computing and Networking, Dallas, United States, ACM Press, 1998.

[9] D. Couto, "High-throughput routing for multi-hop wireless networks," [D]. Massachusetts, Massachusetts Institute of Technology, pp. 55−60, 2004.

[10] C. Perkins and E. Royer, "Ad hoc on-demand distance vector routing," Proceedings of the 2nd IEEE Workshop on Mobile Computing Systems and Applications, 1999.

Wireless Sensor Network, **2009, 1, 1-60**
Published Online April 2009 in SciRes (http://www.SciRP.org/journal/wsn/).

Extending the Network Lifetime Using Optimized Energy Efficient Cross Layer Module (OEEXLM) in Wireless Sensor Networks

T. V. Padmavathy
Department of Electronics and Communication Engineering, SSN College of Engineering, Chennai, India
Email: Padmavathytv@ssn.edu.in
Received February 11, 2009; *revised March* 10, 2009; *accepted March* 13, 2009

Abstract

In wireless sensor network, the primary design is to save the energy consumption as much as possible while achieving the given task. Most of recent researches works have only focused on the individual layer issues and ignore the importance of inter working between different layers in a sensor network. In this paper, we use a cross-layer approach to propose an energy-efficient and extending the life time of the sensor network. This protocol which uses routing in the network layer, and the data scheduling in MAC layer. The main objective of this paper is to provide a possible and flexible approach to solve the conflicts between the requirements of large scale, long life-time, and multi-purpose wireless sensor networks. This OEEXLM module gives better performance compared to all other existing protocols. The performance of OEEXLM module compared with S-MAC and directed diffusion protocol.

Keywords: Routing, Medium Access Control, Life Time of the Network, Energy Efficiency, OEEXLM Module, Wireless Sensor Networks

1. Introduction

Wireless sensor network consists of large number of sensor nodes are randomly distributed in a region. Each node has a limited energy supply and generates information when ever event occurs that needs to be communicated to a sink node. The focus of this paper is on the computation of optimal energy usage for data transfer and link schedule that maximize the network lifetime. However most wireless sensor network energy consumption operations involve sensing, computing, and communicating [1]. Generally, communication between nodes consumes more energy than local processing or collecting data operation. The geographical nature of the deployment space of nodes makes quasi impossible the replacement or the recharging operations of batteries. The challenge is to economize energy inside every node in order to maintain as long as possible the network functionality.

2. Related Works

Many research works are developed for energy efficiency at each layer of protocol stack by proposing new algorithms and protocols. In particular, MAC layer was of great interest for many researchers because it is considered as an important source of energy wastage such as overhearing, collision, control packet overheads and idle listening [2].

In order to decrease or if possible to eliminate these various sources of energy wastage, several protocols has been proposed during last years and which are divided into two main classes: Schedule based protocol TDMA and Contention based protocol.

In TDMA protocols [3] are employed to avoid collisions by associating a slot time for each sensor node in a given cluster. This protocols more complex in the WSN where the nodes in general have a same priority and very limited resources. The Contention-based protocols are known as CSMA-based are usually used in the multi-hop wireless networking. But this protocol generates collisions due to these useless retransmissions which cause energy consumption wastage and time consuming in data transmission.

Some of the power control problems are discussed in [4,5]. Approaches at MAC layer are Dermikol *et al.* [4] infers that some pros and cons of the some of the existing protocol. One of the first attempts at MAC protocol for WSN is PAMAS, which reserves battery power in-

telligently powering off users that are not actively transmitting or receiving packets. This protocol decreased the energy consumption of the network but maximum latency occurs. Raghavendra *et al.* [5] the Power Aware Medium Access protocol and Signaling (PAMAS) is a CSMA based protocol in which the nodes that are not actively transmitting or receiving should power themselves off. The protocol requires the nodes to have two separate channels (control and data), which will require two radios at each node increasing the cost, size and complexity of the sensor design.

Existing MAC protocol [6,7] turn off the transceiver when there is no communication between the nodes also the power savings in these papers results reducing the idle listening power but also decreasing the collisions. In these papers they proposed adaptive listening incurs overhearing. Sleep and listen periods are predefined and constant, which decreases the efficiency of the algorithm under variable traffic load.

A new generation of MAC protocols that is Cross-layer MAC protocols using several layers in order to optimize energy consumption has been emerged. These layers can be divided into interaction mode or unification mode. In the interaction mode, the MAC protocol is built by exploiting the data generated by other adjacent layers.

Approaches at network layer in WSNs are mostly used to implement the routing of the incoming data, as quoted in [8]. It is known that generally in multihop networks the source nodes cannot reach the sink directly. Therefore, intermediate sensor nodes have to relay their packets. Generally, the implementation of routing tables offers the solution. These routing tables contain lists of node options for any given packet destination Definition of the routing tables is the task of the routing algorithm along with the help of the routing protocol for their construction and maintenance.

MAC-CROSS Protocol [9] is an example of Cross-layer approach which allows the interaction between MAC and information of the network layers by making only the communicating nodes in listening mode and by putting other nodes into sleep mode. In order to avoid collisions, MAC-CROSS uses the control messages RTS/CTS/ACK. On the other hand, a Cross-layer design mode by unification requires the development of only one layer including at the same time functionalities of considered layers.

In this paper, a unified cross layer module XLM [10] is developed which achieves efficient and reliable event communication between the nodes with minimum energy expenditure. But in this protocol the end-to-end delay increases for low value duty cycle. When the duty cycle is low δ=0.1, 14% of the transmitted packets are dropped due to retransmission timeout. Because sender nodes cannot find any neighbors that satisfy the constraints.

Weiyan Ge *et al.* [11] addressed the rate optimization for multicast communications at the media access control (MAC) layer, and explore transport layer erasure coding to enhance multicast reliability in wireless sensor networks. In this approach they are not addressed the energy consumption and end-to-end delay.

3. Proposed OEEXLM Module

The proposed cross layer approach replaces the entire traditional layer protocol architecture that has been so far used in WSNs. In this protocol we integrate the medium access control and routing to improve the performance of the network. The communication in OEEXLM module is based on initiative concept. This module allows the each node to decide whether it can participate in communication or not. Consequently, this protocol uses adaptive receiving, stagger scheduling algorithm and logical link decision algorithm.

A node starts a transmission by transmitting to its neighborhood an RTS packet to indicate that it has a packet to send. Upon receiving an RTS packet, each neighborhood node i decide to participate to communication or not, that decision can be determined by an initiative "*I"* defined as follows:

$$I=\begin{cases}\beta = 1 \ if \begin{pmatrix} TA > R+T \\ \gamma = \gamma_{th} \\ E_{rev} = E_{rev}^{thd} \end{pmatrix} \\ = 0 \ otherwise \end{cases} \quad (1)$$

The initiative is set to 1 if all four conditions are true or satisfied. Out of four conditions, the first two conditions related to MAC layer and next two conditions related to network layer. The first condition checks event β occurs or not. If β = 1 then the remaining three conditions checked by the node, otherwise the nodes are go to sleep mode.

Because of this, idle listening and overhearing are avoided. The second condition is adaptive receiving scheme, the receiver node wait for TA seconds if the node does not receive any packets from upper layer it goes to sleep state. The third condition is the node will check the buffer size γ_{th} if the size is less than threshold it will choose the alternate path to reach the destination. Fourth condition is that source node from upper layer checks the lower layer receiver node energy if it is greater than threshold E^{thd}_{rev} then it will transmit packet otherwise it will choose the alternate path.

Using this initiative concept, OEEXLM module overcomes collision, overhearing, idle listening and improve the throughput, link reliability and extend the life time of the network.

3.1. Basic Terms Used in OEEXLM

The following assumption can be considered for OEEXLM protocol to study the performance. The network topology used in this protocol is grid architecture. Data flows from n layer to $n-1$ layer until the data packet reached the destination. For simulation MICA2 mote specification is considered. In this protocol the value of duty cycle is denoted by δ and is defined as ratio of the time a node is active. The duty cycle is varied with re-

spect to data transmission. The sleep time for each node is T_{sleep} sec. The listen period of each node is less than or equal to transmission period of upper layer. Transmission period each layer is 50ms. With in 50ms if lower layer node does not receive any data from upper layer it will wait for TA sec and go to sleep.

3.2. Initiation of Transmission

When the event occurs that is $\beta = 1$ layer n node has a data packet to transmit, it sends RTS signal to the lower layer, the lower layer sends the CTS signal to the upper layer with response the CTS signal the layer *n* sends the data to the layer (*n*−1) for 50ms.During the receiving period, if a node senses that the channel is idle and its neighbours are not communicating for a time TA, it will go to sleep until its subsequent sending periods. After receiving the packet from n layer, the *n*-1 layer route the packets to the destination, each source node determines a path to the destination by selecting a lower layer node under its coverage randomly. Thus messages flow in the correct direction, but do not use the same path every time. Thus this data exchange scheme provides both collision avoidance and reliable retransmission.

4. Mechanism of OEEXLM

Figure 1 explains the mechanism of OEEXLM module. In this module we integrate the MAC and network layer. In MAC layer we proposed Power Efficient MAC protocol which is used to overcome idle listening, collisions, Hidden terminal problem, and also to provide a low latency compared to other existing MAC protocols. The PE-MAC uses the three algorithms to achieve the energy efficiency.

4.1. Clock Synchronization Algorithm

In clock synchronization algorithm layer *n* comprises the source nodes. Initially the nodes in layer *n* are in sending mode for 50ms while those in the layer (*n*−1) are in receiving mode. The remaining nodes are in sleep state. Assume that the source nodes generate packets (layer−n).

As the next layer nodes are in the receiving mode, the source nodes can transmit the packets directly without checking the status of the lower layer nodes. The packets are stored in the buffer space of the lower layer nodes. Once the receiving period of layer (*n*−1) nodes ends, the sending period for layer (*n*−1) starts. The layer (*n*−2) nodes shift from sleep mode to receive mode. The remaining nodes enter the sleep mode.

4.2. Logical Link Decision Algorithm

The LLD algorithm is implemented in this protocol to ensure that two source nodes do not transmit the packets to the same receiver at the same time. This algorithm is implemented initially when each source node determines a link to the sink. When all the source nodes determine their links, the links are compared to ensure that there is no overlap in the existing links. If there is an overlap, the LLD algorithm uses a logical link decision to get the new link to the sink.

4.3. Adaptive Receiving

In Adaptive Receiving algorithm, layer *n* sends RTS packet to the lower layer *n*−1, the lower layer sends the CTS signal to the upper layer *n*. With response the CTS signal from layer *n*−1, the layer n sends the data to the layer *n*-1 for 50ms.Adaptive receiving scheme employs a time interval TA to handle traffic varies.

During the receiving period, if a node in the *n*−1 layer senses that the channel is idle and data from n layer are not communicating for a time TA, it will go to sleep. Suppose with in 50ms if the layer *n*−1 senses any data from the upper layer *n* it wakes up and receive the data. This adaptive receiving scheme reduces the packet drop and improves the throughput of the network.

In network layer we proposed two algorithms: a congestion control and alternate path algorithm. These two algorithms are used to improve the lifetime of multihop sensor network by avoiding the collision.

4.4. Alternate Path Algorithm

In alternate path algorithm, each has routing table. Before route the data packet each source finds a multiple path to the sink. In this each source node initiate *HELLO* message to all lower layer nodes.

The *HELLO* message contains source ID, type of node whether it is sink or intermediate node and energy level which is shown in Figure 2.

Each node in the lower layer updates it table once it receives the *HELLO* message. If any node in lower layer gets more than one *HELLO* message it sends the negative acknowledgement *NACK* signal to the corresponding source node. Then that particular source node chooses the alternate path to reach the sink.

After setting an alternate route the nodes in the routing path check its energy level of receiving node. If the energy level less than the threshold E^{thd}_{rev} again the node choose the alternate path by sending *HELLO* message and the routing table is updated.

4.5. Congestion Control Mechanism and Algorithm

The congestion in the network is due to two traffic. One is due to generated packet that is whenever node detect the events it will generate the data packets and that is to be transmitted to the destination through intermediate nodes. The rate of generated packets at the node *i* is denoted by λ_i.

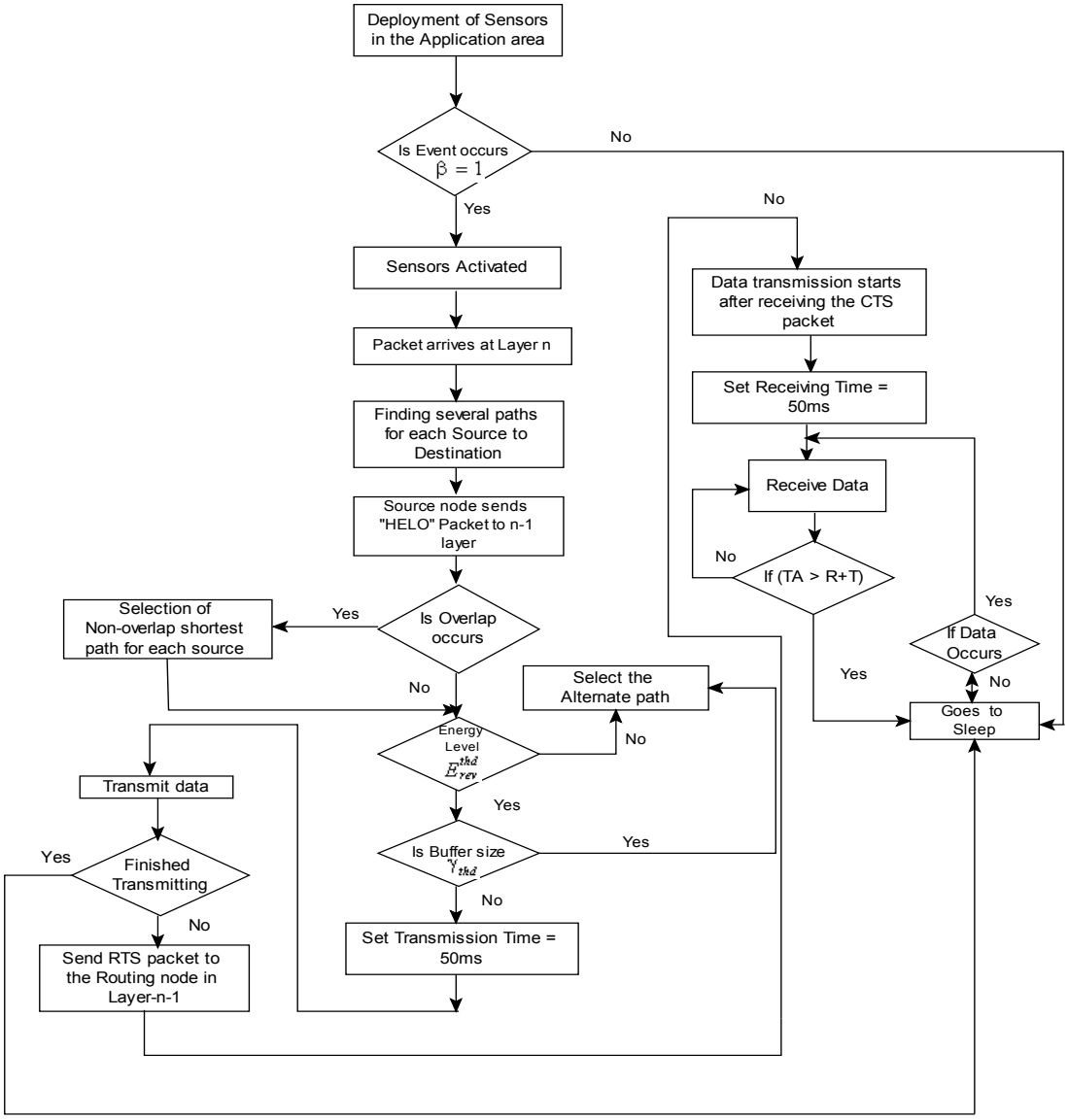

Figure 1. Mechanism of OEEXLM.

Since the network is a multi hop each nodes plays dual role that is it act as source as well as router. During the transmission each node in lower layer receives the data packet from the upper layer until the data packet reached at the destination. These packets are referred as relay packets. If the n−1 layer node receive the data packets from layer n the rate of relay packet of node i of n-1 layer is $\lambda_{i,n-1}^{n}$. The input rate of the buffer for the node i is depends on the rate of relay packets $\lambda_{i,n-1}^{n}$ and the rate of generated packets λ_i. In OEEXLM module the rate of input packet at node i's buffer α_i, can be represented as

$$\alpha_i = \lambda_{i.} + \lambda_{i,n-1}^{n} \quad \textbf{(2)}$$

The node is active for a fraction of duty cycle δ = 50ms. Hence the average time taken a time to transmit and receive data packet can be given by

$$T_{tx} = (1 + e_i)\alpha_i \cdot t_{pkt} \quad \textbf{(3)}$$

$$T_{rx} = \lambda_{i,n-1}^{n} t_{pkt} \quad \textbf{(4)}$$

where t_{pkt} is the average time taken to successfully transmit a packet to another node and e_i is the error packet rate.

The proposed OEEXLM module avoids packet drops due to congestion by not allowing upper layer nodes to transmit data packet if there is not available buffer size γ this is can be controlled by congestion control algorithm. A lower layer node changes the path of transmission based on its buffer status. During transmission, the lower layer node i allow P_i packets to be transmitted by the upper layer nodes. Figure 3 shows the buffer queue model of the node.

Given the condition that the lower layer node has proportionally higher probability to access the medium,

Source ID	Type of Node	Energy level
2 Byte	1 Byte	4 Byte

Figure 2. HELLO message packet format.

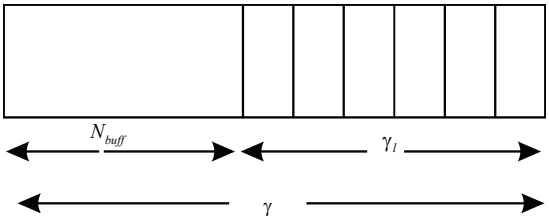

Figure 3. Buffer queue model.

even then the lower layer node may not be able to forward all P_i packets. So, in the next transmission, the lower layer node will have some packets from the previous transmission, which might cause Congestion within few successive transmissions. Therefore, for each transmission upper layer nodes check the routing table if the buffer size γ less than the buffer threshold γ_{thd} upper layer node takes the alternate path. Maximum number of packet hold by the buffer is N_{buff}. The transmission only occur when $\gamma > \gamma_{thd}$

$$\gamma_{thd} = N_{byff} \geq \sum_{i=0}^{i=n} p_i \quad \textbf{(5)}$$

where $N_{buff} = \gamma - \gamma_l$.

As a result of congestion control algorithm, the OEEXLM module avoid the layer to layer congestion occur in the networks. Because of this energy consumed by the node is reduced there by improving the life time of the network.

The medium control access scheme uses three algorithms to improve the energy efficiency and in network layer we use two algorithms to improve the life time of the networks. These two layers are integrated by using initiative conditions as per Equation (1).

5. Network Topology

Figure 4 shows the data flow for the OEEXLM module. The nodes in the network operate in three different modes-sleeping, receiving and sending. Each node goes to sleep periodically to save energy and then wakes up and listens to see if any other node wants to talk to it. During sleep, the node turns off its radio; therefore the energy waste due to idle listening can be reduced.

The nodes with same layer-count are given the same schedule, and the sending and receiving periods are staggered layer by layer such that when one node is in sending mode, its lower-layer node is in receiving mode. After receiving a message from an upper-layer node, each node can transmit it to the lower-layer node in the subsequent sending period. So a packet can be transmitted to sink nodes through multi-layers fleetly and the end-to-end latency is reduced.

5.1. Performance Evaluation

The Table 1 shows the simulation setup used for simulation.

5.1.1. Latency Vs Network Area (MAC)

Figure 5 infers that in S-MAC a node has to wait till its neighbouring node as to awake to transmit the message to it. This results there will be some amount of delay in S-MAC protocol, which is absent in OEEXLM module. In OEEXLM module whenever a node is in send state, the lower layer node is in receiving state. So the source node can transmit the message to the lower layer without checking whether the lower layer node is listening or sleeping mode. Hence the source node can transmit its message fleetly to the sink through multi layers.

5.1.2. Energy Consumption Vs Network Area (MAC)

The Figure 6 infers that depicts the energy consumption of S-MAC and OEEXLM module. The comparison is made for a simulation setup with ten layers, ten nodes in each layer and a four sink. The graph shows that OEEXLM module protocol uses less energy than S-MAC. This is because the idle listening dominates the energy consumption in S-MAC protocol but TA can make OEEXLM module go to sleeping mode earlier, and the energy consumption is reduced. The energy consumption of OEEXLM module is 35% -83% les than existing S-MAC protocol.

5.1.3. Latency Vs Number of Hop (MAC)

The Figure 7 shows that the latency encountered in OEEXLM module compared with that in S-MAC with respect to number of hops. Obviously the latency of OEEXLM

Table 1. Simulation setup.

Parameters	Value
Transmission Range	250 m
Network Area	100 x 100
Number of Sensors	100- 1500
Packet rate	5 pkt/sec
Packet size	512 bytes
Radio Bandwidth	76kbps
Transmitting Power	75mW (270J)
Receiving Power	36mW (129.6J)
Power Consumption in Sleep mode	100μ W (0.36 J)
Sending and Receiving Slot	50msec
Type of mote	Mica2
Inital energy of sensor node	2KJ
Energy Threshold E^{thd}	0.001mJ

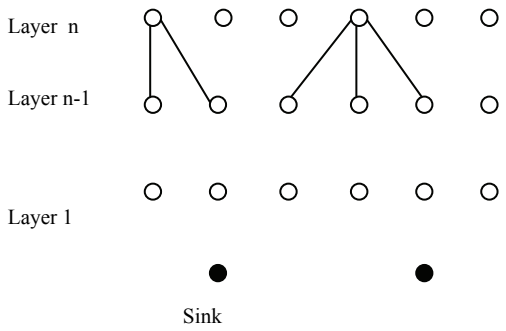

Figure 4. Data flow diagram for OEEXLM module.

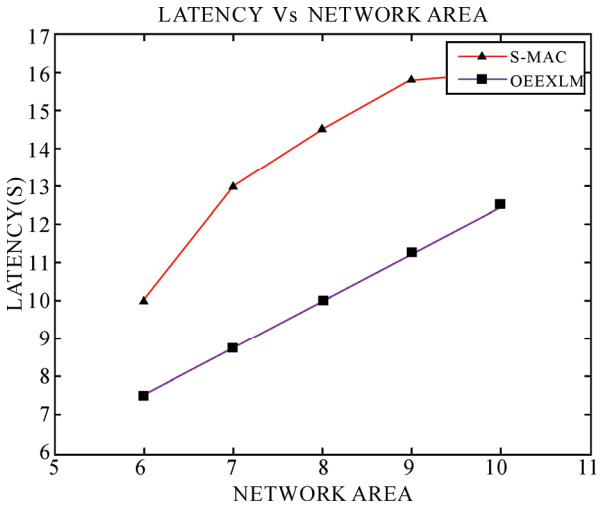

Figure 5. Latency vs network area.

module is lesser than that in the S-MAC because of staggered scheduling algorithm. In S-MAC a node has to wait till its neighbour is awake to transmit the message to it. This problem is not occurring in OEEXLM module. In OEEXLM module whenever a node is in send state, the lower layer node is in receiving state. So the source node can transmit the message to the lower layer without checking whether the lower layer node is listening. Hence the source node can transmit its message fleetly to the sink through multi layers.

5.1.4. Latency Vs Number of Hops (Routing)

Figure 8 infers the delay as a function of the number of nodes in the WSN. The delay increases with the number of hops increasing. Our simulation shows the average delay of the proposed protocol is better than that of the directed diffusion. This is because in OEEXLM module, for each transmission each node in the routing checks the buffer condition, so that no queue of data occurs in the buffer.

Due to alternate path algorithm the shortest delay occur compared to other schemes. As we expected, data packets are routed through different node-with the help of proper design of algorithm in routing. Hence, the network congestion can be avoided.

5.1.5. Energy consumption Vs Number of Nodes (Routing)

Figure 9 infers that energy consumption per node versus number of nodes. The value of node energy consumption gives the average energy dissipated by the node in order to transmit the packet from source to drain. The same metric is used in [6] to determine the energy efficiency level of WSNs. It is calculated as follows:

$$Node\ Energy\ Consumption = \frac{\sum_{i=1}^{N}\left(e_i, initial - e_i, resi\right)}{N\sum_{j=1}^{S} data\ P_j} \quad (6)$$

where N is the total number of nodes, $e_i, initial$ initial energy of nodes, $e_i, resi$ is the residual energy of the nodes, S is the number of sinks and P_j is the number of data packets received by the sink j.

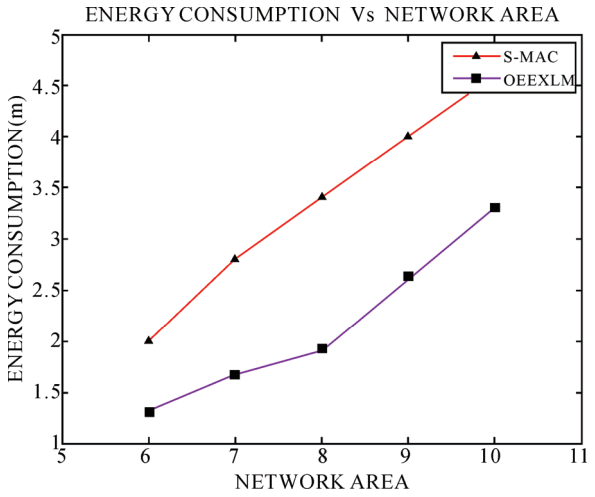

Figure 6. Energy consumption vs network area.

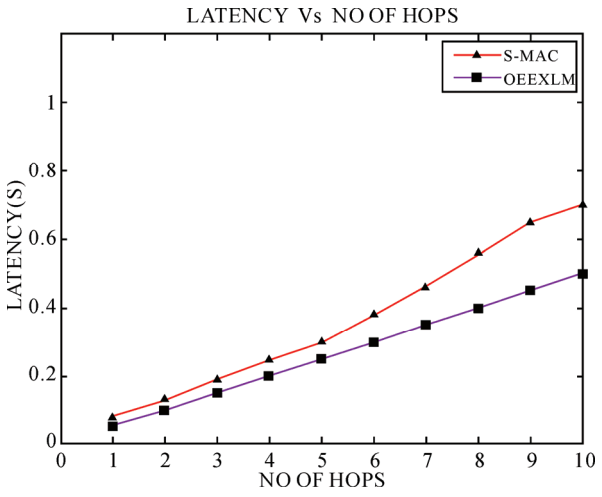

Figure 7. Latency vs number of hops.

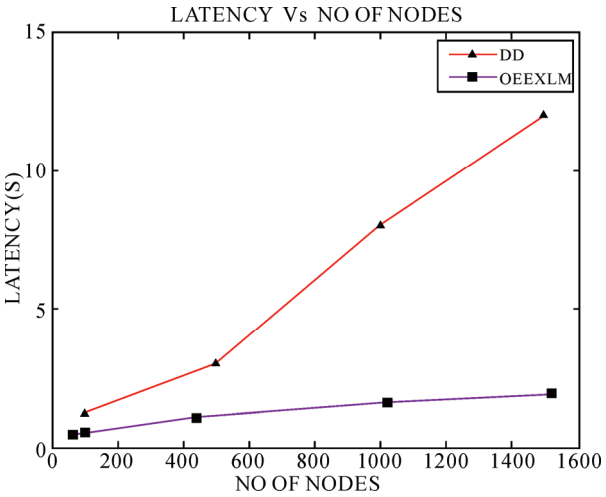

Figure 8. Comparison of latency vs number of hops with DD.

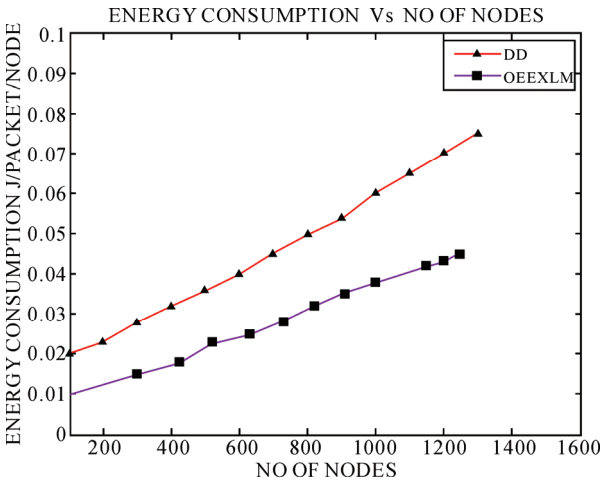

Figure 9. Energy consumption vs number of nodes.

The simulation result infers that there is lower node energy consumption in CRLS protocol over the other schemes., The energy consumption of nodes in OEEXLM module is 34% to 84% lesser than when compared with directed diffusion. This results shows that the energy efficiency of OEEXLM module is stable and has little impact by the increase of the network size, while the performance of other schemes degrades with larger network size.

5.1.6. Network Life Time

The system lifetime is defined as the number of rounds for which 75% of the nodes are still alive. CRSL The transmitted and received energy costs for the transmission of a k-bit data message between two nodes separated by a distance of r meters are given by Equations (6) and (7), respectively.

$$E_t(k,r) = E_{tx}k + E_{amp}(r)k \quad \textbf{(7)}$$

$$E_r(k) = E_{rx}k \quad \textbf{(8)}$$

In Equation (7) $E_t(k,r)$ denotes the total energy dissipated in the transmitter of the source node, while $E_r(k)$ in Equation (8) represents the energy cost incurred in the receiver of the destination node. Parameters E_{tx} and E_{rx} are per bit energy dissipation for transmission and reception, respectively, and $E_{amp}(r)$ denotes the energy required by the transmitted amplifier to maintain an acceptable radio for transferring data reliably. The free-space propagation model is applied, and the transmit amplifier $E_{amp}(r)$ is given by Equation (9)

$$E_{amp} = \varepsilon_{FS} r^2 \quad \textbf{(9)}$$

where e_{FS} is the transmitted amplifier parameter. The set of parameter given in [7,8]. e_{FS} =10 pJ/b/m^2.

From Figure 8, we infer that the network lifetime is increased by using the alternate path and congestion control algorithm. The network lifetime is given in terms of rounds till which 75% of nodes are alive. A network is assumed to be useless when one of the sensor's energy is below the threshold.

5.1.7. Data Packet Delivery Ratio

Data packet delivery ratio can be calculated as the ratio between the number of data packets that are sent by the source and the number of data packets that are received by the sink. It can be denoted as R

$$Data\ Delivery\ Ratio = \frac{Successfully\ delivered\ data}{Required\ data} \quad \textbf{(10)}$$

This parameter R indicates both efficient of the routing protocol and the effort required to receive data. In the ideal scenario the ratio should be equal to 1. If the ratio falls significantly below the ideal ratio, then it could be an indication of some of the packet dropped because of faults in the protocol design. However, if the ratio is higher than the ideal ratio, then it is an indication that the sink receives a data packet more than once. It is not desirable because reception of duplicate packets consumes the more energy. The relative number of duplicates received by the sink is also important because based on that number the sink, can possibly take an appropriate action to reduce the redundancy.

Figure 11 shows the data packet delivery ratio of DD and OEEXLM modules. To eliminate packet loss we use a rate of 5 packets/second. It is found that the delivery ratio of the two protocols increase as the node density increases. When node density is high, there are more nodes available for data forwarding, and this increases the delivery ratio. Directed diffusion protocol offers less packet delivery rates, compared to OEEXLM module because it does not adapt well its behavior to network size increase. The OEEXLM module has maintained constant delivery rates throughout the simulated scenarios because the paths are selected based on the energy availability and buffer size.

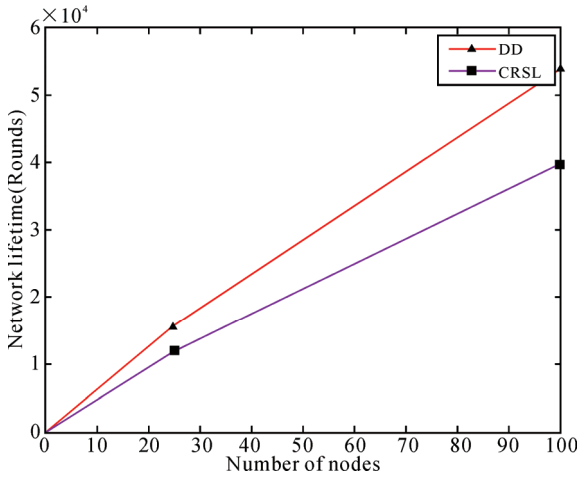

Figure 10. Network lifetime.

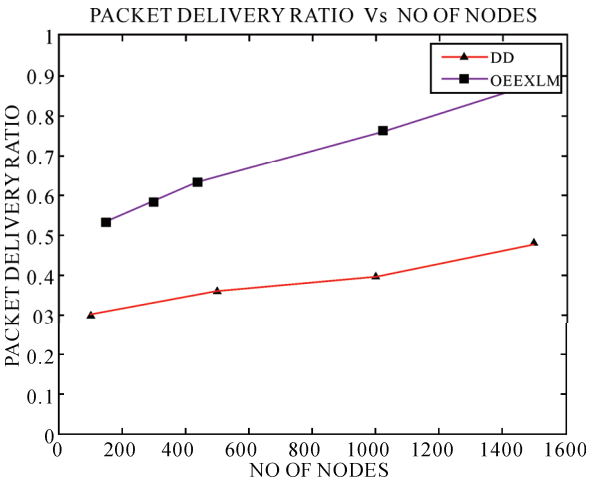

Figure 11. Packet delivery ratio vs number of nodes.

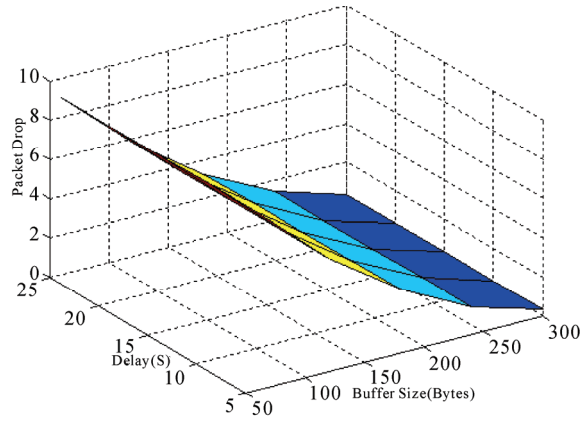

Figure 12. Performance variations with respect to buffer size.

5.2. Performance Variations with Respect to Buffer Size

Figure 12 shows the performance variations when the buffer size varies from 50 bytes to 300 bytes. When the buffer size is 50 bytes number of packets reached at the destination is minimum because of congestion but packet delay is minimum. When the buffer size 300 bytes the number of packets dropped is minimum due to large buffer and the average delay per packet increases due to the increased queuing delay.

5.2.1. Packet Loss with Respect Buffer Size

Figure 13 infers that packet loss get reduced due to increasing buffer size. The number of packets dropped due to buffer overflow in the case of the OEEXLM module almost zero. This is because each time after receiving the packets from upper layer the buffer size is calculated and updated in the routing table. Depending on updated value the routing path algorithm send the HELLO message to the other nodes in the routing.

5.2.2. Packet Delay with Buffer Size

Figure 14 shows Packet delay Vs buffer size. The graph infers that as the buffer size increases the average delay per packet increases due to the increased queuing delay.

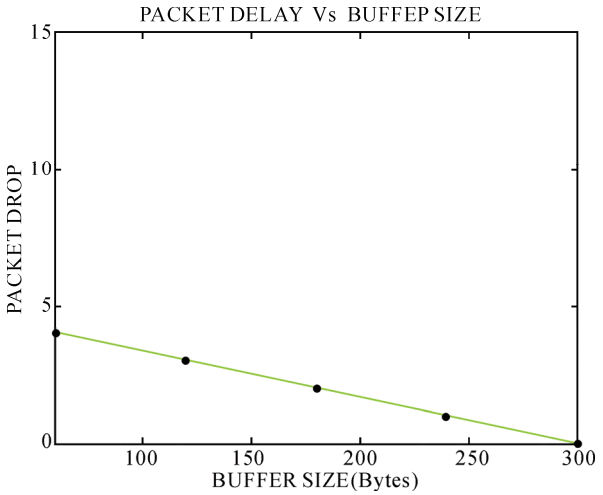

Figure 13. Packet loss vs buffer size.

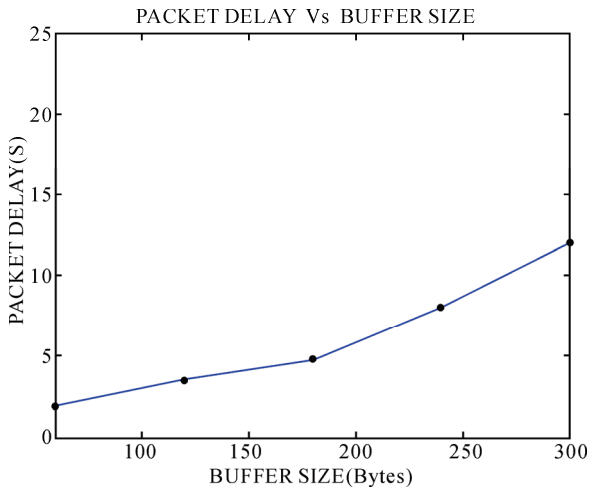

Figure 14. Packet delay vs buffer size.

When the buffer size is 120 bytes, packet delay is only 4 second from source to destination. When the buffer size is 300 bytes length the delay is 12 seconds because of queuing delay. From this graph, we find that as the buffer size increases the packet delay also increases. But throughput is maximum because the packet drop is minimum by compromising the delay.

6. Conclusions and Future Work

In this paper we presented the Cross-Layer Design to improve the performance of the wireless sensor networks. This protocol design is used to give the direct interactions between the Network layer and the MAC layer. The traditional Network layer and MAC layer have been removed, thus simplifying the protocol stack. Simulation results that our proposed scheme has higher node energy efficiency, lower average delay and control overhead than the directed diffusion protocol and S-MAC protocol. The energy consumption of nodes in OEEXLM module is 34% to 84% lesser than when compared with directed diffusion. Further the network life time is 78% improved compared to DD protocol. In future we are going to extend the OEEXML design to Physical layer.

7. References

[1] F. Akyildiz, W. Su, Y. Sankarasubramaniam, and E. Cayirci, "A survey on sensor networks," IEEE Communications Magazine, 40(8), pp. 102–114, August 2002.

[2] O. Zhi-Wen, B. K. Shruthi, and S. K. Sang, "Medium access control for wireless sensor networks," CS258-Advanced Communication Networks, San Jose State University, 2005.

[3] C. Sungrae, K. Kanuri, C. Jin-Woong, L. Jang-Yeon, and S. D. June, "Dynamic energy efficient TDMA-based MAC protocol for wireless sensor networks," Autonomic and Autonomous Systems and International Conference on Networking and Services, ICAS-ICNS, pp. 48, October 23−28, 2005.

[4] I. Demirkol, C. Ersoy, and F. Alagöz, "MAC protocols for wireless sensor networks: A Survey," IEEE Communications Magazine, pp. 115−121, 2006.

[5] S. Singh and C. S. Raghavendra, "PAMAS: Power aware multi-access protocol with signaling for ad hoc networks," ACM Computer Communications Review, 28(3), pp. 5−26, 1998.

[6] W. R. Heinzelman, Chandrakasan and H. Balakrishnan, "Energy-efficient communication protocol for wireless microsensor networks," Proceedings of 33rd IEEE Annual Hawaii International Conference on Systems Sciences, Hawaii, 2000.

[7] W. B. Heinzelman, A. P. Chandrakasan, and H. Balakrishnan, "An application-specific protocol architecture for wireless microsensor networks," IEEE Transactions on Wireless Communications, Vol. 1, 2002.

[8] C. Intanagonwiwat, R. Govindan, and D. Estrin, "Directed diffusion: Ascalable and robust communication paradigm for sensor networks," in Proceedings of ACM MobiCom'00, Boston, MA, USA, pp. 56−67, August 2000.

[9] C. Suh, K. Young-Bae, and S. Dong-Min, "An energy efficient cross-layer MAC protocol for wireless sensor networks," Graduate School of Information and Communication, Ajou University, Republic of Korea, APWeb 2006, LNCS 3842, pp. 410−419, 2006.

[10] Bouabdellah, Kechar1ahmed, and Louazani, "Energy efficient cross-layer MAC protocol for wireless sensor networks," Department of Computer Science, Faculty of Science, University of Oran Es-Senia, BP. 1524 Oran, Algeria, 2002.

[11] W. Y. Ge, J. S. Zhang, and S. M. Shen "A cross-layer design approach to multicast in wireless networks," IEEE Transactions on Wireless Communications, Vol. 6, pp. 1063−1071, March 2007.

Wireless Sensor Network, 2009, 1, 1-60
Published Online April 2009 in SciRes (http://www.SciRP.org/journal/wsn/).

Subarea Tree Routing (STR) in Multi-hop Wireless Ad hoc Networks

Guikai LIU, Chunli SHAN, Gang WEI, Hongjiang WANG
School of Electronic & Information Engineering, South China University of Technology, Guangzhou, China
E-mail: gkliu@scut.edu.cn, spg53@126.com
Received February 28, 2009; *revised March* 15, 2009; *accepted March* 17, 2009

Abstract

Subarea Tree Routing (STR), a new routing protocol for multi-hop wireless ad hoc networks, is proposed. The novelty of the STR protocol is to divide the whole network into many subareas constructed as a result of establishing subarea trees. Its main idea is to identify root nodes by manual configuration or auto-discovery process firstly, then the root nodes originate the process of establishing subarea trees, and finally each node either joins in a subarea tree or become an interconnect node. STR belongs to hierarchical routing protocol and does not attempt to consistently maintain routing information in every node. Furthermore, through the use of tree's intrinsic routing function, the STR protocol exhibits hybrid behavior of proactive and on-demand routing protocols. We prove the correctness of STR, and our simulation results show that the proposed scheme achieves lower route discovery delays, lower route discovery load and better performance of normalized routing load in large, mobile, ad hoc networks as compared with AODV.

Keywords: Wireless Ad Hoc Networks, Hierarchical Routing Protocol, Proactive Routing Protocol, On-Demand Routing Protocol, Subarea Tree Routing

1. Introduction

Multi-hop wireless ad hoc network, also called multi-hop wireless self-organizing network, does not rely on a fixed infrastructure and the network structure changes dynamically due to member mobility. Wireless ad hoc networks are very attractive for tactical communication in military and also expected to play an important role in many fields without the presence or use of a fixed infrastructure such as disaster search-and-rescue operations, data acquisition in remote areas, conference and convention centers etc. Each node in this network not only as a host but also as a router discovers and maintains routes to other nodes that may not be within direct wireless transmission range. To provide communications throughout the network, a sequence of neighbor nodes from a source to a destination form a multi-hop path and intermediate hosts relay packets in a store-and-forward mode.

The major challenges for multi-hop routing in wireless ad hoc networks are continuously changing network topology, low transmission power, and low available bandwidth. In order to support multi-hop routing, much work has been done in this area and many protocols have been proposed. There are different standards to categorize these routing protocols: proactive routing versus on-demand routing, or flat routing versus hierarchical routing and so on.

In proactive protocols [1−6], routes between every two nodes are established in advance even if no data transmission is on demand. This is implemented by a node periodically updating its routing information and every node eventually has consistent and up-to-date global routing information for the entire network. This approach has the advantages of timely exchanging network information such as available bandwidth, delay, topology etc. and supporting real-time services. But it is not suitable for large-scale networks since many unused routes still need to be maintained and the periodic updating may incur overwhelming processing and communication overhead. The on-demand protocol (e.g. [7−10]) is more efficient because each node tries to reduce routing overhead by only sending routing packets when needed for data transmission and a route is released when the data transmission is finished. However, when link breakage is detected due to failure or node mobility, which often occurs in multi-hop wireless ad hoc networks, the delay and overhead of route reconstruction may be significant.

This work was supported in part by National High Technology Research and Development Program of China (863 Program) under contract 2007AA01Z210, and in part by the nature scientific fund of Guangdong province, China (No. 07006488).

As to flat routing and hierarchical routing, this is a classification according to the network structure underlying routing protocols. In flat routing protocol, there is a peer-to-peer relationship between every two nodes and each node participating in routing plays an equal role. Routing algorithm is easily realized. However, it is inferior scalability and limits network's scale in a certain extent. For example, AODV [7], DSR [8] and DSDV [1] are typical flat routing protocols. The hierarchical routing protocol divides the whole network into many logical areas and different routing strategies are used inside and outside the logical area. Compared with flat routing protocol, the hierarchical routing protocol possesses better scalability and is propitious to support large-scale networks. At present, the growing interest in wireless ad hoc network techniques has resulted in many hierarchical routing protocols such as ZRP [11], LANMAR [4], CGSR [12] and HSR [13] etc. In a word, each routing protocol has its own advantages and drawbacks as well. Research is continued on commendably satisfying the demands of multi-hop wireless ad hoc networks on the aspects of reliability, overhead control, efficiency and complexity.

In this paper, a novel hierarchical routing protocol that offers better scalability, low delay, low overhead and low normalized routing load in multi-hop wireless ad hoc networks is presented. The main feature of *Subarea Tree Routing* (*STR*) is to construct subarea trees according to the actual network environment and eventually the entire network will be divided into many logical subareas naturally. In addition, *STR* combines the advantages of proactive routing protocol and on-demand routing protocol, which provide the low route acquisition delay of proactive techniques and the low overhead of reactive methods. The rest of this paper is organized as follows: Next, a detailed description of *STR*, illustrating the key aspects of the protocol's operation, is given. Section 3 proves the correctness of *STR* and we analyze its performance in Section 4. Finally, Section 5 presents our conclusions.

2. Subarea Tree Routing

Our approach to routing in the multi-hop wireless ad hoc networks is based on the notion of *subarea tree*, which is originated by a selected root node. After a subarea tree is established, a logical subarea has already been formed. Namely a logical subarea consists of a subarea tree. Therefore, the whole network is composed of many subarea trees in the end. The *STR* protocol is hierarchical and includes the following components:

1. Identifying the root nodes and interconnecting them
2. Establishing subarea trees
3. Dynamic maintenance of subarea trees
4. Routing mechanism

2.1. Identifying the Root Nodes and Interconnecting Them

In an original network all nodes locate on equal status. Each node has a unique network identifier (ID or address) and its type is configured as "initial node". The root node is also a central node of a future subarea and we can identify the root nodes by static method or auto-discovery process. Static method is to adopt manual configuration to identify the root nodes and set the necessary parameters for them.

Auto-discovery process is more complex and involves the following steps: firstly given a regulation, namely the condition with which the root nodes must satisfy (such as ID Number, number of neighbor nodes, transaction capability, residual energy, stability or other measure values). Then select a node as source node arbitrarily from network (in general convenient for management or operation), and the source node broadcasts root auto-discovering request (*RADRQ*) message which includes source node ID and the given regulation. Those nodes which satisfy the regulation will become root nodes and broadcast their own information such as node ID and node type. Every root node will records other root nodes' information what it has received.

It is interesting that there are two extreme states during the process of identifying root nodes. The first is that there is only one root node in the whole network. Namely the network is composed of one tree. The other is that every node is a root node. Of course, in general the second situation will not happen. However, as a matter of fact, what we want to identify is to find or approach the optimal balance point between these two states according to the real network environment.

Interconnecting root nodes means to build routing information between every two root nodes. The route discovery and route maintenance between root nodes can be realized by adopting existing flat routing protocol such as AODV [7], DSR [8] etc. The initial nodes which route passes through will become "interconnect node (IN)". Both root nodes and interconnect nodes establish routing tables to store the routing information.

2.2. Establishing Subarea Trees

At first, the definition of "tree node" is the nodes that join in subarea trees. The "depth" of a tree node is defined as the hop count between the tree node and its root node. Root node's depth is zero and the depth of initial nodes and interconnect nodes is null. The information of a tree node at least includes node ID, node type, depth, father node, child-node-list, the number of offspring nodes and routing-list, thereinto routing-list stores the routing information of offspring nodes.

The establishing process as follows:

Root nodes and tree nodes periodically broadcast Subarea Tree Establishing Message (*STEM*) which involves node ID, node type, node depth, number of offspring

nodes and other optional parameters (including number of neighbors, residual energy, transaction capability, stability etc.). Its format as Figure 1.

The initial node which receives *STEM* will set its own node type as "tree node"; set father node as the node ID included in the *STEM*; set own depth as the depth included in the *STEM* plus one. Then it returns Tree Node Updating Message (*TNUM*) to its father node. *TNUM* involves destination node ID, source node ID, number of offspring nodes and node routing-list. Its format is shown in Figure 2. After the father node receives *TNUM*, it will update child-node-list, the number of offspring nodes and routing-list; and continue to send *TNUM* to its father node till root node.

If an initial node receives more than one *STEM*, it will select the optimal according to the selecting regulations and discard the others. Selecting regulations involve node depth, the number of offspring nodes or other optional parameters.

If an initial node cannot join in a subarea tree after a stated time T (T>0) since it just connects with interconnected nodes. Here one of the interconnected nodes adjacent with this initial node will be upgraded to become a root node and obtain other root nodes' information from the nearest root node. It also notifies other root nodes that it has become a root node.

At last, all initial nodes will join in subarea trees to become tree nodes. The *STEM* received by root node or interconnect node will be discarded.

2.3. Dynamic Maintenance of Subarea Trees

Child node identifies whether its father node still exists or not through detecting the *STEM* sent periodically by its father node, and vice versa.

If father node inspects that the immediate relationship with one child node is already of nonexistence, it will delete this child node from child-node-list; update the number of offspring nodes and routing-list; then inform its father node by *TNUM*.

If child node inspects that the adjacent relationship with its father node is already failure, it will configure its node type as "initial node"; inform all its child nodes to configure their node type as "initial node" and clear relevant parameters by sending Tree Node Releasing Message (*TNRM*). The format of *TNRM* is shown in Figure 3. Nodes whose type is "initial node" restart to join in subarea trees.

MessageType	NodeID	NodeType	Depth	Num of Offspring	Optional

Figure 1. The format of STEM.

MessageType	DestID	SourceID	Num of Offspring	Routing-List

Figure 2. The format of TNUM.

MessageType	DestID	SourceID	TreeNodesReleased

Figure 3. The format of TNRM.

2.4. Routing Mechanism

From the process of establishing subarea trees, we can see that every root node has acquired the routing information of other root nodes by interconnecting process, and father node has acquired the routing information of all its offspring nodes during the course of establishing a subarea tree. So root node knows the routing information of all the tree nodes in its subarea tree.

Meanwhile, after having finished the process of establishing subarea trees, a hierarchical network structure is formed. There are two tiers: the first tier (namely backbone) consists of root nodes and interconnect nodes; the second tier is each subarea tree. Moreover these two tiers have different routing strategies. The strategy in intra-subarea as well as among root nodes and interconnect nodes is proactive routing; whereas the strategy of inter-subarea is on-demand routing.

Based on the above-mentioned description, the routing mechanism proceeds as follows:

If the destination node of data packet is its own offspring node, the node will forward the packet to the destination directly. If the destination node of data packet is not its own offspring node, the node will forward the packet to its father node. That is to say, there are only two directions-up and down for a tree node to send data packets.

If data packet is sent by interconnected node and no routing information is found, the packet is sent to the nearest root node.

If root node can also not find the routing information, it will send Routing Inquiry Message (*RIM*) to the other root nodes. *RIM* includes message type, destination root node ID, source root node ID, and data packet's destination node ID. Its format is shown in Figure 4. The root nodes or interconnect nodes which know data packet's routing information will return Routing Reply Message (*RRM*) to the source root node. The format of *RRM* is same as *RIM*. Note that there is no demand for establishing a new route in this process and just use the established route.

After receiving *RRM*, the source root node forwards the data packet to the root node or interconnect node which knows the optimal routing. Root node or interconnect node will forward data packet to the destination node according to the known routing information after it receives the data packet.

2.5. Example

A simplified example is illustrated in Figure 5 and there are 22 network nodes. At first all the nodes are "equal" and each node is "initial node" with a unique ID. The line between two nodes denotes a wireless link and these two nodes can communicate directly.

MessageType	DestRootID	SourceRootID	DataDestID

Figure 4. RIM/RRM format.

Assume the condition of becoming a root node in this example is that the number of neighbors is more than or equal 4. Let node S broadcasts *RADRQ* message and nodes A, B, C will become root nodes. These three root nodes will broadcast their information so that they can know each other. Afterwards through existing routing protocol such as AODV or DSR, they will build routing information (routing metrics: hop count or burthen is least in this example): A↔B; A↔D↔C; B↔E↔F↔C. During this procedure, nodes D, E, F will become "interconnect node", illustrated as Figure 6.

Root nodes A, B, C start the establishing process of subarea trees by broadcasting *STEM*. The initial nodes receiving this message will join in subarea trees and become "tree node" simultaneously. Then tree nodes also send out *STEM* periodically. In this example, all the initial nodes except nodes H, I, R will join in subarea trees successfully through such a process. Under this circumstances, interconnect node E will be upgraded to become root node and it will gain other root nodes' information from the nearest root node B as well as notify other root nodes of its own information. And then nodes E, H, I, R form a new subarea tree. At last the entire network is composed of four subarea trees illustrated as Figure 7 and two tiers of network structure is obvious.

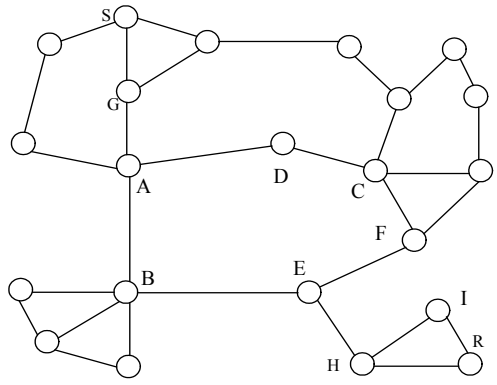

Figure 5. Original network.

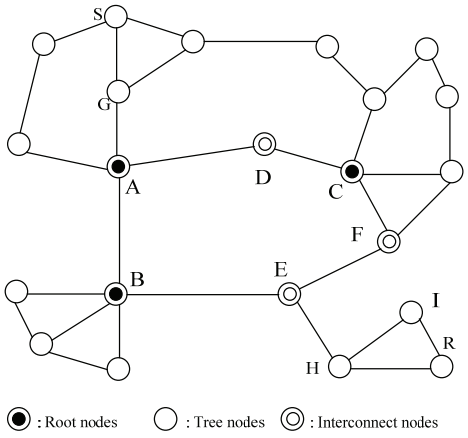

Figure 6. Root nodes and their routing.

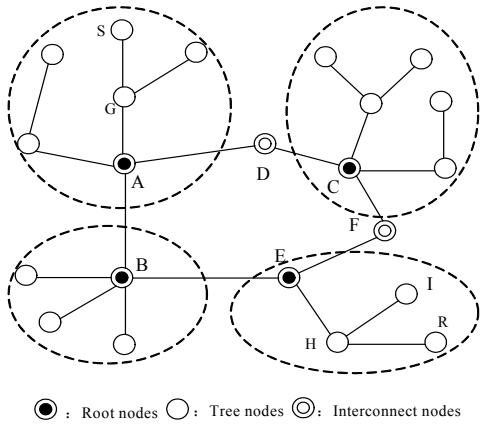

Figure 7. Subarea tree formed network.

Assume node S wants to send data packets to node R. Firstly S sends the data packets to its father node G. Node G finds node R is not its offspring node and sends the data packets to root node A. Root node A will lookup routing information for node R, but it cannot find the route. And then A sends *RIM* to root nodes B, C, E and node E will answer this message with *RRM* because it knows node R is its offspring node. Node A will send data packets to node E while it receives *RRM* from node E. Finally node R can receive the data packets through nodes E and H. The forwarding path is shown in Figure 8.

3. The Correctness of STR

According to the definition, initially every node in the network is an initial node. Well then can *STR* act on all these nodes and create a complete network structure after having finished the process of establishing subarea trees? Strictly speaking, this question is concerned with the effectiveness of *STR* and the correctness wants to be proved. The following theorem assures it.

Theorem 1 We model the network as a graph G =(V, E), where V is the set of vertices and E is the set of edges.

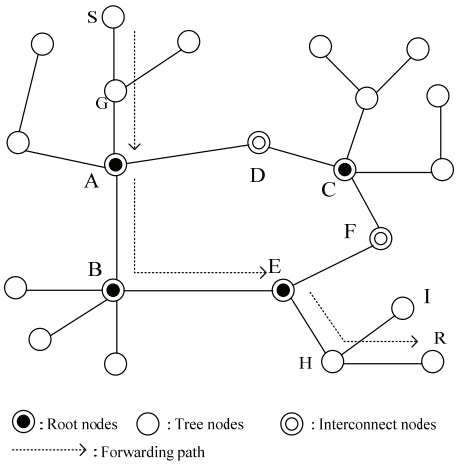

Figure 8. Data forwarding.

Assume G is connected, and then there are two situations for $\forall v \in V$ through the process of establishing subarea trees:

1) v belongs to a subarea tree, namely $\exists$ T=(V_T, E_T) makes $v \in V_T$, thereinto $V_T \subseteq V$, $E_T \subseteq E$; or

2) v is an interconnect node (IN).

Proof:

If v satisfies the condition of selecting root node, then v becomes a root node; thereupon v belongs to the subarea tree whose root node is v.

If v is not a root node, but a node which interconnect routes of root nodes pass through, then v is an interconnect node (IN).

If v is neither a root node, nor a interconnect node, then there are four cases:

(1) $\exists$ a root node r, makes edge (r, v) $\in$ E; or

(2) $\exists$ a tree node t, makes edge (t, v) $\in$ E; or

(3) $\exists$ a interconnect node i, makes edge (i, v) $\in$ E; or

(4) All the neighbors of v are initial nodes.

For cases (1) and (2), v can receive message *STEM* from r or t at least and join in a subarea tree because both r and t broadcast *STEM* periodically.

For case (3), i will be upgraded to become a root node when v cannot join in a subarea tree in a stated time, upon that v will receive *STEM* from i and join in a subarea tree.

For case (4), since G is connected, so $\exists v_0 \in$ a subarea tree T, makes

Path (v_0, v) = (v_0, v_1, v_2, …, v_n, v_{n+1}=v) exists, thereinto v_j (j=1,2, …, n, n+1) are initial nodes. The following will prove that v can receive *STEM* and join in a subarea tree through mathematical induction:

Since $v_0 \in$ T, so v_0 sends *STEM*.

When j=1, v_1 is the neighbor of v_0; v_1 can receive *STEM* from v_0 and become a tree node.

When j=2, v_2 is the neighbor of v_1; v_2 can receive *STEM* from v_1 and become a tree node.

When j=n, assume v_n can receive *STEM* and become a tree node.

Thereupon, when j=n+1, since v_{n+1} is the neighbor of v_n, so v_{n+1} can receive *STEM* from v_n and join in a subarea tree. Namely $\exists$T= (V_T, E_T) makes $v \in V_T$.

4. Performance Analysis

4.1. Simulation Model

We used NS2 (Network Simulation 2) to evaluate the performance of *STR*. The simulation modeled a network in a 2500m×2500m area with 50 mobile nodes. Radio transmission range is 250 meters. The mobility of each node is arranged from 2m/s to 8m/s, and the pause time of the mobile nodes is zero. Traffic sources are continuous bit rate (CBR) with the rate of 15kbit/s. The source-destination pairs are randomly selected over the network.

Four important performance metrics are evaluated: (1) Normalized routing load-the number of routing control packets transmitted per data delivered at the destination. Each hop-wise transmission of a routing control packet is counted as one transmission. (2) Route discovery delays-the delay between a route requests being issued and a reply with a valid route being received. (3) Route discovery load-the route discovery packets being used to find a valid route to the destination. (4) Packet delivery ratio-the ratio between the number of received data packets and those originated by the sources.

4.2. Simulation Result

In our experiments, we compare the performance of *STR* with that of AODV. Figure 9 reports the normalized routing load. For small number of pairs (say 10), we can see that the normalized routing load increases with the mobility of each node in both two protocols. And the performance of AODV is little better than *STR*. *STR*'s poor performance can be attributed to route control messages used to maintain the connection between child-father pairs. However, with the increase of source-destination pairs (say 30); the normalized load of AODV is higher than *STR*, especially when the mobility speed increases to a high level. This is because AODV has a much higher O/H than *STR*.

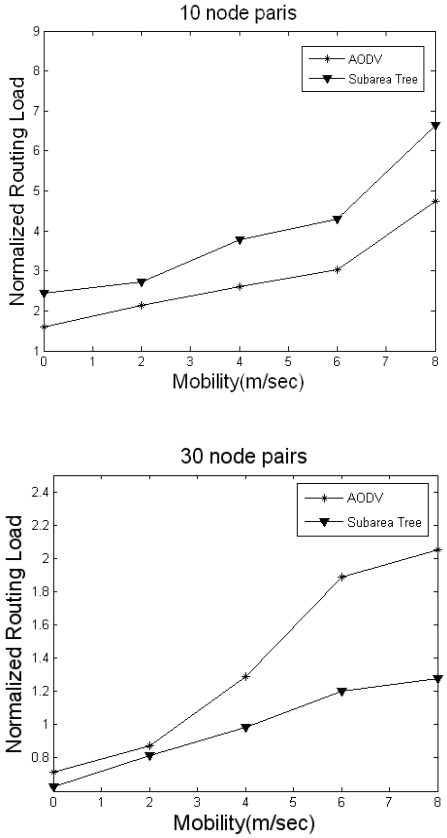

Figure 9. Normalized routing load.

In Figure 10, the route discovery delays are reported. Here we assume that all source-destination pairs are in different subarea and the node speed is fixed at 2m/s. When the hop count of the source-destination is small, the performance of these two protocol a quite similar. The route discovery delays increases with hops between source and destination. However, we can see from the figure that AODV has a higher increase rate than *STR*. Because, in *STR* protocol, route discovery process only need to find a route within root nodes. On the other hand, if the source-destination pairs are in the same subarea, there will be no route discovery delays by using *STR* protocol.

Experiment in Figure 11 shows the effect of distance between source and destination on route discovery load. Clearly in both protocols the route discovery load is increased with distance. At the beginning, the route discovery load of *STR* is almost zero, since when source-destination pair is close to each other, they are usually in the same subarea, no route packet need to be used. The poor performance of AODV is because that it uses an expanding ring search technique to disseminate the RREQs, while in *STR* only the root nodes and interconnect nodes need to handle the Routing Inquiry Message (*RIM*).

Figure 12 shows the packet delivery ratio of *STR* under various offered load with different speeds. Packet delivery ratio declines both with speeds and offered load. We note that at low speeds, packet delivery ratio is sensitive with offered load. Packer delivery ratio declines while

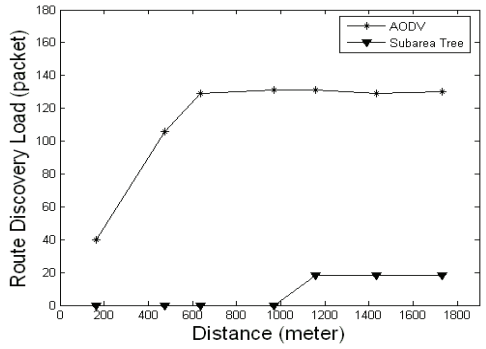

Figure 10. Route discovery delay.

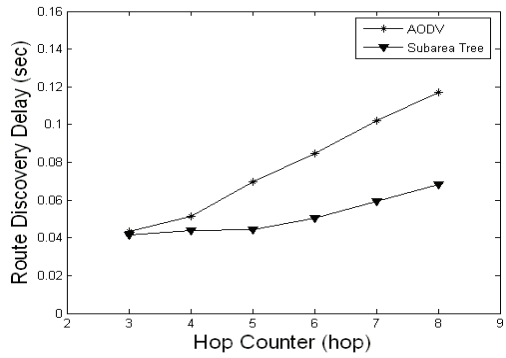

Figure 11. Route discovery load.

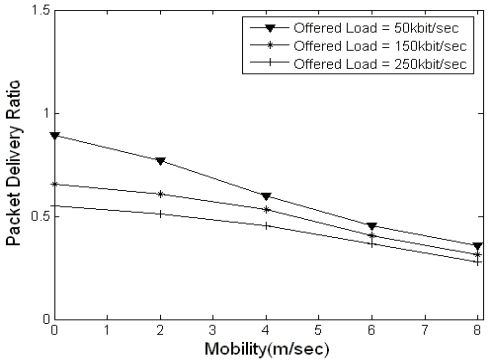

Figure 12. Packet delivery ratio of STR.

offered load is increasing. This is because most data packets are sent to their father node before they go to the destination in *STR*. And it will probably lead to traffic congestion in some father nodes and cause packet loss. As mobility increase, the packet delivery ratio is less sensitive with offered load. Since most packet loss ascribe to the fiercely change of network topology.

5. Conclusions

Subarea Tree Routing (*STR*), a novel routing protocol for multi-hop wireless ad hoc networks based on the idea of establishing subarea trees and dividing the whole network into many logical subareas, has been proposed. This protocol constructs a hierarchical network structure with two tiers in which different routing strategy is adopted, and routing mechanism combines the advantages of proactive routing and on-demand routing. Indeed, since the extents of proactive routing are restricted in intra-subarea as well as among root nodes and interconnect nodes, *STR* does not incur heavy overhead due to maintaining routing information, especially in large, mobile, ad hoc environment. Furthermore, since on-demand routing is operated only between root nodes whose number is very small in general, the delay due to route searching is also low. Theorem 1 assures the correctness of *STR* and our ns-2-based simulation has confirmed the advantages of *STR* and demonstrated a significant routing efficiency and scalability improvement.

6. References

[1] C. E. Perkins, "Highly dynamic destination-sequenced distance-vector routing (DSDV) for mobile computers," Proceedings of ACM SIGCOMM, pp. 234−244, 1994.

[2] G. Pei, M. Gerla, and T. W. Chen, "Fisheye state routing in mobile ad hoc networks," in Proceedings of the 2000 ICDCS Workshops, Taipei, Taiwan, pp. D71−D78, April 2000.

[3] J. J. Garcia-Luna-Aceves and M. Spohn, "Source-tree routing in wireless networks," Proceedings of IEEE International Conference on Network Protocols (ICNP), pp. 273−282, 1999.

[4] G. Y. Pei, M. Gerla, and X. Hong, "LANMAR: Landmark routing for large scale wireless ad hoc networks with

group mobility," Proceedings of IEEE/ ACM Workshop on Mobile Ad hoc networking & Computing, MobiHOC'00, Boston, MA, USA, MA, USA, pp. 11−18, 2000.

[5] T. Clausen and P. Jacquet, "Optimized link state routing protocol (OLSR)," IETF Internet RFC3626, October 2003.

[6] R. Ogier, F. Templin, and M. Lewis, "Topology broadcast based on reverse-path forwarding (TBRPF)," IETF Internet RFC3684, February 2004.

[7] C. E. Perkins, E. M. Belding-Royer, and I. Chakeres, "Ad hoc on demand distance vector (AODV) routing," IETF Internet RFC3561, July 2003.

[8] D. Johnson, Y. Hu, and D. Maltz, "The dynamic source routing protocol (DSR) for mobile ad hoc networks for IPv4," IETF Internet RFC4728, February 2007.

[9] V. Park and S. Corson, "Temporally-ordered routing algorithm (TORA) Version 1 functional specification," IETF Internet draft (draft-ietf-manet-tora-spec-04.txt), July 2001.

[10] C. K. Toh, "Associativity-based routing for ad hoc mobile networks," WLPersonal Communications Journal, Special Issue on Mobile Networking and Computing Systems, Kluwer, Vol. 4, No. 2, pp. 103−139, March 1997.

[11] Z. J. Haas and M. R. Pearlman, "The performance of query control schemes for the zone routing protocol," IEEHACM Transactions on Networking, Vol. 9, No. 4, pp. 427−438, August 2001.

[12] C. C. Chiang and M. Gerla, "Routing and multicast in multihop, mobile wireless networks," Proceedings of IEEE ICUPC '97, San Diego, CA, pp. 546−551, October 1997.

[13] G. Pei, M. Gerla, and X. Y. Hong, *et al*., "A wireless hierarchical routing protocol with group mobility," Proceedings of IEEE WCNC'99, New Orleans, LA, pp. 1538−1542, September 1999.

Wireless Sensor Network, 2009, 1, 1-60
Published Online April 2009 in SciRes (http://www.SciRP.org/journal/wsn/).

Research on ZigBee Wireless Sensors Network Based on ModBus Protocol

Chengbo YU[1], Yanfei LIU[1,2], Cheng WANG[2]
[1]*Research Institute of Remote Test & Control, Chongqing Institute of Technology, Chongqing, China*
[2] *National Engineering Research Center for Information Technology in Agriculture, Beijing, China*
E-mail: yuchengbo@cqit.edu.cn
Received January 17, 2009; *revised March* 3, 2009; *accepted March* 5, 2009

Abstract

The information transmission is transparent for the user in the ZigBee wireless sensors network, which are lack of interactivity and self-constrain. The information in the ZigBee wireless sensors network can not be viewed in a real time by a friendly interface. Modbus protocol is embedded into ZigBee stack, in this way, we can implement interaction well and the information can be viewed in a friendly interface. The paper presents the measures to embed the Modbus protocol into the ZigBee stack provided by Chipcon company, which contains address bound mechanism, information centralized storage, and flexible monitoring, by which we can monitor the real time information from the ZigBee wireless network and use some instructions to control the remote device in a friendly interface, which can be used well in the middle and small ZigBee monitoring wireless sensors network. We implement it in the plant physiological ecology monitoring system.

Keywords: ModBus Protocol, ZigBee Stack, Monitoring

1. Introduction

Wireless ZigBee is a very low-cost, very low power consumption, two-way, wireless communications technology [1,2], which can be used widely in consumer electronics, home and building automation, industrial controls, PC peripherals, medical sensor applications, toys and games [3,4]. Now ZigBee technology also can be used in Agriculture monitoring and control [5]. ZigBee wireless communication is transparent to the user, which is not convenient for the user to know the consecutive data information in a real-time system. We need a friendly interface to observe the information in the wireless network. ModBus protocol is widely used in industrial monitoring and test, which is an application layer messaging protocol, positioned at level 7 of the OSI model, that provides client/server communication between devices connected on different types of buses or networks [6]. In the plant physiological ecological monitoring system, the information transmission between the coordinator and PC by ModBus protocol, we can easily observe the real-time data from the remote field-device. This paper presents the method to implement ModBus protocol based the TI ZigBee stack, and the plant physiological ecological system hardware platform and test results are proposed.

2. Implementation Platform

The implementation platform contains software platform and hardware platform. The basic software platform is the TI ZigBee-stack 2006, and the ModBus Protocol is embedded into the ZigBee-stack, then we implement the wireless field-bus protocol. The ZigBee module connected with some sensors which measure the environment parameters and the plant physiological ecological information. By that information we can analyse the plant health status.

2.1. System Overview Framework

The plant physiological ecological monitoring system is composed of PC, some sensors node, and a coordinator. PC is the friendly interface to show the information in the wireless network, which connects with the Coordinator by RS-232 interface. Sensors nodes send the data to the Coordinator, and it stores the data by Modbus protocol. When the PC sends some instructions to query the sensor node information, the Coordinator will response to the query instructions. Figure 1 is the system structure.

2.2. Hardware Platform

The chip CC2430 is as the core of the hardware, CC2430

integrated RF transceiver, CPU, and 128K flash memory, and very few external components are required in the CC2430 typical application [7]. In the system the CC2430 module connects with some different kinds of sensors, and The Coordinator node has the same structure with the sensor node except the sensor module.

2.3. Software Platform

Using the TI ZigBee stack as the software platform, Figure 2 shows the structure of the project built in the ZigBee stack 2006.

APP directory is the area for the project creature, which contains the application layer files and the main contents of the project. HAL directory contains hardware configuration, driver, and relevant functions. MAC directory contains MAC layer parameters config files and some API libraries. MT directory contains some serial operator files. NWK directory contains network layer parameters configuration files. OSAL directory contains the operator system files. Profile directory contains AF layer functions. Security directory and Services directory are with respectively security layer functions and address processing functions. Tools directory contains the memory space partition files. ZDO directory includes the ZigBee device object information files. ZMAC directory contains MAC layer parameters configuration files and some libraries. ZMAIN directory contains the entrance function of the project. Output directory is the output results of the project [8]. In this system we used Modbus protocol and ZigBee protocol. ZigBee protocol is used for the data transparent transmission in the wireless network, and Modbus protocol is used to query and control the filed device information between the Coordinator and host computer.

ZigBee stack runs in an operator system called OSAL (Operator System Abstract Layer). OSAL takes task scheduling mechanism. Each task contains some events, and each events own the only events ID. Task scheduling is implemented by the event trigger of the task. When an event appears, the corresponding event of the task will set an event ID, then the task scheduling will call relevant task processing function.

The operator system task scheduling flow is as shown in Figure 3; the system begins to run from the main () function of the ZMain directory. In main () function the osal_init_system () function will be called, which is used to initial the OSAL system. In this function it will call osalAddTask () function in which the osalTaskAdd () function will be called to add the events needed to be processed. The osalNextActiveTask () function in the OSAL directory will keep querying the event and judge whether it can be executed. When the host computer sends a Modbus function code to query the information, it will be treated as an event, and the corresponding event ID will be allocated. The task processing function in the APP directory will process the event and output the result.

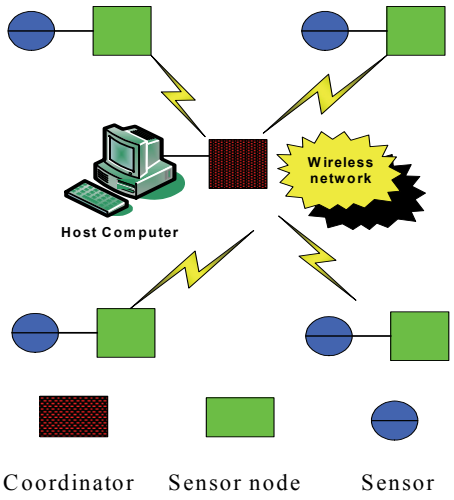

Figure 1. System structure.

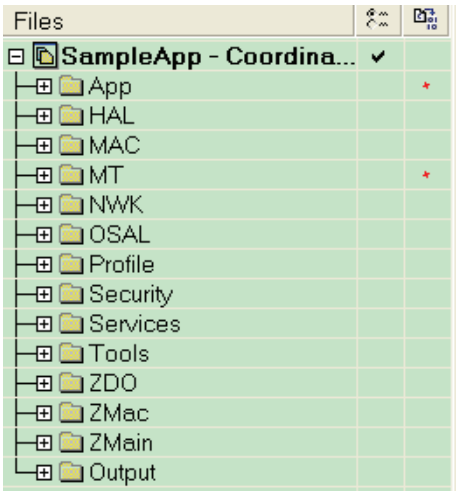

Figure 2. The structure of the project.

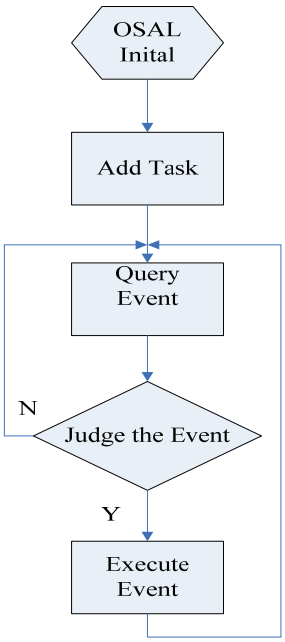

Figure 3. Task scheduling flow.

In order to combine the modbus protocol into Zigbee network we take some measures such as address bound mechanism, information centralized storage and flexible monitoring, which will be discussed in the Section 4.

3. Test Results

Modbus protocol is widely used in industrial automation field. The typical transmission characteristic is that no query, no reply. If we want to query the sensor node's information we should send the command first, then the sensor node will reply the relevant information to the host computer. There are two message frame structures in Modbus protocol, of which we take RTU message frame structure, as shown in Figure 4.

Modbus Poll is a very convenient software platform for the Modbus transmission test. The Coordinator is connected with the host computer by serial port. When the ZigBee wireless sensor network is running stably, we can set the Modbus Poll as shown in Figure 5.

Slave is the object that we want to observe, and we write the sensor node's Modbus ID here. Function is one of the command options, and 03 function command is chosen to read holding register. Address is the start address of the register need to read, and Length is the number of register need to read consecutively. Scan rate is the interval between two commands. All these configurations are following the Modbus protocol frame structure. Then we will get the replied modbus package as shown in Figure 6.

In the test there are four sensor nodes in the ZigBee wireless network, each node has a only Modbus ID. We put node 1,2 and 4 around the coordinator, which is not too far. Node 3 is away from the coordinator but near to node 1. Then it makes the wireless network keep working.

Figure 6 is the test result of the plant physiological and ecological monitoring system. We used Modbus poll to query and control the field-device. From the results we can know the sensors value, the network short address of the node, and the parent's network short address, and so on.

Slave Address	Function code	Data	Error check

Figure 4. Modbus frame structure.

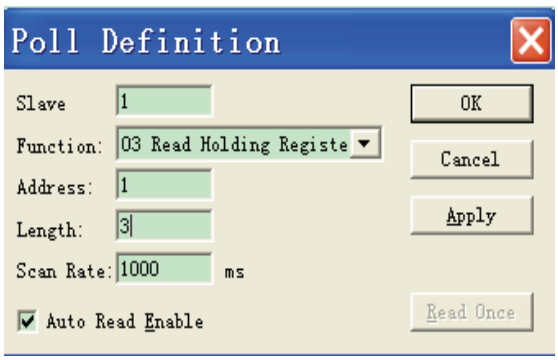

Figure 5. Test configuration.

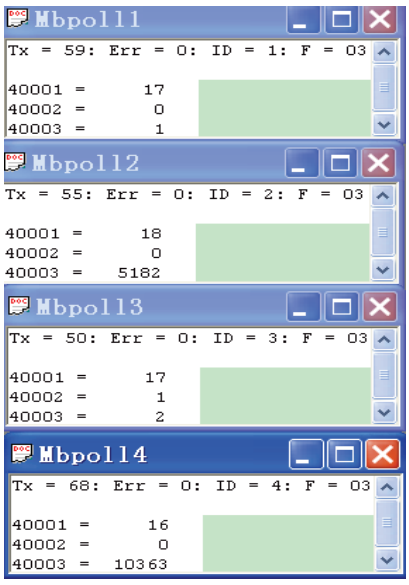

Figure 6. Test result.

As shown in Figure 6, register 40001 is the sensors value, register 40002 is the short network address, and the register 40003 is the parents' short network address. We can get the network topological structure by the test result. In Figure 4, the ID 1, ID 2, and the ID 4 are connected with the coordinator. The ID 3 is the child node of the ID 1.

4. Discussion on the Implementation Method

4.1. Address Bound Mechanism

In the Modbus protocol communication mechanism each node has an address, which we call Modbus ID. In the ZigBee wireless network each node has a 64 bit IEEE address, which is a constant, and each node also has a 16 bit network short address, which may be changed when the network state changes. So each node has three kinds of address. In different communication network we use different address. But we should know clearly the Modbus poll viewed value which node it comes from. Each 64 bit IEEE address corresponds to a Modbus address. Modbus address scope is from 1 to 255, which is an 8 bit address. In order to make the Constant 64 bit IEEE address consistent with the 8 bit Modbus address, we use the 8 bit Modbus address as the low 8 bit of the

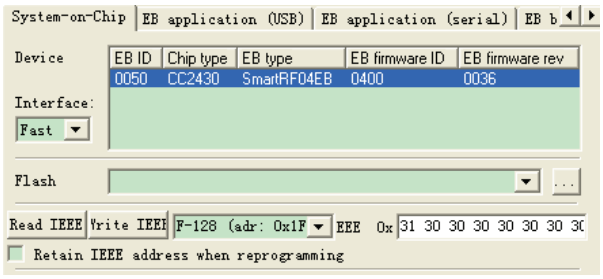

Figure 7. Write IEEE address.

64 IEEE address, and the remain bits set to 0. Each sensor node will read the low 8 bit of the 64 bit IEEE address as their Modbus address when the nodes send information to the coordinator. In this way, we can know clearly which nodes we are operating. Figure 7 shows that we are writing the 64 bit IEEE address into the flash memory of the CC2430.

4.2. Information Centralized Storage

If the sensors nodes store the information by themselves, we should go through wireless network to get the node information. If the sensor node is far away form the host computer there will be a delay for the information transmission. And also when we query too many nodes at the same time it may cause network communication jam. So we take measures to store all sensor node information in the coordinator. We store the information by the Modbus address, and when the coordinator gets the ZigBee package form the sensor node, first of all it parses the package and gets the Modbus address, to make sure the storage address of the information, then stores the relevant information to the register. Host computer connects with the coordinator by serial port, so information centralized storage is very reliable for the communication.

4.3. Flexible Monitoring

Modbus protocol has a typical advantage, if there is no query for the node, there will be any response information to the host computer. If the nodes in the ZigBee wireless network are too many, and we only care for some nodes in the node, we can choose the nodes which we want to monitor. It also can reduce the load of the processor of the coordinator.

4.4. Communication Course

The communication course of the system was divided into two parts. First of all, the Modbus poll sends Modbus query data package to the Coordinator, when the coordinator receives the Modbus package, parses the package and stores the query information, which contains the Modbus address function code, and so on. After that, the coordinator executes the function code instruction. Figure 8 shows the 03 function code instruction to query node 1 information. That's a typical query course.

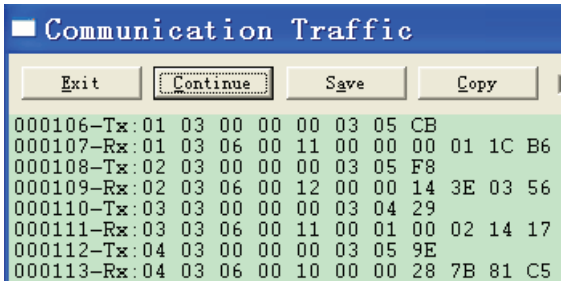

Figure 8. Communication package.

As shown in Figure 8, at first the Modbus poll sends a query instruction, 01 is the Modbus ID and it is also the low bit of the 64 bit IEEE address. 03 is the function code, following double 00 is the start address to query, following 00 is the high bit of the number of the register, 03 is the low bit, and the last 05CB is the 16 bit CRC. When the Coordinator receives the Modbus package, the Modbus ID, function code, and the number of byte to be queried register will be stored. Then the Coordinator executes the 03 function instruction, and reads the information in the registers. The information will be stored in the return Modbus package. As shown in the figure, RX is the PC received Modbus package. 01 is the Modbus ID, 03 is the function code, 06 is the number of bytes to be queried register, and the following 6 bytes is the registers value. At last it adds the 16 bit CRC code into the package.

The registers information comes from the sensors node. The sensors node sends a package to the Coordinator which contains Modbus ID, 64 bit IEEE address, the short network address, and its parent's short network address, and the sensor information. When the Coordinator receives the OTA (over the air) package, first it confirms the Modbus ID, then it stores the relevant information to the appointed registers. The sensors nodes send the periodic information to the Coordinator, and the information updates in a real time.

4.5. Limitation of the System

The limitation of the system is its only application to middle and small networks. Due to each Modbus network only allowes 255 nodes as the maximum Value.

In the course of the system test, we have found that if the communication distance is too long, the remote sensor node's information will be delayed. We can take some remedial measures, such as to fix the sensors node higher, to use some directional antenna, etc.

5. Conclusions

ZigBee wireless sensors network based on Modbus protocol can be used well in the Plant physiological ecological monitoring system. The advantages of the ZigBee wireless sensors network system based on Modbus protocol are as follows:

1) The wireless sensors system is of high convenience in the course of the system installation.

2) The ZigBee technology makes the power consumption very low.

3) The Modbus protocol provides a friendly interface for the system observation.

4) Modbus protocol, as a mature field bus standard, provides a general interface for the system. So we can use this interface to connect with GPRS, Industry Ethernet and so on. So this system can be expanded well.

6. Acknowledgment

The work is supported by the foundation of National Key Technology R&D Program (2006BAD11A10, 2006BAD 30B03), and is supported by the foundation of chongqing natural science (CSTC2007BA2023).

7. References

[1] IEEE STD 802.15.4 [S], http://www.zigbee.org.

[2] ZigBee Alliance, ZigBee Specification [Z], http://www. ZigBee. org.

[3] L. T. Cao, W. Jiang, and Z. L. Zhang, "Networked wireless meter reading system based on ZigBee technology," Control and Decision Conference, Chinese, pp. 3455−3460, 2008.

[4] W. K. Park, C. S. Choi, J. Han, and I. Han, "Design and implementation of ZigBee based URC applicable to legacy home appliances," Consumer Electronics, ISCE 2007, IEEE International Symposium, pp. 1−6, 2007.

[5] Y. M. Zhou, X. L. Yang, X. S. Guo, M. G. Zhou, and L. R. Wang, "A design of greenhouse monitoring & control system based on ZigBee wireless sensor network," Wireless Communications, Networking and Mobile Computing, WiCom 2007, International Conference, pp. 2563−2567, 2007.

[6] Modbus Application Protocol Specification [S], http:// www.Modbus-IDA.org.

[7] Texas Instruments, Datasheet, CC2430[Z], http://www.ti.com.

[8] WXL. Zigbee Stack User Guide [Z], http://www.C51rf.com.

Wireless Sensor Network, 2009, 1, 1-60
Published Online April 2009 in SciRes (http://www.SciRP.org/journal/wsn/).

Policy Based Self-Adaptive Scheme in Pervasive Computing

Jian Quan OUYANG[#*1], Dian Xi SHI[#2], Bo DING[#3], Jin FENG[※4], Huai Min WANG[#5]
[#1]*School of Computer, National University of Defence Technology, Changsha, China*
[*]*School of Computer and Communication, Hunan Institute of Engineering, China*
[※]*Nanchang Military Academy Unit Battle, Nanchang, China*
E-mail: [1]*kissingman1@gmail.com,* [2]*dxshi@nudt.edu.cn,* {[3]*maildb,* [5]*whm_w*}@163.*com,* [4]*fengjin*0510@126.*com*
Received February 15, 2009; *revised March* 6, 2009; *accepted March* 10, 2009

Abstract

Nowadays, application systems in pervasive computing have to be self-adaptive, which means adapting themselves to dynamic environments. Our aim is to enable systematic development of self-adaptive component-based applications. The paper first introduces a novel policy based framework for self-adaptive scheme in pervasive computing. Then the proposed policy ontology and policy language are well expressive and easily extensible to support the design of policy which is based on the Separation of Concerns principle. Furthermore, the context-driven event channel decouples the communication between the suppliers and consumers for asynchronous communication. The proposed framework can provide both a domain-independent and a flexible self-adaptation solution.

Keywords: Policy Ontology, Self-Adaptive, Policy Language, Pervasive Computing

1. Introduction

Technology of software evolution drives the need for software self-adaptive. Moreover, while pervasive computing environment is open and dynamic, application systems in pervasive computing have to be self-adaptive, which is adapt themselves to work in dynamic environments. Previous adaptation work is based on predicting future circumstances and adapting themselves by way of embedding the adaptation decisions in the program code. It is clearly that it is done in an ad hoc way. While policy can define the behaviour of adaptive are applied by different research projects for the flexible reconfiguration systems, it seems that a feasible approach to be decoupled from functional concerns and systematically develop self-adaptive applications. Moreover, as it can separate the business logic (rules) from the controls (programming code) of the implementations, policy-based scheme are typically more flexible and adaptable than non- policy-based approach. In a word, policies can specify and adapt the behavior of a system and can be applied to various areas: auction mechanisms, access control, Privacy (Information Collection Policies), Context aware computing, etc.

In this paper, we present a policy based adaptive architecture for pervasive computing. Different from current policy approach, in the view of the proposed scheme, the context information is used as meta data and the policy is applied to meta protocol, thus it can materialize a reflective approach in the adaptation architecture. In additional, the proposed policy ontology and policy language can support for knowledge representation and reasoning and knowledge sharing. And they are feasible to support the design of policy which is based on the Separation of Concerns principle.

The rest of the paper is structured as follows. In next section, we introduce the current state of the art. Section 3 discusses the requirements of self-adaption. Section 4 describes the overview of adaptation architecture. Following this, Section 5 proposes a policy descriptive language for pervasive computing. Section 6 illustrates the event scheme. Section 7 will give an introduction to the prototyping applications in fire alarm scenario and preliminary experiments. Finally we summarize our work and give future plan in Section 8.

2. Current State of the Art

There are several ways for proposing polices. Previously, the approaches to policy specification are proposals for policy language specification. Lobo [1] depicted the PDL (policy description language) to describe the strategies for mapping a series of events into a set of actions. Damianou [2] described a policy language (Ponder) applying for both management and security policies for distributed systems. Anthony [3] introduced a policy

definition language which is designed to permit powerful expression of self-managing behaviours. Moreover, a prototype library implementation of the policy support mechanisms which can facilitate adaptive-policy deployment is illustrated. Ahn [4] proposed a high-level policy description language for formally specifying context entity relation, and introduced the translator which can provide automatic generation of Java classes for ubiquitous entities.

The other approach is based on logic programming for supporting well defined semantic. Semantic Web Languages for policy specification: KaoS [5] and Rei [6]. Uszok [5] proposed a framework for specification, management, conflict resolution and enforcement of policies which is used OWL ontology. Kagal [6] introduced a policy language (Rei) for pervasive computing environment which can express the behaviour of entities and it is used as part of a secure pervasive system.

Recently, there are several policy based applications in the ubiquitous/pervasive computing scenarios. Rukzio [7] presented policy based adaptive services for mobile commerce, but the event scheme is not mentioned. Erradi [8] introduced policy-based middleware, Manageable and Adaptive Service Compositions (MASC), for dynamic self-adaptation of Web services compositions. David [9] presented an adaptive framework which is based on the Fractal component model. In the framework context-awareness service can provide information about the execution context. Chan [10] proposed an event model for a highly adaptive mobile middleware, Web Proxy for Active Deployable Service (WebPADS). Bandara [11] applied Event Calculus to transform both policy and system behaviour specifications into a formal notation. However, these methods did not concentrate the Separation of Concerns principle to support reconfiguring system based on reflective scheme.

Lately, Adamczyk [12] proposed a lightweight framework called the Autonomic Management Toolkit, which can support dynamic deployment and management of adaptation loops.

3. Requirements of Adaptation in Pervasive Computing Environment

Generally, self-adaptive applications need to control how and when decisions and actions are taken. Policy-based scheme can specific the adaptation layer and adaptation time [13]. Different from the three basic requirements (Uniformity, Separation and Generic) for the development of adaptation architecture [7], we define the following three basic requirements of policy in pervasive computing environment:

-Expressiveness: The first requirement is that suitable expression of policies is important for describing the rules to specify the behavior of a system. On the one hand, it is need to be restricted to avoid ambiguities or ill-defined policies. On the other hand, it can not be too complex for untrained user to write rules.

-Well-defined semantics: The next requirement is well-defined semantics. Obviously, Well-defined policy can support for knowledge representation and reasoning and knowledge sharing of polices. Moreover, it can enable interoperability of heterogeneous rules.

-Usability: As the perspective pervasive computing is to seamless integration of computing into the user's everyday life, make it easy for users to write rules is one of the critical requirement of policies. Make rules intelligible to the common user and declarative, human readable interface is favourable for design polices

-Lightweight: Foe the reason of limitation of resource in pervasive computing environment, strong rule engine is difficult to run for the various devices in pervasive computing environment. Lightweight policy architecture is necessary for devising the rule engine.

4. Overview of Adaptation Architecture

4.1. Core Idea

The core idea of the adaptation architecture is shown in Figure 1. The architecture is based on the tenets of policy-driven systems which are applied in various adaptive systems.

We are using policies which can be seen as a set of sophisticated rules modelled by Event-Condition-Action rules for the definition of the adaptive behaviour in pervasive computing environment. Thus it can react to changes of the context information by reconfiguring the application.

Our proposed policy engine is based on the Separation of Concerns [14] principle: extract explicit rules of business logic from various applications. In the first step in a cycle, Context data is provided by context-aware component, PolicyController matches all polices with the Context data and select the appropriate policy. Then judge whether the conditions in the "action-event" table are met. If they are met, EventMonitor triggered by relevant events and notify PolicyExecutor. As the next step PolicyExecutor will executes the predefined rules and lead to a change of the context information.

4.2. Reflective Scheme

A reflective scheme can ensure that can support structural reconfiguration while examining and change environment, aiming to self-adapt at runtime. As shown in Figure 2, in our architecture, the strategy of the separation of component and policy can gain the decoupling of meta-level scheme and based-level implementation. The advantage of the reflective scheme can conclude two parts:

1) The policy-based application system can be flexible, extensible and adaptive, since the policy can be deployed and modified in the course of runtime of systems.

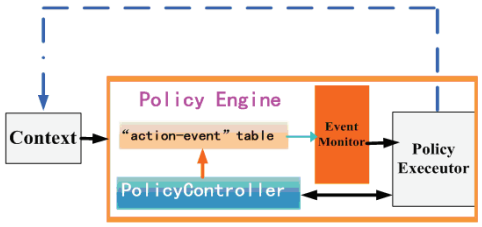

Figure 1. The core idea of the adaptation architecture.

2) Policy-based scheme decouples the reusable component between the developments and deployability stage. The developer can only focus on using policy to describe the base-level business logic, and the deploymentor can designate the component according to the application environment.

Context is the provider of the meta-level data, policy is the meta-level protocol between the business logic and context, policy engine is meta-level procedure, and behaviour component is the base-level computing entity.

4.3. Context-driven Mechanism

Context is one of the most important features of pervasive computing. As the dynamic character of pervasive computing, it is necessary to model and specify context in a way such that context information can easily exchange, share and reuse their knowledge. For simplicity, we define context as four tuple ConData=(ConSup, ConType, Value, TimeStamp), ConSup is the supplier of context data, ConType indicates the type of the context (e.g., location, temperature), Value gives the content of the context data, Timestamp describes the generation time of the context.

Here, we classify the components into two classes: Context-aware components which gain and aggregate the context data and Behaviour components which carry out the actions according to the predefined rules in policy engine. The policy engine is driven by policies which are a set of rules in XML files and describe how the behaviour component reacts in a specific context to support deployable application. As shown in Figure 2, context is the only starting point of self-adaptation and also the end point of adaptation.

4.4. Context-driven Policy Based Framework

The model of context-driven policy consists of three layers, which is shown as Figure 3. The bottom layer is context layer. The top layer is self-adaptive layer, while the policy layer is in the middle. Context layer can abstract the state of physic and information space in pervasive computing environments and context-driven events. The policy layer is used for describing self-adaptive rules including context constraint, description of actions. Self-adaptive layer is based on context-driven scheme. Context based event is the jumping-off point of the course of adapt procedure and the sole driver for adapt procedure.

5. Policy Descriptive Language for Pervasive Computing (PDLPC)

5.1. Policy Ontology

To attain better semantic language understanding and share knowledge for reusable, Figure 4 illustrates the policy ontology we are developing to express the structure of polices precisely.

The proposed policy ontology defines the vocabularies for indicating rules that perform different types of actions. To describe policy rules, the ontology define the basic concepts of "policy ontology" including "Priority", "Event", "Precondition" and "LogicType". Furthermore, we use "Unionof" relation to design the hierarchical structure of the policy ontology.

The structure of the policy ontology is as follows.

Priority: The "Priority" class defines the priority between policies. It has been further classified into "High" and "Low" subclass.

LogicType: LogicType class indicates types of logic including two-valued logic and fuzzy logic.

Precondition: Preconditions are constraints on the action and environment. We use "Unionof" relation to model the composition of the value restriction.

Event: The "Event" class implies the policy is triggered by the changed environment context. The "Event" class include:

1) "EventTpye" subclasses comprise "AtomEvent" and "Composite" subclasses. In the meantime, "Composite" subclass is composed by "EventOperator" and "AtomEvent" via "Unionof" relation.

2) "LogicTpye".

3) "Precondition".

4) "Component" subclasses can indicate the related component which can perform a specific action.

5) "Action" subclasses can represent an invocation to certain type of computing procedures to acquire user information or provide services in the pervasive environment.

Also, the "Unionof" relation can describe the "EventTpye", "LogicTpye", "Precondition", "Component" and "Action" to form "Event" class.

5.2. Policy Descriptive Language for Pervasive Computing (PDLPC)

Policies can be described at different levels of abstraction. At a high level, Policies could be specified using natural language. At a low level, the method of logic or algebraic can be applied to specify policy description. In the intermediate point, production rules are be found to specify policies. In this paper, we prefer in the intermediate point for effectively computing in pervasive computing

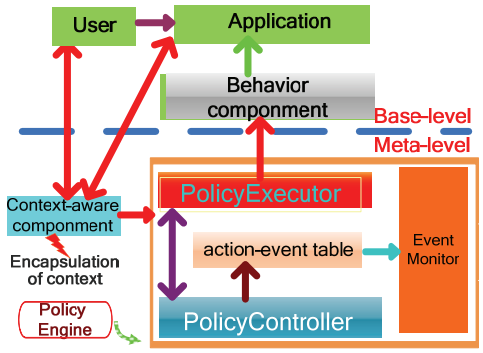

Figure 2. Reflective scheme of context-driven policy scheme.

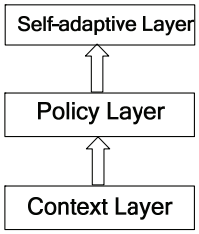

Figure 3. Model of context-driven policy.

environments. For this reason we propose a Policy Descriptive Language for Pervasive Computing (PDLPC) based on the proposed policy ontology.

The syntax of PDLPC is defined based on the BNF notation. The most important features of BNF used in this paper are as follows:

• =is the defining symbol. On the left-hand side is the name of the grammar rule and on the right-hand side is the definition of that name.

• | indicate optional elements.

• {and} indicate repetition. Zero or more elements.

• , is the definition separator symbol. It separates alternatives in a grammar rule.

• ; is the terminator symbol. Every rule is terminated by this symbol.

The definition of PDLPC is as follows.

<PolicySet>::={<Policy>};
<Policy>::= <PolicyID>,<Priority>,<LogicType>, <EventPreconditionGroup>,<Event>;
<Priority>::=<High>|<Low>;
< LogicType >::=<Two-Valued >|<Fuzzy>;
<EventPreconditionGroup>::= {<EventPrecondition>};
<EventPrecondition>::= <EventPreconditionid>, <EventCondition>,<Restriction>;
<EventCondition>::=<Context>|<State>;
<Context>:==<ContextTime>,<ContextAattribute>,<DataType>;
<DataType>:==<int>|<char>|<float>|<double>|<datetime>;
<Restriction>::=<LogicOperator>,<Value>;
<LogicOperator>::=<Over>|<Below>|<Equate>;
<Event>::=<EventType>,<LogicType>, <PreconditionGroup>,<Component>,<ActionGroup>;
<EventType>::=<AtomEvent>|<CompositeEvent>;
<AtomEvent>::=<ContextValueEvent >|<StateEvent>;
<CompositeEvent>::=<AtomEvent>,<EventOperator>;
<EventOperator>::=<→>|<and>|<or>|<not>|;
<LogicType>:=<Two-valued>|<Fuzzy>;
<PreconditionGroup>::={<Precondition>};
<Precondition>::=<PreconditionID><Context>,<Restriction>;
<ActionGroup>::={<Action>};
<Action>:: =<ActionID>, <Component>, <Method>, <ParameterSet>;

PDLPC consists of there layers: policy-event-action. Policy is at a high level and could be a set of rules which govern the behaviour of a system can be triggered by events. At a low level, Action is a domain dependent action and Precondition is constraints on the Action and Component. It can reveal the execution of actions and consider greater understanding of the action and its parameters. In the middle level, Event is used to trigger policy and represent the execution of action reacts in a specific context.

From the above description, it is convenient to be able to define polices separately, and re-use them via PDLPC.

5.3. XML Based Representation

For rules are intuitive and natural way of thinking, there is need to write rules conveniently. As XML becomes the de facto standards for data representation and interchange, and XML data which can be viewed as a hierarchically-structured rooted tree is convenient for represent the policy descriptive language. Here, we prefer to use XML-based representation for PDLPC.

We use the fire alarm example to illustrate PDLPC using XML, as show in Figure 5. From the example, we can find the useful features of our approach.

1) Policy is a hierarchically-structured that can be favourable to XML parser.

2) Events and parameters are attached to a component.

5.4. The Lifecycle of Polices

The lifecycle of polices is as shown in Figure 6. It includes the main steps and related activities in the policy life cycle.

The step of policy analysis is to parse the policy set via XMLParser. In the meantime, for the efficiency and simplify of policy management, priorities of policies fall into two main categories: low and high. The conflict between the two policies can be resolved at run-time.

When PolicyController check the policy is high priority, the policy will be activated, otherwise it will be deactivated. According to the reflective scheme, application developer can adjust relevant policies to the new situation including insert, modify and delete policy in Policy Set. The policy maintenance mechanism is convenient to improve the policy definition and deployment.

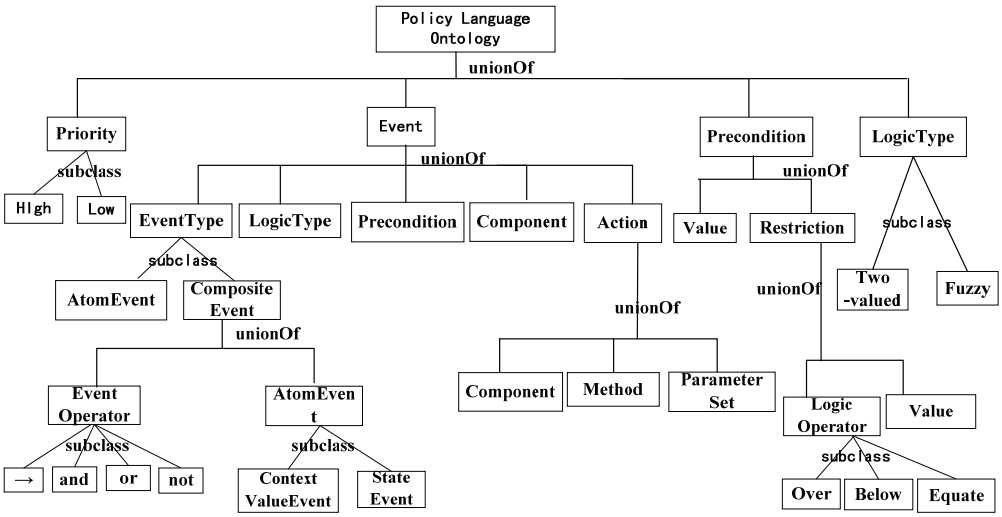

Figure 4. Policy ontology.

```
<PolicySet PolicyID=”FireAlarm”>
  <Policy>
    <Priorities>High</Priorities>
    <LogicType>Two-Valued</LogicType>
    <PreconditionGroup>
      <Precondition PreconditionID=”First”>
        <Context>
          <ContextTime>180506</ContextTime>
    <ContextAattribute>temperature</ContextAattribute>
          <DataType>float</DataType>
        </Context>
        <Restriction>
          <Over>
            <Value>200</Value>
          </Over>
        </Restriction>
      <Component>Temperature_sensor_demo</Component>
        </Precondition>
      </ PreconditionGroup>
  <Event>
        <EventType>ContextEvent</type>
        < LogicType >IF-THEN</Type>
        < PreconditionGroup>
          < Precondition PreconditionID=”first”>
            <Context>
              <ContextTime>180507</ContextTime>
              <ContextAattribute>fog</ContextAattribute>
        <DataType>float</DataType>
      </Context>
      <Restriction>
        <Over>
          <Value>0.3</Value>
        </Over>
      </Restriction>
      <Component>Fog_sensor_demo</Component>
    </Precondition>
  </ PreconditionGroup>
  <ActionGroup>
    <Action ActionID=”Fire_alarm”>
      <Component>Fire_alarm_demo</Component>
      <Method>Forecast</Method>
        <ParameterSet></ParameterSet>
      </Action>
    </ActionGroup>
  </Event>
 </Policy>
</PolicySet>
```

Figure 5. Fire alarm example in XML.

6. Event Scheme

6.1. Context-Driven Event Channel

The context-driven event channel decouples the communication between the suppliers and consumers for asynchronous communication. Event scheme supports asynchronous communication and lets one or more suppliers to send events to more than one consumers occurring at the same time. Context-driven event channel is as shown in Figure 7.

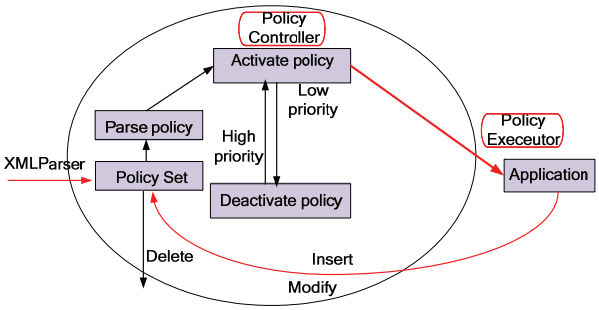

Figure 6. The lifecycle of polices.

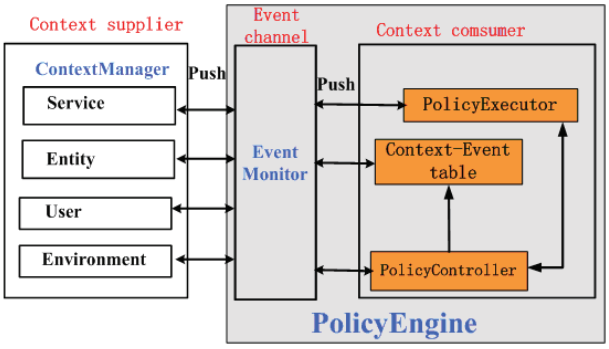

Figure 7. Context-driven event channel.

Context Suppliers and Consumers: ContextManager is the context suppliers consist of context data which is organized as hierarchical ontology including Service, Entity, User and Environment. When the context data is changed, context suppliers will push events to consumers. Context consumers which are managed by PolicyController are final goals of the events generated by the context suppliers pushing the events.

Event Channel: The event channel plays the role of a central mediator between the context consumers and suppliers. Both the suppliers and consumers connect to one or more event channels which are managed by EventMontior. An event channel is responsible for transferring events from the suppliers to the consumers.

Reflective Scheme: PolicyExecutor can dynamically change context data via EventMonitor for reflection. Moreover, when the policy in Policy Set is modified or deleted, it will lead to relevant change in ContextEventTable and EventMonitor.

6.2. Event Composition

An adaptation policy consists in a set of rules, each of the form Event-Condition-Action (ECA). The event can be classified into two classes: AtomEvent and CompositeEvent. AtomEvent consists of two types: ContextValueEvent represents the change of the context data, while StateEvent gives a clue to the state of the system.

There is four event operators that allow various kinds of complex events to be specified:→, and, or, not.

• →: If A and B are events, A→B denotes that event B must only be triggered after event A or that event A and B must be triggered in sequence.

• and: If A and B are events, A and B denotes that CompositeEvent is triggered when both event A and B have been happened no matter the occurrence time of event A, B.

• or: If A and B are event s, A or B denotes that CompositeEvent is triggered when either event A or B is happened.

• not: If A is a event, not A denotes that CompositeEvent is triggered when event A is not happened.

The event composition can be composed via simple Boolean expressions. The hierarchical event composition consists of multiple levels of atom events. The example

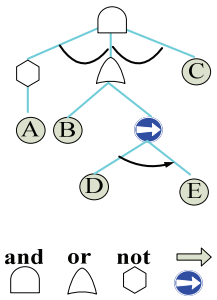

Figure 8. Hierarchical event composition example.

is as shown in Figure 8, The composition event F is composed by five atom events A,B,C,D,E: (not A) and (B or (D→E)) and C.

7. The Implementation of Adaptation Architecture

For the convenience of implementing the self adaption, we extend the CCM component container for supporting policy scheme. As shown in Figure 9, We augment the infrastructure of CCM component container including increasing the context list, Context-Event table, PolicyController, Policy Table and Policy Executor for supporting the parse and handle of policy. Context list is a two-dimension table, which consists of component name, context name and the value of the context data. Context-event table can describe the change of physical and information space. It includes the field of context name, event ID and event name. PolicyController is responsible for matching all polices with the Context data and select the appropriate policy. Policies are defined as a set of sophisticated rules which is described in XML (EXtensible Markup Language). The Policy Table can maintain the policy information which contains policy ID, policy priority, event ID, The reference of PolicyExecutor pointer. They indicate the execution of action reacts in a specific context and are storaged by hash table.

The functionality of Policy Engine is monitoring the change of the value of Context and executing the predefined polices. It comprises the Event Monitor, Policy Executor, PolicyController, Policy Table, Policy Parser and POA (Portable Object Adapter).

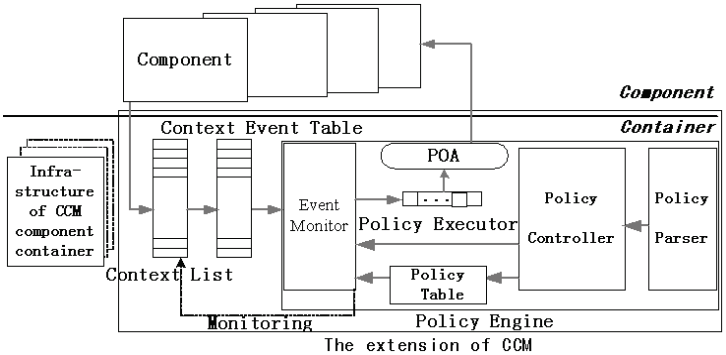

Figure 9. Extension of CCM component container for component fault detection.

◆ Policy Parser is a CORBA object, which is a XML parser. The functionality of Policy Parser is to match all polices in the Context Event Table and select the appropriate policy to dynamically generate the Policy Executor.

◆ Policy Executor is a two dimension pointer array. The first dimension is context name, and the second is a pointer which point to a group of CORBA objects and corresponding interfaces. The policy is storied as a structure of policy condition, action type, component name, method of component. Policy Executor can check the condition of policy is met, if it is true, the method of the component can be triggered by POA.

◆ PolicyController takes charge loading, uninstalling, activating/deactivating the polices. In the meantime, it can adjust the priority of the polices according the demand of the applications.

◆ Policy Table is initialized by PolicyController and can providing the query operation. For instance, it can retrieve the reference of the corresponding Policy Executor by event ID.

◆ Event Monitor is also initialized by PolicyController. The role of Event Monitor is to register the event to the Context Event Table or remove the event from the Context Event Table. The event ID is unique and can be bound to the Policy Table. It can periodically monitor the change of value the Context List. When the change is detected, it judge whether the context event is in the Context Event Table, if it is false, insert the context event into Context Event List.

8. Prototype Implementation

8.1. Fire Alarm Scenario

The first prototype implement is based on fire alarm scenario, as shown in Figure 9. There are temperature infrared sensor, sprinkler control valve and fire warning light in a room. The fire alarm application consists of sprinkler control valve component, fire warning light component, temperature-aware component and fire alarm policy. The temperature-aware component aggregate the context information from the temperature sensor and the aggregated data which is the occurrence likelihood of fire alarm (0%-100%) is displayed by fire monitor terminal. When the captured values from temperature sensor exceed the threshold, fire alarm component will drive the fire alarm lamp give off flashes of light and sprinkler control valve begin to sprinkle water which can be activated by sprinkler control valve component. As the predefined value which is assigned by policy stored in XML file is update from 200 to 150, it is need to only restart the fire alarm application without recoding the program code. Moreover, while the temperature exceeds the threshold, policy engine will result in a change of the context information by way of executing the predefined polices.

The XML parser is based on TinyXML parser (from SourceGauge Website). In the mean time, the register/ recall mechanism is used in the communication between the temperature-aware component and context manager component.

8.2. Error Tolerant Policy

As pervasive computing environments is open and dynamic, the technology is sustainable and high confident if it is inconspicuous to the user and does not disturb the user's attention. This necessitates the pervasive computing system has to be resilient to faults and should be able to be error-tolerant.

Here, a prototype implementation of component error recovery has been realized based on fire alarm scenario.

The instance of error tolerant policies is as shown in Figure 11. It means that "If temperature context name= [CompomentStatus], and context value=[Component Failure], then call the activate () method of temperature-aware component".

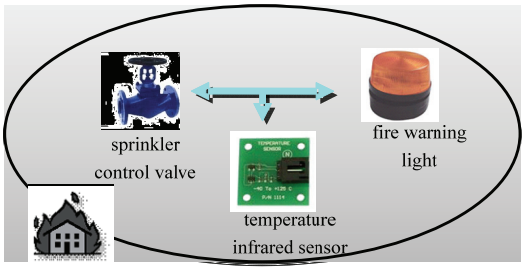

Figure 10. Fire alarm scenario.

```
<PolicySet>
  <Policy>
    <Policy Description>Temerature error tolerent policy</Policy
Description >
    <Priorities>High</Priorities>
    <Event>
     <Event Description >Platform cotext event</Event Descrip-
tion >
     <EventType>ContextEvent</type>
     <Type>IF-THEN</Type>
     <PreconditionGroup>
       <Precondition>//Error event triggered
         <Contextid>
           <Component>Temperature_sensor</Component>
           <ContextTime>180506</ContextTime>//
           <Attribute>ConponentState</Attribute>
           <LogicType>Bool</LogicType>//
           </Contextid>
           <Restriction>
             <Equate>
               <Value>Failure</Value>//The Component is failed
             </Equate>
           </Restriction>
           </Precondition>
       </PreconditionGroup>
       <ActionGroup>//action
           <Action>
            <Component>Temperature_sensor</Component>
            <Method>activate</Method>//reload the component
            <ParameterSet></ParameterSet>
           </Action>
       </ActionGroup>
    </Event>
  </Policy>
</PolicySet>
```

Figure 11. Instance of error tollrant policy.

8.3. Comparison with Current Methods

The proposed self-adapt model is based on reflective scheme for adaptive middleware support. It means that context information is used as meta data and policy can be regarded as meta protocol. Thus it can separate self-adapt functionality from business logic of a system. Compared with David [9], the proposed framework can be more reusable and flexible. Compared with Adamczyk [12], the proposed policy ontology is well defined semantic. This means that it can adapt the behaviour of applications in the pervasive computing without re-coding functionality, and a change in the applications can be applied without restarting the system. Moreover, the proposed policy language is based on the policy ontology, which has a common semantic understanding of aadaptive rules for well-defined semantics, thus it is well expressive and easily extensible to support the design of policy engine which is based on the Separation of Concerns principle.

However, there is still a limitation of the proposed scheme that has an impact on the complexity of component management because there both exist behaviour component in the base-level and context-aware component in the meta-level.

9. Conclusions

In this paper, we have presented policy based adaptive architecture for pervasive computing. The proposed policy ontology can support for knowledge representation and reasoning and knowledge sharing and integration for defining adaptive rules. Also, the proposed policy descriptive language for pervasive computing can enable define polices separately, and re-use them. Moreover, policy management allows application developers to ensure flexibility and adaptability. Furthermore, the policy mechanism is based on not only event- condition-action rules, but also more abstract utility/goal policies.

Now our ongoing work is to apply the adaptive architecture to the museum monitor scenario in China in practice.

10. Acknowledgment

This work was supported by the National High-Tech Research and Development Plan of China under Grant No 2006AA01Z198 and China Postdoctoral Science Foundation Grant No 20070420187.

11. References

[1] J. Lobo, R. Bhatia, and S. Naqvi, "A policy description language," 16th National Conference on Artificial Intelligence, Orlando, Florida, USA, 1999.

[2] N. Damianou, N. Dulay, E. Lupu, and M. Sloman, "Ponder: A language for specifying Security and management policies for distributed systems, V 2.3," Imperial College Research Report DoC 2000/1, October 2000.

[3] R. J. Anthony, "A policy-definition language and prototype implementation library for policy-based autonomic systems," 2006 IEEE International Conference on Autonomic Computing, pp. 265−276, 2006.

[4] J. Ahn, B. M. Chang, and K. G. Doh, "A policy description language for context-based access control and adaptation in ubiquitous environment," Emerging Directions in Embedded and Ubiquitous Computing, pp. 650−659, 2006.

[5] Uszok, Bradshaw, Jeffers, Suri, Hayes, Breedy, Bunch, Johnson, L. Kulkarni, "KAoS policy and domain services: Toward a description-logic approach to policy representation, deconfliction, and enforcement," in POLICY, pp. 93−96, 2003.

[6] K. Lalana, F. Tim, and J. Anupam, "A policy language for a pervasive computing environment," Proceedings of the 4th International Workshop on Policies for Distributed Systems and Networks, Washington, DC, USA: IEEE Computer Society, pp. 63−74, 2003.

[7] E. Rukzio, S. Siorpaes, O. Falke, and H. Hussmann, "Policy based adaptive services for mobile commerce," 2nd Workshop on Mobile Commerce and Services (WMCS 2005), Munich, Germany, pp. 183−192, July 19, 2005.

[8] P. C. David and T. Ledoux, "Towards a framework for self-adaptive component-based applications," Proceedings of Distributed Applications and Interoperable Systems 2003, Lecture Notes in Computer Science 2893, pp. 1−14, November 2003.

[9] A. Erradi1, P. Maheshwari, and V. Tosic, "Policy-driven middleware for self-adaptation of web services compositions," Middleware 2006, LNCS 4290, pp. 62–80, 2006.

[10] A. T. S. Chan, S. N. Chuang, J. N. Cao, and H. V. Leong, "An event-driven middleware for mobile context awareness," The Computer Journal, 47(3), pp. 278−288, 2004.

[11] A. K. Bandara, E. Lupu, and A. Russo, "Using event calculus to formalise policy specification and analysis," 4th IEEE International Workshop on Policies for Distributed Systems and Networks, pp. 26−39, 2003.

[12] J. Adamczyk, R. Chojnacki, M. Jarząb, and K. Zieliński, "Rule engine based lightweight framework for adaptive and autonomic computing," International Conference on Computational Science 2008, LNCS 5101, pp. 355−364, June 23−25, 2008.

[13] P. McKinley, S. Sadjadi, E. Kaste, and B. Cheng, "Composing composing adaptive software," IEEE Computer, 37(7), pp. 56−64, July 2004.

[14] W. Hürsch and C. V. Lopes, "Separation of concerns," Technical Report NU-CCS-95-03, Northeastern University, Boston, Massachusetts, 1995.

Wireless Sensor Network, 2009, 1, 1-60
Published Online April 2009 in SciRes (http://www.SciRP.org/journal/wsn/).

The Analysis of the Structure and Security of Home Control Subnet*

Chengyi WANG[1], Yun ZHANG[2,3]
[1]*School of Electronic Engineering, Hubei University of Economics, Wuhan, China*
[2]*International School of Software, Wuhan University, Wuhan, China*
[3]*Research Center of Spatial Information and Digital Engineering, Wuhan University, Wuhan, China*
Email: wcytjx@126.com
Received November 16, 2008; *revised January* 10, 2009; *accepted February* 5, 2009

Abstract

A lot of technologies can be used in home control subnet, but the hardware and software resources available for the home control subnet are limited. There are security problems easily seen. The paper gives the systematic analysis of the structure and function of home control subnet based on the general model of home network. The paper has also analyzed two types of major equipment, namely sub-gateways and terminal equipment. The major networking technology used in home control subnet is summarized and concluded. In combination with relationship among home control subnet, home network, as well as the outside main network, the paper has systematically studied various safety problems related to home control gateways and the possible solutions to those problems have been made.

Keywords: Home Network, Home Control Subnet, Network Architecture, Network Security

1. Introduction

Home network is developed from the concept of home LAN, Intelligent home. It is the integrated networks of home control networks and multimedia information network, which is an integrated business platform with a voice, data, multimedia, video, control and management. Home network can be roughly divided into the high-speed backbone-network and low-speed control subnet. Subnet of control, there is a lot of technology and standards can be used, can be connected with home backbone-network, and even be connected with the Internet. Therefore, in building control network function, security issues associated with the network exists. The paper gives the analysis of the technology, structure and security issue of home subnet and also gives the description of the possible solutions.

2. The Architecture of the Home Control Subnet

2.1. The Reference Model of the Home Network Structure

Home control Subnet is one part of home network. It is described in detail in the structure reference model [1], as shown in Figure 1. The home backbone-network is linked with Internet and the management by home network gateway. Home control Subnet is connected with home backbone-network through sub-subnet gateway. Home backbone-network equipment can communicate with each other, getting access to external networks through the main gateway, holding the control operations of the equipment through the sub-subnet gateways. Home control subnet device can communicate through sub-gateway and the main gateway with the external home network.

2.2. Main Functions of the Control Subnet

The functions of home control subnet should be [2]:

- Inquiry function: the adoption of home control subnet gateway can query the status of subnet equipment;
- Control function: It can control the devices under the home control subnet through subnet gateways, but also implement the remote control through the main gateway;
- Configure function: implementation of the home sub-

*Fund Project: Hubei Province education department scientific research project (D200619006)

net configuration control operation;

- Message function: For auto-discovery, device management to provide basic information, it is able to take the initiative to send its status report to sub-gateways.

2.3. The Typical Structure of Home Control Subnet

A home network can have one or more home control subnet, each subnet network consisting of a subnet gateway and a number of terminal equipment. They can be connected through twisted pair, power line, radio frequency, infrared fiber and optical fiber, etc. One typical structure is shown in Figure 2.

2.4. The Structure of Subnet Gateway

Subnet gateway is one of the home control network equipment, whose functions are to enquire about the home control network device, parameter setting and control and to allocate and manage, home subnet equipment. In terms of hardware, sub-gateway is based on the 32-bit embedded system (such as the S3C2410x) to achieve implementation, shown in Figure 2. For the software, sub-gateways are based on embedded operating system (such as ARMlinux), Web server (such as boa), data base management system (such as SQLite) and so on to get the implementation.

As the central equipment of home control subnet, it is necessary for subnet to provide services for main network and external network, such as user authentication, remote control. It is needed for subnet to offer the service to the subnet equipment, such as the provision of the dynamic registration of terminal equipment, collecting the relevant data of terminal equipment. Subnet will also have the maintenance of a variety of information databases [3] and give sustained, reliable data information for information exchange and management. Its logical structure is as shown in Figure 3.

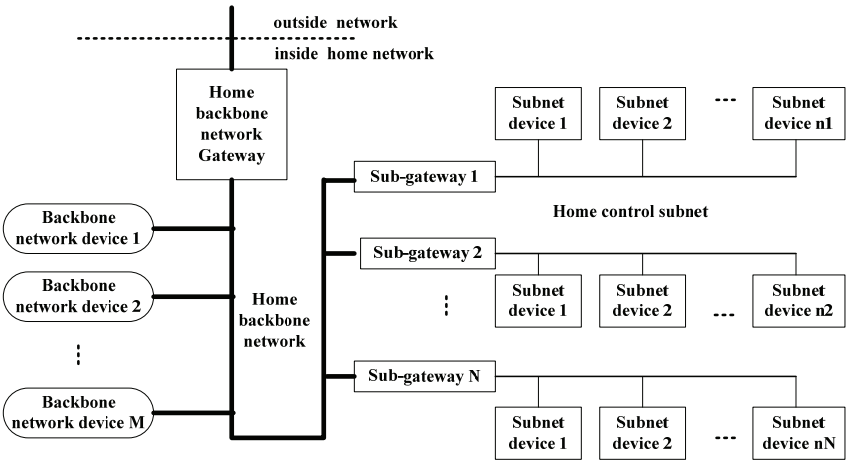

Figure 1. Home network structure reference model.

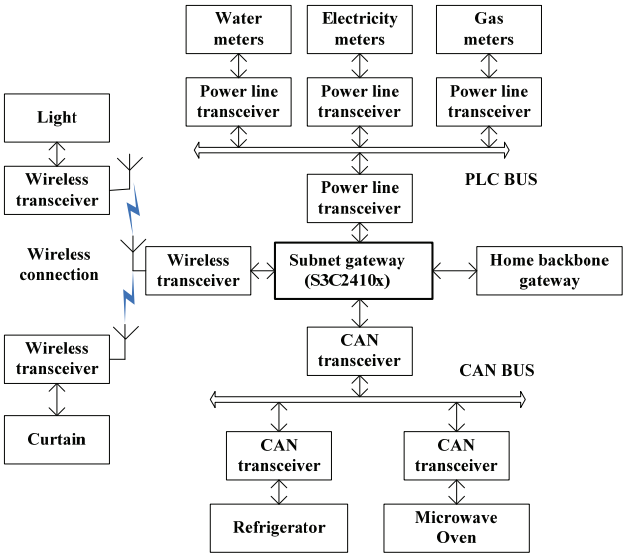

Figure 2. The typical structure of home control subnet.

Subnet gateway can provide remote services and remote control for the outside network user, the software architecture is as shown in Figure 4.

3. Networking Technology of Home Control Subnet

Home control subnet networking technology, according to the introduction of home network technology at the source, can be divided into bus technology, Ethernet technology and wireless network technology. Among them, the Ethernet technology mainly refers to industrial Ethernet technology. In terms of reliability, redundancy and other aspects of treatment improved the Ethernet technology is improved, but with less applications. Wireless network technology includes the 802.11 series, radio frequency, infrared, Bluetooth, ZigBee, etc. Bus technology can best bear the real-time control network, orderly and interoperable features. The typical of the bus technology is as shown in Table 1.

4. The Security Problems and Related Measures of Terminal Equipment and Wire

The Security risks of home control subnet may come from different levels, such as from the physics, the vulnerability of technology or man-made attack. The details are as follows.

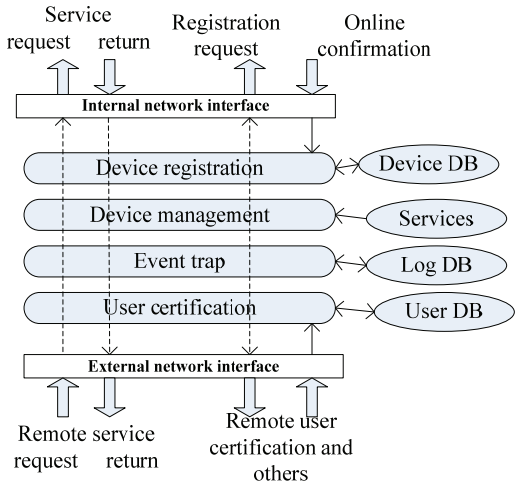

Figure 3. Subnet logical structure.

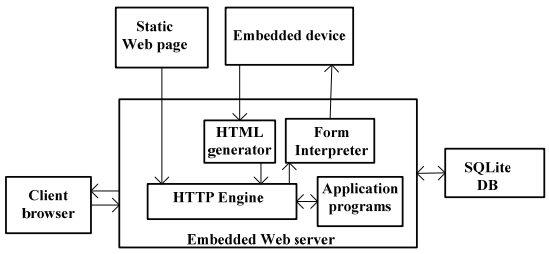

Figure 4. The subnet gateway software architecture.

Table 1. Typical bus technology.

Bus type	Relevant standards	The transmission medium	Maximum transfer rate
X-10	The standard in fact	power line	60bps
CEBus	ANSI IS-60/EIA-600	twisted pair, power line, coaxial cable, wireless	10kbps
LonWorks [4]	ANSI/EIA-709	Twisted pair, power line, coaxial cable, wireless and optical fiber	1.25Mbps
EIB	European Installation Bus Association	twisted pair, power line, wireless, infrared	10kbps
CAN [5]	ISO 11898-1	twisted pair, coaxial cable, and optical fiber	1Mbps

4.1. The Physical Security of Equipment

Problem 1: the physical security of equipment is the home control subnet gateway equipment, terminal equipment their own safety, including accident damage and man-made events, such as home gateways, connecting wires, home appliances equipment having been illegally linked, external electromagnetic interference, fire and other natural disasters.

Related measures: To set up password for access to essential equipment and more stringent measure of gateway certification is needed.

Problem 2: the power network security of the equipment and the security of weak power supply system.

Related measures: the use of effective protective circuit (such as the circuit with the energy absorption or photoelectric isolation function) for security.

Problem 3: There being more wireless networking technology in home control subnet, it may be overlapped with the frequency bands of other networks.

Related measures: the application of frequency bands approved by local relevant agencies for networking.

Problem 4: power line information security, including EMC (Electromagnetic Compatibility) and the signal separation.

Related measures: strict and effective grounding equipment, the use of isolators to isolate carrier.

4.2. The Protocol Security of Low Layer Network

Problem 5: RF wireless technology security, such as 802.11b technological security. Take 802.11b as an example, it shared key authentication by using one-way authentication method so that the access point can verify the identity of the user, but **users** can not verify the identity of the access point. If a false place is put to WLAN access points, it will hijack the legitimate client to launch a platform of DOS (denial of service stacks).

Related measures: By using two-way authentication mechanism so that detecting and isolating a false access point becomes possible. MAC address filtering, Wired Equivalent Privacy, etc. will be jointly used.

Problem 6: wireless coverage and information security. Neighbor device gets involved.

Related measures: One solution is to manually set ID for terminal equipment. The other is to verify the identity of terminal equipment.

5. The Security Problems and Related Measures of Subnet Gateway

As for the home control subnet, security of the gateway is most complex. In addition to the above mentioned similar device safety problems, more problems will occur at the top of network protocols. The security of subnet gateway is closely related with the location, structure and functions of subnet gateway. In terms of the location, the sub-gateway is key equipment between home control subnet and home backbone-network, being a member of the main network. In terms of the functions, the sub-gateways take the responsibilities of equipment registration, management and control, of verifying authentication of remote users, of information services and operational control. The sub-gateways for are responsible for the communication links between the main network and subnet, for the implementation of the centralized control and remote control of home control subnet terminal equipment, for bridging UPnP network upper protocol of main network. In terms of the protocol, the sub-gateways are involved in the multi-layered protocol stack. See Figure 5, showing that they result in different levels of network security problems.

The main security problems of subnet gateways are:

- Security of information: By the home sensors, an attacker can intercept domestic information of one family, such the working status of home appliances and personal privacy.
- User authentication: The attacker will illegally play as family members or staff of property management to read data and announce false instructions.
- User license: The attacker will illegal use or steal the authorization of the owner to take sabotage activities on purpose;
- Data integrity: An attacker will undermine the integrity of data through tampering the user's data and instructions. Specific analysis is as follows.

Problem 7: The safety of subnet gateway HTTP Authentication [6]. If the system is based on the HTTP basic authentication (Basic Authorization), and when the client makes requests to the HTTP server, HTTP server will determine the legality of the user through the basic certification process of verifying the client's name and password. In this certification process a user's name and password is submitted to the Web server after a 64-bit encoded files are put on the HTTP headers, but the password and user name is transmitted in plaintext way so that it can easily be intercepted and any user with that name and password can have access to these protected resources.

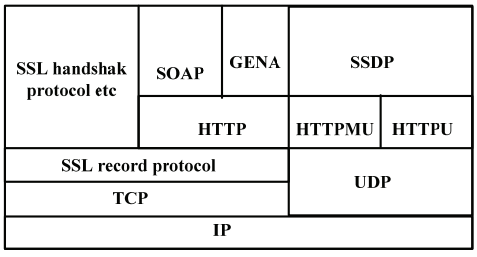

Figure 5. Subnet gateway protocol stack.

Related measures: For the weaknesses of basic authentication, HTTP/1.1 proposed to improve the user authentication program, known as the digest access authorization. With the similarity to the basic certification, digest access authorization is also a testing key know to both sides, but the transmission is not in plaintext way transmission, but in cipher text way transmission. Access control on the client can be divided into three steps, namely, identification authentication of clients and home gateway, the identification and authentication of client name and password, the check of the permissions of customer account.

Problem 8: How to encrypt and transmit important information.

Related measures: One solution is to use SSL (Secure Sockets Layer) protocol to simplify the information so that it applies to a subnet gateway of home network [7]. The protocol stack is as shown in Figure 5.

With the introduction of SSL protocol, it can upgrade the Web server and client communication confidentiality, data integrity and effective authentication. In combination with HTTP digest access authorization, different authentication can be done based on different levels of security. The visiting right is grouped. Through user groups of different terminals for different access control, and thus a more comprehensive security control can be achieved. The detailed measure is that different levels of equipment and its operation of home appliances will use different security systems. High security can hold SSL secure communication through the port of 443, or otherwise through the transfer port of 80 for HTTP, just use an easy authentication at the application layer. The main process of Web server is monitoring 80 ports and 433 ports. When 80 ports received request from HTTP, HTTP server would have digest access authorization to the clients. Upon completion of authentication, data will start to be transmitted. When there is a request of connection from the port of 443, the simplified SSL system which ensures security of transmission and authentication will be used.

Problem 9: Non-repudiation problem. It mainly refers to interaction between the two sides not denying the exchange of information, focusing on the user who cannot deny the operation on the home gateway and the terminal equipment.

Related measures: A basic approach is to log the user operations, to set up a log database. All users will be recorded for all operations. If the problem of non-repudiation is tackled, the adoption of digital signatures will matter.

Problem 10: Access Control security.

Related measures: For characteristics of home subnet, manager and user is usually the home member, therefore it is needless to grasp the complex set of internal details of permissions. As we know, there will be more types of electrical appliances at home their functions will become more and more complex. A possible solution is to establish the control strategy based on the object-model. From the perspective of the controlled object, the object-model will directly link the access to the subject with the controlled access object. On one hand, it is easy to operate the definition of the access control list object, deletion, addition and modification. On the other hand, when the controlled object feature changes, or the controlled object has the action of inherit and derivation, there is no need to update the access to the subject with the permissions, only need to modify the corresponding access of the controlled object, thereby reducing access to management of subject and decreasing the complexity of the authorized data management.

Problem 11: The security of device auto-discovery mechanism based on UPnP (Universal Plug and Play) [8] [9]. In order to get the intelligence of home backbone-network, there will be implementation of equipment, service auto-discovery protocol stack. The most typical one is UPnP. Because of malicious intrusion to the equipment, UPnP as the main equipment of home backbone-network, by subnet gateway as bridge, will get information of control subnet terminal equipment, and can do further attacks.

Related measures: the log can be used to record the user's operation, alarm. Subnet gateway can use the appropriate sub-gateway packet filtering strategy.

Problem 12: The security problem of virus attack and hacker attack.

Related Measures: The main solution is that the main gateway of home network is armed with firewall function so that it can block and prevent the attack of viruses, Trojans, hacker, and so on.

6. Conclusions

Through systematic analysis of the home control subnet structures, networking, and the relations of home control subnet and home backbone-network, especially the structure, functions of subnet gateway of home network and protocol stack, safety issues of home control subnet in different levels and aspects, including security of physical security equipment, the safety of the underlying protocol and the protocol level, are analyzed in detail and workable solutions are provided step by step. In short, as long as we make the full use of limited resources of the control subnet, make a reasonable choice of technology and build different levels of security precautions, a reliable and practical home control subnet will be surely constructed.

7. References

[1] SJ/T 11316-2005, "Home network system architecture and reference model," People's Republic of China Electronic Industry Standard, September 2005.

[2] SJ/T 11314-2005, "Specification for home subnet communication protocol," People's Republic of China Electronic Industry Standard, September 2005.

[3] SJ/T 11317-2005, "Home network device description file specification," People's Republic of China Electronic Industry Standard, September 2005.

[4] F. Q. Wu, J. Li, and D. S. Hu, "Application of LON works field bus technology in home network system," Journal of Chengde Petroleum College, Chengde, No. 4, pp. 31−56, 2008.

[5] Bosch, "CAN specification Version 2.0," September 1991.

[6] Y. Zhu, "Design and realization of an improved HTTP digest authentication scheme," Study on optical communication, Wuhan, No. 4, pp. 59−62, 2008.

[7] Y. Y. Zeng and Z. H. Zuo, "Design and implementation of SSL protocol on embedded devices," Journal of Chengdu University of Information Technology, Chengdu, No. 4, pp. 389−392, 2008.

[8] UPnP Forum, "UPnP device architecture 1.0," April 2008.

[9] SJ/T 11310-2005, "Information device intelligent grouping and resource sharing Part1: Core protocol," People's Republic of China Electronic Industry Standard, September 2005.

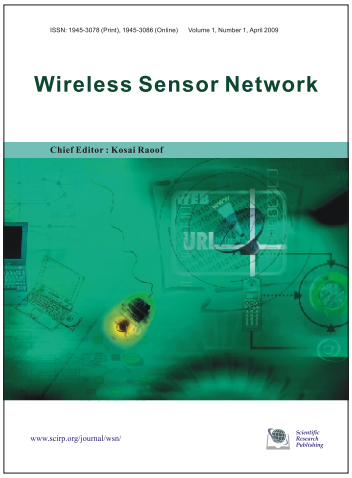

Wireless Sensor Network (WSN)

Call For Papers

http://www.scirp.org/journal/wsn

ISSN 1945-3078 (Print) ISSN 1945-3086 (Online)

WSN is an international refereed journal dedicated to the latest advancement of wireless sensor network and applications. The goal of this journal is to keep a record of the state-of-the-art research and promote the research work in these areas.

Editor-in-Chief

Dr. Kosai Raoof , GIPSA LAB, University of Joseph Fourier, Grenoble, France

Subject Coverage

This journal invites original research and review papers that address the following issues in wireless sensor networks. Topics of interest are (but not limited to):

- Network Architecture and Protocols
- Self-Organization and Synchronization
- Quality of Service
- Data Processing, Storage and Management
- Network Planning, Provisioning and Deployment
- Integration with Other System
- Software Platforms and Development Tools
- Routing and Data Dissemination
- Energy Conservation and Management
- Security and Privacy
- Developments and Applications
- Network Simulation and Platforms

We are also interested in short papers (letters) that clearly address a specific problem, and short survey or position papers that sketch the results or problems on a specific topic. Authors of selected short papers would be invited to write a regular paper on the same topic for future issues of the WSN.

Notes for Intending Authors

Submitted papers should not have been previously published nor be currently under consideration for publication elsewhere. Paper submission will be handled electronically through the website. All papers are refereed through a peer review process. Authors are responsible for having their papers checked for style and grammar prior to submission to WSN. Papers may be rejected if the language is not satisfactory. For more details about the submissions, please access the website.

Website and E-Mail

http://www.scirp.org/journal/wsn Email: wsn@scirp.org

Wireless Sensor Network, 2009, 1, 1-60
Published Online April 2009 in SciRP (http://www.SciRP.org/journal/wsn/).

TABLE OF CONTENTS

Volume 1 Number 1 **April 2009**

Bandwidth Efficient Three-User Cooperative Diversity Scheme Based on Relaying Superposition Symbols
M. W. CAO, G. G. BI, X. F. JIN..... 1

The Influence of LOS Components on the Statistical Properties of the Capacity of Amplify-and-Forward Channels
G. RAFIQ, M. PÄTZOLD..... 7

Parameter Optimization for Amplify-and-Forward Relaying Systems with Pilot Symbol Assisted Modulation Scheme
Y. WU, M. PÄTZOLD..... 15

An Energy Balanced Reliable Routing Metric in WSNs
J. ZHU, H. ZHAO, J. Q. XU..... 22

Extending the Network Lifetime Using Optimized Energy Efficient Cross Layer Module (OEEXLM) in Wireless Sensor Networks
T. V. PADMAVATHY..... 27

Subarea Tree Routing (STR) in Multi-Hop Wireless Ad hoc Networks
G. K. LIU, C. L. SHAN, G. WEI, H. J. WANG..... 36

Research on ZigBee Wireless Sensors Network Based on ModBus Protocol
C. B. YU, Y. F. LIU, C. WANG..... 43

Policy Based Self-Adaptive Scheme in Pervasive Computing
J. Q. OUYANG, D. X. SHI, B. DING, J. FENG, H. M. WANG..... 48

The Analysis of the Structure and Security of Home Control Subnet
C. Y. WANG, Y. ZHANG..... 56

9771945307008 01